PHYSICOCHEMICAL STUDIES OF POTASSIUM CATION INTERACTIONS WITH NEUTRAL LIGANDS AND WITH ANIONS

By

Emmanuel Schmidt

A DISSERTATION

Submitted to
Michigan State University
in partial fulfillment of the requirements
for the degree of

DOCTOR OF PHILOSOPHY

Department of Chemistry

1981

ABSTRACT

PHYSICOCHEMICAL STUDIES OF POTASSIUM CATION INTERACTIONS WITH NEUTRAL LIGANDS AND WITH ANIONS

By

Emmanuel Schmidt

The kinetics of complexation of the potassium cation with the ligand 18-crown-6 (18C6) were studied in five solvents or solvent mixtures by potassium-39 nuclear magnetic resonance. The salt used was potassium hexafluoroarsenate or iodide. The solvent systems were acetone, methanol, 1,3-dioxolane, acetone-1,4-dioxane (80-20% vol.) and acetone-tetrahydrofuran (80-20% vol.). In solutions containing equimolar amounts of solvated and complexed K^+ ions, a kinetic process is observed in which the potassium cation exchanges between the solvated and the complexed site. The kinetic parameters were obtained from a quantitative analysis of the line width of the apparent resonance of the solvated cation.

In 1,3-dioxolane and probably in other solvents too, the cation exchange proceeds via the bimolecular exchange

mechanism instead of the dissociative mechanism which other workers found to be operative in water. The activation energy for the bimolecular exchange strongly depends on the solvent; it is 9.2 kcal mol^{-1} in acetone and methanol, 13.8 kcal mol^{-1} in the acetone-dioxane mixture and about 16 kcal mol^{-1} in dioxolane. The differences in activation entropies, which vary between -4 cal mol^{-1} deg^{-1} in acetone and +15 cal mol^{-1} deg^{-1} in dioxolane, largely compensate the differences in activation energies so that the exchange rates at 25°C vary by a factor of less than 50. The results point to a "loose" transition state in which bond breaking would occur prior to bond forming.

Carbon-13 NMR studies were performed on the free cryptand 221 (C221) in twenty solvents over a large temperature range. It was shown that C221 interacts with acceptor solvents such as water, formamide, nitromethane, acetonitrile, methanol and dichloromethane. In these solvents, as the temperature decreases, the conformation of the cryptand molecule tends towards that found in the $C221 \cdot K^+$ cryptate whereas in other solvents such as acetone and dimethylformamide (DMF) the C221 conformation does not change with temperature. Hydrogen-bonding is likely to be responsible for the cryptand-solvent interaction.

The temperature independence of the potassium-39 chemical shift of the $C221 \cdot K^+$ cryptate in several solvents indicates that, in solution, there is only one kind of

complex formed. The relatively large paramagnetic shift, which varies between 10 and 15 ppm, suggests that the K^+ ion is tightly embedded in the cryptand cavity.

Potassium-39 and carbon-13 NMR studies were also performed on the potassium ion complexes with dibenzo-21-crown-7 (DB21C7), dibenzo-24-crown-8 (DB24C8) and dibenzo-27-crown-9 (DB27C9). Only the presence of 1:1 complexes was detected by both techniques. With DB24C8, the logarithm of the formation constants (measured by ^{13}C) are 1.44±0.08, 3.46±0.17, 3.70±0.16 and ≥ 4 in DMF, pyridine, acetonitrile and nitromethane respectively. In nitromethane, the three aliphatic carbon peaks coalesce at K^+/DB24C8 mole ratio of 1, indicating the formation of a tridimensional "wrap-around" complex. In the other solvents, where the complex is less stable, the coalescence is not observed, indicating that a strong K^+-solvent interaction might prevent a complete stripping of the cation solvation shell by the ligand. The DB24C8 ligand has the minimum size required to wrap around the K^+ ion.

The ^{23}Na, ^{39}K, ^{133}Cs and ^{205}Tl chemical shifts of the crown complexes with the corresponding monovalent cations in various solvents were collected from the literature. An analysis of these data in terms of the repulsive overlap effect provides detailed information about the ion size-cavity size relationship, the conformational properties of crown molecules and the cation-solvent interactions.

Emmanuel Schmidt

Potassium-39 chemical shifts in molten salts correlate those in aqueous solutions of these salts but cover a much larger range.

ACKNOWLEDGMENTS

The author wishes to express his deepest appreciation to Professor Alexander I. Popov for his guidance and encouragement throughout the course of this work. Professor Popov will be particularly remembered as a master in the difficult titration of necessary guidance with necessary freedom.

Professor Stanley R. Crouch is acknowledged for his helpful suggestions as second reader. Thanks are also extended to Professors James L. Dye and Michael J. Weaver for interesting and helpful discussions concerning the kinetics study and to Dr. Jean-Pierre Kintzinger (Université Louis Pasteur, Strasbourg, France) for his precious last-minute help during his visit at MSU.

The financial assistance of the Department of Chemistry, Michigan State University, and the National Science Foundation is gratefully acknowledged.

Many thanks go to Wayne Burkhardt, Tom Clarke and Alan Ronemus for their efforts in keeping the NMR spectrometers in operating condition and for allocating me expanded time slots on these instruments.

Deep appreciation is given to Professor Bernard Tremillon (Université Pierre et Marie Curie, Paris, France)

for "sending" me to America to make sure that Professor Popov practices his French on a regular basis and for "sending" his son Jean-Michel to check that I did not forget mine.

Special thanks go to all the past and present members of the research group (alias the U.N. lab) and in particular to Dale, Davette, Elisabeth, Lee, Richard, Sadegh, and Zhi-fen for their friendship and stimulation during these intense years.

Finally, I wish to thank Catherine for her love, patience and unending encouragement throughout this study. Her everyday letter considerably shrank the ocean.

TABLE OF CONTENTS

Chapter Page

Chapter Page

LIST OF TABLES

LIST OF FIGURES

LIST OF ABBREVIATIONS

DNMR	Dynamic Nuclear Magnetic Resonance
C222B	Benzo cryptand 222
DMF	Dimethylformamide
PC	Propylene carbonate
THF	Tetrahydrofuran
THP	Tetrahydropyran
DMSO	Dimethylsulfoxide
DB	Dibenzo
PY	Pyridine
EDA	Ethylenediamine

CHAPTER I

HISTORICAL REVIEW

1. Introduction

The coordination chemistry of alkali metal cations (M^+), which for many years was thought to be non-existent, has matured in the last fifteen years to become a coherent discipline. Two major discoveries prompted chemists to develop the field very rapidly. The recognition of the biological role of Li^+, Na^+ and K^+ cations (1-3) was soon followed by the synthesis of macrocyclic polyethers, called crowns (4), and of macrobicyclic ligands, called cryptands (5-7). Crowns and cryptands display strong and selective complexive abilities towards alkali metal cations. The recent and fascinating chemistry of these ions has evolved from this property.

Syntheses of new multidentate macrocycles, some of which exhibit complicated topologies and fluctuating ring sizes (8), are reported almost weekly. The equilibrium properties associated with the interactions of alkali cations with these macrocycles have been investigated by a number of physicochemical techniques (9) and collected in several reviews (10-13). Some of the most useful techniques are potentiometry, calorimetry and conductometry as well as electronic, vibrational and nuclear magnetic resonance (NMR) spectroscopy.

In this laboratory we probe directly the immediate chemical environment of the alkali ions in solution by using alkali metal NMR. This sensitive technique has proved valuable for studying ionic solvation and complexation reactions, particularly in nonaqueous solvents (9,14). Potassium-39 NMR, however, has been used only sparingly in the past due to the very low sensitivity of this nucleus, as compared to those of the other alkali elements. However, with the advent of superconducting magnets and the development of Fourier transform NMR, high quality ^{39}K NMR spectra may be obtained even in dilute solutions.

In this dissertation we describe various aspects of the kinetics and thermodynamics of complexation of the potassium cation with some crown ethers and cryptands in nonaqueous solvents.

In the first part of this thesis we investigated by ^{39}K NMR the solvent dependence of the kinetics of complexation of the potassium cation with a crown ether molecule.

The second part is devoted to a ^{13}C NMR study of the solvent and temperature dependences of the conformation of a cryptand. Cryptands and their complexes, cryptates, exist as equilibrium mixtures of three conformations but nothing is known about the conformational equilibria in solution. Likewise the ligand-solvent interactions have not been explored, except in water and methanol solutions.

The third part of this work describes the extension of the thermodynamic studies of potassium cation-crown ether complexes initiated by Shih (15) in this group. In particular, we examined the possibility of measuring the stability constants of complexes by ^{13}C NMR. Some exploratory studies of alkali complexes with the so-called "classical" or "conventional" ligands are also reported. We selected 2,2'-bipyridine for this investigation.

The last part is devoted to some ^{39}K NMR measurements in low melting salts of eutectics. The object of this exploratory study was to investigate the influence of a direct K^+-anion interaction on the ^{39}K resonance in the absence of a solvent.

We will review separately each of the four topics outlined above except the third one. The literature up to early 1978 on potassium complexes has been covered in the Ph.D. thesis of J. S. Shih (15).

2. Kinetic Properties of Alkali Cation Complexes

Thus far, the kinetics of alkali cation complexes have received rather limited attention despite their importance for the understanding of ion transport processes in organic or biological membranes (1) and of catalytic phenomena (18).

Naturally occurring antibiotic macrocycles such as valinomycin, monactin (Figure 1) and enniatin, have been

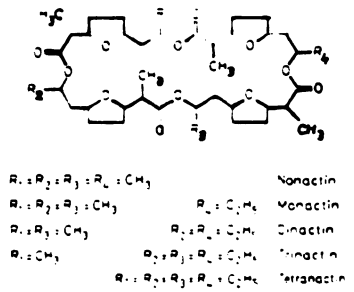

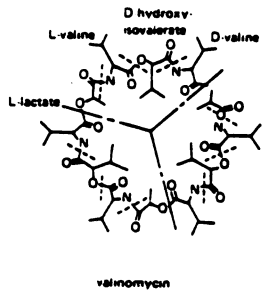

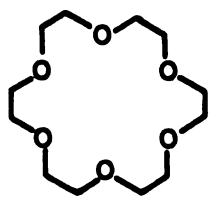

18-CROWN-6 (18C6)

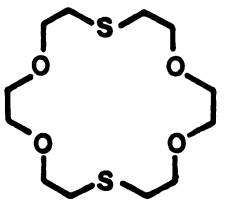

1,10-DITHIA-18C6 (DT 18C6)

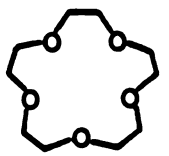

15-CROWN-5 (15C5)

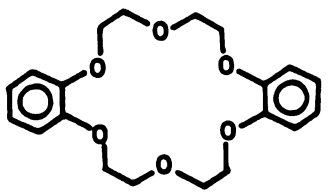

DIBENZO-18-CROWN-6 (DB18C6)

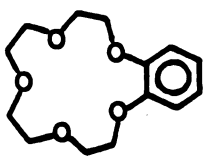

BENZO-15-CROWN-5 (B15C5)

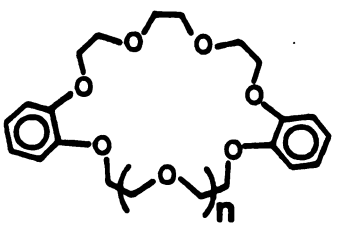

n=1 DB21C7
n=2 DB24C8
n=3 DB27C9

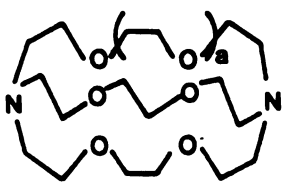

a=0 CRYPTAND 221 C221
a=1 CRYPTAND 222 C222

Figure 1. Structures of some naturally occurring and of some synthetic macrocyclic compounds.

better characterized in terms of their complexation kinetics than their synthetic counterparts (10,19) although most studies were performed only in methanol solutions because of problems of low solubility and low complex stability in water (16).

Grell et al. (17) investigated the formation of the M^+-valinomycin complexes in methanol, using an ultrasonic absorption method. The data indicated that the uncomplexed valinomycin undergoes some rapid conformational equilibria, and the mechanism could be simply described as shown below.

$$M^+(\text{solvated}) + L(\text{solvated}) \underset{k_{21}}{\overset{k_{12}}{\rightleftarrows}} M^+(\text{solvent})L \underset{k_{32}}{\overset{k_{23}}{\rightleftarrows}} ML^+ . \qquad (1)$$

A diffusion controlled bimolecular collision, between an open form of the ligand molecule and the solvated cation, is followed by the rate-determining conformational change of the ligand leading to the compact final structure of the M^+-valinomycin complex. Chock et al. (16) reported extensive relaxation studies on complex formation of macrocyclic (e.g., nonactin, monactin) and open chain (e.g., monensin) antibiotics with monovalent cations. Their data indicated the existence of a ligand conformational change prior to complexation:

$$L_1 \underset{k_{21}}{\overset{k_{12}}{\rightleftarrows}} L_2 \qquad (2)$$

$$L_2 + M^+ \underset{k_{32}}{\overset{k_{23}}{\rightleftarrows}} ML_2^+ \qquad (3)$$

The formation rates k_{23} approach the limits imposed for diffusion controlled processes. Degani (20) used ^{23}Na NMR to monitor the kinetics of complexation of Na^+ by the open chain antibiotic, monensin, in methanol. The dominant sodium exchange pathway was found to be the first order dissociative mechanism

$$Na^+ + \text{monensin} \underset{k_{32}}{\overset{k_{23}}{\rightleftarrows}} Na^+\text{-monensin} \qquad (4)$$

The small activation entropy for complexation ($\Delta S^{\neq}_{23}$ = -3.9 cal. $mol^{-1}deg^{-1}$) indicates a small conformational rearrangement of the monensin anion prior to complexation.

The kinetic parameters for the formation of some M^+-antibiotic complexes in MeOH are collected in Table 1. The formation rates (k_{23}) approach the limits imposed for diffusion controlled processes. It is clear from Table 1 that alkali metal complexes show wide variations in the dissociation rates (k_{32}). Indeed, for the cryptates, these rates may vary by as much as ten orders of magnitude (21).

Table 1. Kinetic Parameters for M^+-Antibiotic Complexes in MeOH at 25°C.

Ligand	Cation	K_f[a] $\underline{M}^{-1}$	k_{12}[b] $M^{-1}\ s^{-1}$	k_{21} s^{-1}	K_{12}[c] M^{-1}	k_{23}[d] $M^{-1}\ s^{-1}$	k_{32} s^{-1}	K_{23}[e] M^{-1}	Method
Monensin[f]	Na^+					6.3×10^7	63	1×10^6	^{23}Na NMR
Val[g]	Na^+	4.7	7×10^7	2×10^7	3.5	4×10^6	2×10^6	2	US[i]
Val[g]	K^+	3×10^4	4×10^8	1×10^8	4.0	1×10^7	1.3×10^3	7.7×10^3	US,TJ[j]
Val[g]	Rb^+	6.5×10^4							TJ
Val[g]	Cs^+	8×10^3							TJ
Val[g]	NH_4^+	47	1×10^9	1.5×10^8	6.5	2×10^6	2.5×10^5	8	US
Monactin[h]	Na^+	1.1×10^3							V.P.O.[k]
Monactin[h]	K^+	2.5×10^5							V.P.O.
Dinactin[h]	Na^+	1.1×10^3	6.5×10^7	1.1×10^8	0.6	1.3×10^8	4.3×10^4	3×10^3	US
Dinactin[h]	Na^+					1.6×10^8	5.4×10^4	3×10^3	TJ
Dinactin[h]	Cs^+	4.2×10^3	6.5×10^7	1.1×10^8	0.6	7.8×10^8	5.1×10^4	1.5×10^4	US
Trinactin[h]	Na^+	1.7×10^3			1.2	1.6×10^8	4.2×10^4	3.8×10^3	TJ

[a]Apparent stability constant determined by spectrophotometric titrations (in the presence of 0.1 $\underline{M}$ tetrabutylammonium perchlorate except for Val-Na^+ and Val-NH_4^+). [b]Units are s^{-1} for dinactin. [c]No units for dinactin and trinactin. $K_{12}=k_{12}/k_{21}$. [d]Units are s^{-1} for Val. [e]No units for Val. $K_{23}=k_{23}/k_{32}$. $\Delta H^{\neq}_{23}=-0.8$ kcal.mol^{-1}. $\Delta S^{\neq}_{we}=-3.9$ e.u. [f]See Equation (3) for notations. Data from Reference 20. [g]See Equation (1) for notations. Data from Reference 17. [h]See Equation (2) for notations. Data from Reference 22 (monactin) or 16. [i]US denotes ultrasonic absorption. [j]TJ denotes temperature jump relaxation. [k]VPO denotes vapor phase osmometry.

Here lies a major difficulty for doing kinetic studies of the alkali complexes. In general, as seen in Table 1, several techniques are needed to cover the large range of exchange rates exhibited by a given macrocycle complexing several alkali cations, even in a single solvent.

In a review published in 1978, Eyring (19) noted that kinetic studies of alkali metal complexation are impeded by such factors as high reaction rates, which render experiments difficult, and lack of color of the complexes which makes the spectrophotometric measurements rarely possible. However, in the sixties, Eigen and coworkers (22) had developed a series of chemical relaxation techniques in which a reaction mixture is perturbed by an external parameter (23). Some of these techniques are temperature-jump, pressure-jump, sound absorption and electric field-jump relaxation (for charged reaction partners). These methods cover the microsecond to the nanosecond range, but most of them require the detection of concentration changes by optical or conductometric techniques and are difficult in practice (23). At the same time, dynamic NMR (DNMR) spectroscopy was commonly thought to be limited to rate constants less than 10^4 s^{-1} (24). By 1970, the whole range of chemical exchange rates from the very slow reactions to the diffusion controlled ones could be explored by a variety of methods. Hence the necessity to use several delicate techniques, rather than the mere lack of these, may explain

the rarity of kinetic studies of alkali complexes.

More interesting qualitative features can be drawn from Table 1. A comparison of the values of K_f and k_{32} for different cations with one ligand (e.g., Val) indicates that the cation selectivity of the biological carriers arises mainly from differences in the dissociation rates. Also the high values of the formation rates imply that the substitution of the solvent molecules from the inner solvation sphere of M^+ is most likely accomplished by a stepwise process (22). These early findings by Diebler et al. (22) which are also pertinent to the synthetic multidentate macrocyclic compounds, were fully confirmed by the recent work of Chock et al. (16).

The structures of some crown-ethers and cryptands are illustrated in Figure 1. Kinetic studies on cryptate formation were reported more extensively than those for the crown ether complexes. The smaller decomplexation rates of the cryptates fall in the range observable by a number of techniques: cyclic voltammetry (25), stopped-flow conductometry (26-30), spectrophotometry (31), ^1H NMR (32) and alkali metal NMR (33-38). By contrast the rates of decomplexation of the crown complexes are usually high and are measurable only by ultrasonic absorption (39-42), temperature-jump (43,44) or dynamic NMR methods (36,38,45-50).

Even dynamic NMR does not easily lend itself to kinetic

measurements of macrocyclic complexes.

The major factor responsible for the scarcity of kinetic data for both crown complexes and cryptates is the small ^{1}H or ^{13}C NMR chemical shift of the ligand nuclei between the complexed and the uncomplexed forms (0.1 - 0.5 ppm for both nuclei, see References 45, 51, 52). Crown ethers containing benzene rings and those containing ester functions and pyridine moities are noticeable exceptions (45,53). Even if high fields are used, the coalescence temperatures are very low for the kinetically labile crown complexes, and the temperature range where the kinetic process occurs is narrow. This severely limits the accuracy of the results (54). With a few exceptions mentioned later (55), the Arrhenius activation energy (E_a) of decomplexation cannot be obtained. We are usually limited to the determination of the exchange rate and of the free energy of activation for decomplexation, $\Delta G_d^{\neq}$, at the coalescence temperature T_c (32,54). In many cases T_c falls below the liquid range of common solvents, and the use of the very low melting freons ($CHCl_2F/CHClF_2$ mixtures) becomes necessary (49-52). This obviously precludes the study of the solvent dependence of the complexation kinetics by ^{1}H or ^{13}C NMR.

Before we describe in some detail the crown kinetics, we mention briefly the characteristic features of the better known cryptate kinetics which have been discussed

by Lehn (6) and more recently by Cox *et al*. (30).

The effects of varying the cation, the anion, the cavity size, the metal oxidation state and the solvent upon the cryptate kinetics have been investigated (25-38). From the data summarized in Tables 2-4, the following picture emerges.

- The cation exchange between the free and the complexed site proceeds via the association-dissociation mechanism ($M^+ + L \rightleftarrows M^+L$) and not via the alternate bimolecular exchange. However, this is a very simplified description of the mechanism since it does not take into account the possible conformational changes of both the free and the complexed cryptand.

- The association rates in H_2O ($\sim 10^6$ $\underline{M}^{-1}$ s^{-1}) are much lower than the diffusion controlled rates ($\sim 10^{10}$ $\underline{M}^{-1}$ s^{-1}). This is in contrast with the high rates found (in MeOH) for macrocyclic or open chain antibiotics complexes with the alkali cations (16). The solvent effect on the formation rates is very strong since cryptates also form very rapidly in MeOH (Table 2), particularly in view of the relative rigidity of the ligands (30).

- Within a given solvent, variations in stability constants, whether resulting from changes in cation or ligand, are essentially reflected in the dissociation rates. For 221 and 222 cryptates the restriction due to the solvent may be lifted (30).

Table 2. Rate Constants and Activation Parameters for the Formation of Some Cryptates at 25°C.[a]

Cation	Cryptand	$\Delta G_f^{\neq}$[b] kcal.mol^{-1}	$\Delta H_f^{\neq}$[b] kcal.mol^{-1}	$\Delta S_f^{\neq}$[b] kcal.mol^{-1}
Li^+	C221	13.1[c]	15.6[c]	7.6[c]
	C221			
Na^+	C221	7.2[e]		
	C221	8.5	6.9[d]	-5.5[d]
	C222	8.9	8.7[d]	-0.5[d]
K^+	C221	7.6[e]		
	C222	8.9	9.3[d]	2.4[d]
Rb^+	C221			
	C222	8.6[e]		
Cs^+	C221			
	C222			

Table 2. Continued.

Cation	Cryptand	k_f (M^{-1} s^{-1})					
		H_2O	MeOH	EtOH	DMSO	DMF	PC
Li^+	C211	8.0×10^3	4.8×10^5	1.8×10^5	1.5×10^4	1.4×10^5	$<3 \times 10^7$
	C221		1.8×10^7	$\sim 3 \times 10^6$			
Na^+	C211	2.2×10^5	3.1×10^6	8.8×10^6	2×10^5		2.1×10^7
	C221	3.6×10^6	1.7×10^8	4.2×10^7	7.2×10^6	1.8×10^7	
	C222	1.2×10^6	2.7×10^8	1.1×10^8			
K^+	C221	1.8×10^7	3.8×10^8	4.9×10^7		$\sim 1.3 \times 10^7$	2.8×10^8
	C222	2.0×10^6	4.7×10^8	1.3×10^8	3.5×10^7	3.8×10^7	4.6×10^8
Rb^+	C221		4.1×10^8	8.3×10^7			8.0×10^7
	C222	3.1×10^6	7.6×10^8	1.7×10^8			1.8×10^8
Cs^+	C221		$\sim 5 \times 10^8$				$\sim 3.3 \times 10^7$
	C222		$\sim 9 \times 10^8$				$\sim 5 \times 10^6$

[a]Data from Reference 30 unless otherwise indicated. [b]The activation parameters are given in water. [c]Calculated from References 35 and 56. [d]Reference 25. [e]Calculated from k_f in H_2O.

Table 3. Dissociation Rates of Some Cryptates in Several Solvents at 25°C.[a]

Cation	Cryptand	k_d (s^{-1}) H_2O	MeOH	EtOH	DMSO	DMF
Li^+	C211	2.5×10^{-2}	4.4×10^{-3}	6.0×10^{-4}	2.3×10^{-2}[b]	1.3×10^{-2}[b]
	C221	1.2	7.5×10^{1}	1.3×10^{1}		
Na^+	C211	1.4×10^{2}	2.5	7.1×10^{-1}		
	C221	1.45×10	2.35×10^{-2}	2.6×10^{-3}	7.5×10^{-1}	2.5×10^{-1}
	C222	1.47×10^{2}[c]	2.87	3.0×10^{-1}		
K^+	C221	2.0×10^{3}	1.09	1.3×10^{-1}		∿2.6
	C222	7.5	1.8×10^{-2}	4.1×10^{-3}		
Rb^+	C221		7.5×10	1.1×10		
	C222	1.4×10^{2}	8.0×10^{-1}	9.2×10^{-2}		
Cs^+	C221		$\sim2.3\times10^{4}$	$\sim2\times10^{3}$		
	C222		$\sim4\times10^{4}$			9.0×10^{6}[d]
	C222B					

Table 1. Continued.

Table 3. Continued.

Cation	Cryptand	k_d (s^{-1}) PC	EDA	THF	PY	Formamide
Li^+	C211				1.2×10^{-4} [b]	7.4×10^{-3} [b]
	C221					
Na^+	C211					
	C221	$<10^{-2}$				
	C222	<1	165 [c]	8.0 [c]	1.1 [c]	
K^+	C221	3.7×10^{-2}				
	C222					
Rb^+	C221	7.5				
	C222	1.7×10^{-1}				
Cs^+	C221	$\sim 4 \times 10^2$				
	C222	$\sim 3 \times 10^2$				
	C222B	3.4×10^5 [d]				

[a] Data from Reference 30 unless otherwise specified. [b] Reference 35. [c] Reference 34. [d] Reference 37.

Table 4. Activation Parameters for the Dissociation of Some Cryptates at 25°C.

Cation	Cryptand	Solvent	E_a kcal. mol^{-1}	$\Delta G_d^{\neq}$ kcal. mol^{-1}	$\Delta H_d^{\neq}$ kcal. mol^{-1}	$\Delta S_d^{\neq}$ kcal.mol^{-1}	Method	Ref.
Li^+	C211	H_2O	21.3	20.6	20.7	+ 0.4	^{7}Li NMR	35
	C211	Py	19.6	22.7	19.0	-12.5	"	"
	C211	DMSO	16.1	19.7	15.5	-13.8	"	"
	C211	DMF	16.0	20.0	15.4	-15.5	"	"
	C211	Formamide	14.1	20.8	13.5	-22.8	"	"
	C221	Py	13.5	17.9	12.9	-14.9	"	"
Na^+	C221	H_2O	12.9	15.8	12.3	-11.7	C.V.[a]	25
	C222	H_2O	16.7	14.5	16.1	+ 5.3	^{23}Na NMR	34
	C222	Py	14.2	17.4	13.6	-12.6	"	"
	C222	THF	14.4	16.2	13.8	- 8.1	"	"
	C222	EDA	12.9	14.4	12.3	- 7.6	"	"
K^+	C222	H_2O	20.9	16.3	20.3	+13.9	C.V.[a]	25
Rb^+	C222	H_2O		14.5[b]			conduct.[c]	30
Cs^+	C222	DMF	13.5	8.0	12.9	+16.5	^{133}Cs NMR	37
	C222B	PC	14.9	9.9	14.3	+15.	^{133}Cs NMR	37

[a]C.V. denotes Cyclic Voltammetry. [b]Calculated from Reference 30.

[c]Conductometric method.

- The transition state for complex formation lies very close to the reactants. Apparently only a small amount of desolvation of the cation has occurred on formation of the transition state.

- The dissociation rates increase sharply with the donor ability of the solvent (this rule has a few exceptions (34)).

- The dissociation of the cryptates is acid catalyzed (26,29).

These general features were mostly found from rate data. Very few activation parameters have been reported, particularly in nonaqueous solvents (see Table 4 and Reference 57).

Kinetic studies of crown ether complexes have been rather sparse. They require a great deal of effort since none of the classical optical techniques are applicable.

Alkali metal NMR seems to offer a more general approach than ^{1}H or ^{13}C NMR to the investigation of the complexation kinetics (46). It can yield exchange rates in a large temperature range so that the activation energies may be obtained. When a quadrupolar nucleus, e.g., ^{23}Na and ^{39}K, is placed in an environment which does not have cubic symmetry, the line width of the NMR signal increases due to the asymmetry of the electric field at the nucleus (34). In general the lines are broader for the crown complexes than for the cryptates, sometimes by one order

of magnitude or more (47,58). This indicates that the electric field produced by the planar structure of the former is less symmetrical than that created by the tri-dimensional cavity of the latter. A noticeable exception to this behavior was found for the 2:1 (ligand:metal) "sandwich" crown complexes, e.g., $Na(15C5)_2$ (59), which give quite narrow signals because the cation is surrounded by a large number of binding sites not coplanar with it. Both the number and the position of these sites are essential in determining the alkali metal NMR line width. For example Kintzinger and Lehn (60), studying the sodium cryptates, found that the ^{23}Na quadrupole coupling constant (which determines the line width, see Chapter III) decreases as more and more oxygen atoms are disposed around the cation.

When the signals are relatively narrow, i.e., $\Delta\nu_{1/2} \lesssim$ 100 Hz, and if the cation exchange is slow, two separate alkali resonances are observed in solutions containing an excess of the salt. Only in this case can a complete line shape analysis be performed to obtain the kinetic parameters. This method was used by Ceraso et al. (33,34) for the Na^+-C222 cryptates and by Cahen et al. (35) for the Li^+-C211 and Li-C221 cryptates in various solvents (Table 4). Mei et al. (36,37) also applied this technique to the Cs^+C222 and Cs^+C222B cryptates in DMF and PC, respectively.

Unfortunately this technique fails for crown complexes

except for nuclei like ^{133}Cs which have a small quadrupole moment (61) and give narrow signals. Mei et al. (38) found by ^{133}Cs NMR small activation enthalpies (∿8 kcal. mol^{-1}), but large negative activation entropies (∿-14 e.u.) for the release of Cs^+ ion from the crowns 18C6 and DC18C6 in PY and PC respectively (Table 5). For the nuclei with large quadrupole moments, the line width of the bound site is usually broad and sometimes undetectable. In the last case only one apparent resonance is observed (46), but in some cases the exchange kinetics may still be deduced from the line shape analysis (62,63) with an approximate treatment (see details in Chapter III).

Ten years ago, Shchori et al. (46,47) studied by the above technique the kinetics of complexation of the Na^+ ion with DC18C6, DB18C6 and its derivatives in DME, DMF and MeOH solutions using ^{23}Na NMR (Table 5). They observed that the cation exchange proceeds via the dissociative mechanism, the same as that which is favored for the cryptates. Table 5 shows that the apparent activation energy E_a for the release of the Na^+ ion from DB18C6 and its derivatives is nearly independent of the solvent. The much smaller value of E_a, i.e., 8.3 kcal.mol^{-1}, found for DC18C6, compares well with the result of Mei et al. (38) for the Cs^+-DC18C6 complex in PC.

Shchori et al. (47) suggested that the energy barrier for the release of the Na^+ ion is determined by the energy

Table 5. Rate Constants and Activation Parameters for Some Crown Complexes at 25°C.[a]

Crown	Cation	Solvent	k_{23} M^{-1} s^{-1}	k'_{23}[b] $M^{-1}s^{-1}$	k_{32} s^{-1}	E_a kcal.	$\Delta H^{\neq}_{32}$ mol^{-1}	$\Delta S^{\neq}_{32}$ e.u.
15C5[c]	Na^+	H_2O		$2.4x10^8$	$4.8x10^7$			
	K^+	H_2O		$4.3x10^8$	$7.8x10^7$			
	Rb^+	H_2O		$4.6x10^8$	$1.2x10^8$			
18C6[d]	Li^+	H_2O	$\sim 8x10^7$		$\sim 6x10^7$			
	Na^+	H_2O	$2.2x10^8$		$3.4x10^7$			
	K^+	H_2O	$4.3x10^8$		$3.7x10^6$	10.8	10.2	3.1
	Rb^+	H_2O	$4.4x10^8$		$1.2x10^7$			
	Cs^+	H_2O	$4.3x10^8$		$4.4x10^7$			
	Cs^+	Py[e]			$9.5x10^3$	8.4	7.8	-14.2
DC18C6(IA)[e]	Cs^+	PC				8.5	7.9	-14.
DC18C6(IB)[f]	Na^+	MeOH				8.3		
DB18C6[f]	Na^+	MeOH	$3.2x10^8$		$1.4x10^4$	11.7		
	Na^+	DMF	$6x10^7$		$1x10^5$	12.6		
	Na^+	DME	$6.5x10^7$		$1.5x10^4$	13.3		
	K^+	MeOH			610(-34°C)	12.6		
NDB18C6[f]	Na^+	DMF				12.5		
AmDB18C6[f]	Na^+	DMF				13.1		

Table 5. Continued.

Crown	Cation	Solvent	k_{23} $M^{-1}s^{-1}$	k'^{b}_{23} $M^{-1}s^{-1}$	k_{32} s^{-1}	E_a kcal.	$\Delta H^{\neq}_{32}$ mol^{-1}	$\Delta S^{\neq}_{32}$ e.u.
DMDB18C6[g]	Na^+	THF-d8			3200(2°C)	12.5		
DB30C10[h]	Na^+	MeOH	$>1.6x10^7$		$>1.3x10^5$			
	K^+	MeOH	$6x10^8$		$1.6x10^4$			
	Rb^+	MeOH	$8x10^8$		$1.8x10^4$			
	Cs^+	MeOH	$8x10^8$		$4.7x10^4$			

[a]See equations 6 and 7 for notations.

[b]$k^1_{23} = k_{23}/(1+K_{21})$ with $K_{21} = k_{21}/k_{12}$ (see a).

[c]Reference 41.

[d]Reference 40. $\Delta H^{\neq}_{21}$ = 10.2 kcal. mol^{-1} and $\Delta S^{\neq}_{21}$ = 7.7 cal. mol^{-1}. deg^{-1}.

[e]Reference 38. IA stands for Isomer A.

[f]Reference 47. IB stands for Isomer B. NDB18C6 = dinitro-DB18C6. AmDB18C6 = diamino-DB18C6.

[g]Reference 55, k_{32} in $M^{-1}s^{-1}$ (see text). DMDB18C6 = dimethyl DB18C6.

[h]Reference 44.

required for a conformational rearrangement of the crown (47). In this case, the greater flexibility of DC18C6 as compared to DB18C6 could account for the lower E_a associated with this crown (47). This hypothesis was supported by other studies. In 1969, Wong et al. (55) reported a ^1H NMR kinetic study of the complexation of dimethyl-DB18C6 with the fluorenyl sodium ion pair (Na^+Fl^-) in THF-d8 solutions. This is a special case in which the fluorenyl ring currents cause large chemical shifts of the ligand protons, thus making possible the measurement of the activation energy E_a for the exchange process, which the authors assumed to be the bimolecular process shown below

$$Fl^-C^*Na^+ + C \rightleftarrows Fl^-CNa^+ + C^* \qquad (5)$$

The value of E_a, 12.5 kcal.mol^{-1}, closely matches that measured by Shchori for DB18C6 (Table 5). Similarly Shporer and Luz (48) measured by ^{39}K NMR an activation energy of 12.6 kcal.mol^{-1} for the release of the K^+ ion from DB18C6 in MeOH solution. However, they could not detect by ^{87}Rb NMR any kinetic process for the Rb^+-DB18C6 complex, the decomplexation rates being much faster. The results of Eyring et al. (42) were along the same lines. Using an ultrasonic absorption method these authors observed that in water the enthalpy of activation for a conformational rearrangement of 18C6 (vide infra) closely

resembles that required for the dissociation of the $K^+ \cdot 18C6$ complex (see Table 5). According to these authors the simplest conceivable mechanism consistent with the relaxation data is the two-step process represented by the equations

$$CR_1 \underset{k_{21}}{\overset{k_{12}}{\rightleftarrows}} CR_2 \qquad (6)$$

$$M^+ + CR_2 \underset{k_{32}}{\overset{k_{23}}{\rightleftarrows}} MCR_2^+ \qquad (7)$$

where CR_1 and CR_2 denote the unreactive and the reactive form of the crown respectively. This mechanism involves a fast ligand conformational change followed by a stepwise substitution of the coordinated solvent molecules by the CR_2 conformer of the crown. It is identical to the mechanism originally proposed by Chock for the complexation of various monovalent cations with DB30C10 (44). We have already encountered this two-step process in the case of antibiotic ionophores (16).

The above series of studies, except Wong's in THF-d8, are restricted to four solvents with high and similar donicities (34) so that the observed apparent constancy of E_a for DB18C6 and its derivatives may be coincidental, as Shchori _et al_. themselves (46) pointed out in their original paper. The same comment applies to 18C6 and to

DC18C6 complexes. In order to ascertain if the energy barrier to exchange is determined by the barrier for a conformational twist of a crown molecule, it would be necessary to have kinetic data for a single crown ether reacting with more than two metal ions, in several solvents over a substantial temperature range (42).

The various mechanisms proposed for the formation of crown complexes are worth being examined. Eyring et al. (39-42) carried out ultrasonic absorption studies of the conformational equilibrium of 18C6 and its complexation with Li^+, Na^+, K^+, Rb^+, Cs^+, Tl^+, Ag^+, NH_4^+ and Ca^{2+} ions as well as of 15C5 and its complexation with Na^+, K^+, Rb^+, Tl^+ and Ag^+ ions in aqueous solutions (Table 5). The equilibrium constants for the conformational change (Equation 5) are $K_{21} = k_{21}/k_{12} = (2 \pm 2)\ 10^{-2}$ for 18C6 and $K_{21} \leq 0.1$ for 15C5. This means that most of the free crowns are in the "reactive" CR_2 form and that the observed formation rates $k'_{23} = k_{23}/1 + K_{21}$ are very close to the actual ones k_{23}. For a given cation, the values of k_{23} are about the same for both crowns (Table 5) and also for the much larger and more flexible antibiotic macrocycles (Table 1). In contrast k_{32} increases for all the cations in going from 18C6 to 15C5, due presumably to the smaller ring size and the increased rigidity of 15C5 (41). As seen for the cryptates the selectivity arises mainly from differences in the decomplexation rates.

Turning back to the formation rates, Liesegang et al. (40) observed that for the crown complexes with the K^+, Rb^+ and Cs^+ ions, the k_{23} values level off at 4.3×10^8 $\underline{M}^{-1}$ s^{-1} whereas for the EDTA and nitrilotriacetic acid complexes they are in the order $K^+ < Rb^+ < Cs^+$. In addition, for the crowns the k_{23} values are all about one order of magnitude smaller than the corresponding specific solvent exchange rate constants k_{ex} (22). The first point suggests a ligand dependence of the complexation kinetics due, for example, to the presence of a second conformational change. Since typically the rate determining step in ligand substitution of an aquo ion is the rate of loss of primary coordinated water from the ion, the second point may indicate that binding the ligand to the ion will require the loss of more than one inner layer water molecule. Thus the kinetic evidence appears to suggest a mechanism more complex than the elementary two-step process previously considered.

Several conformational processes (in small crowns) with free energy barriers ranging from 6 to 10 $kcal.mol^{-1}$ were reported by Krane (49,50,66,67) who used low temperature ($\sim$-100°C $\rightarrow$ -160°C) DNMR techniques in $CHClF_2/CHFCl_2$ mixtures and in some other low melting solvents. The blocking of the inversion of the ether linkages either in the free ligand (50) or in the complex (49) provokes at low temperature a split of the peaks corresponding

to different sets of ligand nuclei. The NMR relaxation times T_1 also yield conformational information. Fedarko (68) detected by this method segmental motion in the free DC18C6 and DB18C6 molecules.

Many factors other than the donor ability of the solvent and the rigidity of the crown may affect the kinetic parameters for crown complexes. Among these factors are the dielectric constant of the solvent, the structure of the anion and that of the cation, the solvation state of the ion pair, the ligand solvation (H-bonding, etc.).

Since all the alkali cations have the same "noble gas" electronic structure, we must include in this discussion some studies concerned with organic cation - crown ether complexes (M^+_{org} C). De Jong et al. (51,69,70), using a DNMR method with the cation protons, found the activation energy E_a for the release of t-$BuNH_3^+(PF_6^-)$ from 18C6 in $CDCl_3$ to be 18 ± 1 kcal.mol^{-1}. This high value is unexpected since most reported values of E_a for alkali crown complexes (M^+C) fall in the range of 10-14 kcal.mol^{-1} (46-48,55). Indeed it resembles the E_a values measured for the cryptates (Table 4). No explanation was proposed by the authors. Instead of the dissociative mechanism which applies to most M^+C complexes, the bimolecular process (Equation 4) was found to be predominant. Both the structure of the cation and the low polarity of the solvent may be responsible for these facts. Recently

Krane et al. (52) studied by ^{13}C DNMR the ring size effect on the decomplexation barrier of crown complexes with aryl diazonium tetrafluoroborate salt in $CHCl_2F$. The preferred host for this salt is the crown ether 21C7 ($\Delta G_d^{\neq}$ = 11.1 kcal.mol^{-1} at T_c = -52°C). For 18C6, $\Delta G_d^{\neq}$ = 10.1 kcal.mol^{-1} at T_c = -75°C. A comparison of these values with other data obtained at 25°C is impossible since $\Delta S_d^{\neq}$ is unknown. Once again the chemical shift difference between the free and the complexed form of the ligands is too small to permit the measurement of the activation energy E_a. In general the organic cations (51,71) as well as Ag^+ and Tl^+ (40,41) complex much faster with 18C6 than do the alkali cations (40,41). For these cations the association rates in $CDCl_3$ or CD_2Cl_2 (10^9 = 10^{10} $\underline{M}^{-1}$ s^{-1}) are characteristic of a diffusion controlled process (51,71). Thus the orbitals of the metal ions appear to play as decisive a role in the complexation kinetics as do dissimilarities in the ligands (19).

In low dielectric media, the cation-anion interactions may also affect the exchange rates. If the forward and reverse reaction rates vary in a significantly different extent, the resulting thermodynamic parameters will also change. Consequently a different selectivity order can be observed in a polar solvent and in a low polarity medium such as THF or THP. For example Wong et al. (55) found the stability sequence with dimethyl-DB18C6 in THF to be

$Na^+ > K^+ > Cs^+ > Li^+$ whereas both Pedersen (4) and Izatt *et al*. (10) found an affinity order in water of $K^+ > Cs^+ > Na^+ > Li^+$ for DC18C6. The polarity of the solvent, rather than the difference in the ligand molecules was found to be responsible for this effect (55,72). Ionic association can give either contact or solvent-separated ion pairs (73), and contact ion pairs can be externally solvated or complexed (74). Furthermore, complexation by the crowns induces the formation of another kind of species, namely the ligand-separated ion pairs (74). Smid *et al*. (72,74) extensively studied the complexation of alkali metal fluorenyl salts (Fl^-M^+) with various small crowns (C) in THF and THP by electronic spectroscopy. They obtained the equilibrium constants for the formation of externally complexed ion pairs (Fl^-M^+C) and ligand-separated ion pairs (Fl^-CM^+). In this particular case where only contact ion pairs exist in the absence of crown at 25°C, the following equilibria were considered

$$Fl^-M^+ + C \rightleftarrows Fl^-M^+C \qquad K_1 \qquad (8)$$

$$Fl^-M^+ + C \rightleftarrows Fl^-CM^+ \qquad K_2 = K_1K_3 \qquad (9)$$

$$Fl^-M^+C \rightleftarrows Fl^-CM^+ \qquad K_3 \qquad (10)$$

$$Fl^-M^+C + C \rightleftarrows Fl^-CM^+C \qquad K_4 \qquad (11)$$

The first type of ion pair prevails over the second one, i.e., $K_1 > K_2$, in the less polar solvent THP, as it does for potassium salts in both solvents due probably to the weaker specific solvation of K^+ as compared to Na^+ or Li^+. In general the formation of an Fl^-CM^+ complex from Fl^-M^+C is exothermic and so is the formation of Fl^-SM^+ from Fl^-M^+ where S is a cyclic ether solvent molecule (72). Therefore a temperature decrease results in an increase in the concentration of both the solvent-separated and the ligand-separated ion pairs. This also has a profound effect on the selectivity order (72). The kinetic origin of the variations seen in the thermodynamic parameters is unknown.

Considering the large number of species present in such systems, i.e., contact, solvent and ligand-separated ion pairs, 1:1 and 2:1 ($C:M^+$) complexes, solvated and complexed ion pairs, ion triplets . . ., and the necessity of taking into account the temperature dependence of the concentration of each species, the treatment of data obtained by any technique may be extremely complicated, as shown by the work of Khazaeli (75). Usually a single technique cannot "see" all the species present. Electronic spectroscopy, whenever possible, and NMR spectroscopy of several nuclei, as well as electrical conductance and electrochemical techniques must all be used to assemble the puzzle.

The solvation state of the ion pairs and the kinetic parameters may be altered by changing the solvent, the

temperature and, last but not least, the anion. A striking example of the anion effect was recently reported by Lin and Popov (59). They studied by ^{23}Na NMR the exchange of the Na^+ ion between its solvated site and its 18C6 complex in THF and 1,3-dioxolane, using the salts $NaBPh_4$, $NaClO_4$ and NaI. With $NaBPh_4$ the exchange is slow at 25°C in both ethereal solvents, whereas it is fast with the other salts. The coalescence temperature decreases by about 60°C when BPh_4^- is replaced by ClO_4^- or I^-. This effect has not been fully rationalized yet, but it is most likely related to the fact that, in THF at 25°C, $NaBPh_4$ is a solvent-separated ion pair (76) whereas $NaClO_4$ is a contact ion pair (76,77).

Cation-anion interactions can drastically affect the rates of the decomplexation step even for cryptates. For example Lehn et al. (32) observed that the coalescence temperature of the ^1H NMR peaks of C222 and $TlC222^+$ decreases from +39°C to -6°C upon replacement of TlCl by $TlNO_3$. Yee et al. (25) found a strong association between the tripositive Eu^{3+} and Yb^{3+} cryptates and small anions F^- and OH^-. They could not decide if the cation-anion interaction is direct or not, but the presence of significant concentrations of the OH^- and F^- ions had a marked accelerating effect on the dissociation. In their detailed IR study of the nitrate ion structure in the system $Na^+ \cdot C221\ NO_3^-$ (in DMSO-d6 solutions), Edgell et al. (72)

detected two NO_3^- sites. One of them was attributed to the solvent-separated ion pair. The second site was tentatively assigned to a "close ion pair" in which the NO_3^- would interact with the sodium cation through the strands of the cryptand molecule having replaced one or more solvent molecules.

Crystallographic studies of solid macrocyclic complexes have shown that the cation is either coordinated to one macrocyclic ligand only (79,80) or to the ligand plus (i) one anion (81,82) or (ii) two anions (83) or (iii) a water molecule which in turn is H-bonded to an anion (84,85) or (iv) a second ligand molecule (86) or (v) two solvent molecules and two anions alternatively (87). This list is not exhaustive. X-ray crystallographic data, although very useful, indicate rather than demonstrate the geometrical structure of the ion pairs in solution (88).

In summary, the kinetics are better understood for cryptates than for crown complexes. Fast rates and ion pairing effects for the latter drastically increase the complexity of the data collection and the data interpretation, respectively. For both systems the actual mechanisms might be much more involved than the apparent ones. A clear picture of the mechanisms will not emerge before the conformational equilibria are fully understood.

C. Conformation and Solvation of Cryptands and Cryptates

A recent compilation of thermodynamic data on macrocyclic complexes (10) reveals that most cryptates and crown complexes are enthalpy stabilized and entropy destabilized. Only a few cryptates in water do not follow this rule (56). In nonaqueous media the release of solvent molecules from the cation and the free ligand upon complexation introduces a favorable entropy term. On the other hand, the conformational contribution to the entropy of complexation is negative since the number of conformations available to the ligand decreases upon complex formation (89). This effect is important enough to overcome the entropy increase associated with desolvation of the ion and the free ligand.

Cryptands exhibit interesting conformational properties. Like the macrobicyclic diamines of Simmons and Park (90, 91), cryptands exist as equilibrium mixtures of three conformational isomers (6). These forms, which are denoted as in-in, in-out, and out-out, depending on the respective positions of the bridgehead nitrogen lone pairs inside or outside the cryptand cavity (Figure 2), may interconvert rapidly via nitrogen inversion.

It has been shown (6,92) that in the solid state the cryptand C222 is in the in-in form whether it is free or complexed. In solution the situation is far from clear for the free ligand but the in-in form is strongly favored

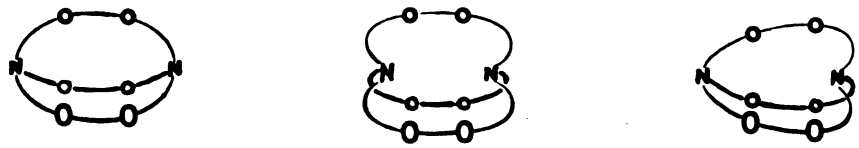

out-out in-in out-in

Figure 2. Three possible forms of Cryptand 222.

in the complex since it allows both nitrogen to contribute to the complex stability. The formation of cryptates brings about an increase in the rigidity of the ligand which results in the non-equivalence of the two protons of certain CH_2 groups of the non symmetrical ligands, e.g., C221 (93).

Crystal structures of C222.M^+ with cations of increasing sizes (M^+ = Na^+ (94), K^+ (95) and Cs^+ (96)) show a progressive opening up of the C222 cavity with torsion of the ligand around the N...N axis. For a given molecular cavity the larger the cation size, the larger is the extent of the overlap between the outer orbitals of the cation and those of the ligand binding sites, and the larger the downfield shift observed by alkali metal NMR. For the tight fitting inclusive C222•Cs^+ complex, Kauffmann et al. (97) reported a ^{133}Cs NMR chemical shift of +244 ppm (vs aqueous Cs^+). Conformational information may be obtained

by ^1H NMR; however, except for the highly symmetrical C222, the complexity of the patterns and superimposition of the signals render the analysis difficult (93). Knöchel et al. (98) found a relationship between the donicity of the solvent and the chemical shift of the N-$C\underline{H}_2$ protons of C222. According to them the position of the signal of the N-CH_2 groups allows an estimation of the conformation of the cryptand in solution. However their data are restricted to only three solvents, $CDCl_3$, CD_3OD and D_2O, and this precludes a completely general interpretation.

Ligand solvation and ligand conformation are intimately related. For example, strong ligand-solvent interactions may limit the number of conformations available to the ligand. It has been stated that the solvation of cryptands and cryptates is small or at least does not change very much from solvent to solvent when compared with the ionic solvation (99). Indeed several authors even proposed that cryptates might provide a new method for obtaining single-ion enthalpies (ΔH_t) and free energies (ΔG_t) of transfer (99-101). However in 1977 Abraham et al. (102) found by direct calorimetric measurements that the enthalpy of transfer of C222 from water to methanol, ${}^{M}_{W}\Delta H(C222)$, is +13.9 kcal.mol^{-1}. This represents about three times (in absolute values) the corresponding ΔH_t for Na^+ and K^+ ions (-4.9 and -4.5 kcal.mol^{-1}, respectively). The same

authors showed that the extrathermodynamic assumption [ΔH_t (C222.M^+) = 0] does not hold for enthalpies of transfer in the H_2O-MeOH system (103-105). The very large ${}^{M}_{W}\Delta H_t$ (C222) is almost totally compensated by the entropy of transfer [${}^{M}_{W}\Delta S_t$ (C222) = 43 cal.mol^{-1}.deg^{-1}] to give ${}^{M}_{W}\Delta G_t$ (C222) = 1.1 kcal.mol^{-1}. The large increase in entropy indicates desolvation of C222 and/or an increase in the number of conformations available to the ligand. Besides, the substantial variation in ${}^{M}_{W}\Delta G_t$ (C222.M^+) with the central ion M^+ indicates that the central ion is not shielded from the environment (103-105).

Water and methanol form strong hydrogen bonds with the two amine nitrogens and, to a lesser extent, with the ether oxygens of an uncomplexed cryptand. The hydrogen bonding is, at best, considerably weaker in a cryptate in which the ether oxygens and the two nitrogens are bonded to the metal ion (106). Between dipolar aprotic solvents S_1 and S_2, the transfer activity coefficients ${}^{S_1}\gamma^{S_2}$ of C222·M^+ with M^+ = Na^+, K^+, Tl^+ and Ag^+, are almost equal to that of the cryptand, but due to H-bonding this equality does not hold if S_1 is methanol (105).

D. Interaction of Conventional Ligands with the Alkali Cations

In view of the rapid expansion of the coordination chemistry of alkali and alkaline earth cations, recent

studies of the alkali complexes with the non macrocyclic ligands are rather sparse, although as a review article by Poonia and Bajaj (13) shows, some attempts to study such complexes have been made even in the pre-macrocycle days (107). In most cases, however, such work was directed towards the isolation of new adducts of the alkali salts with a variety of chelating or non chelating ligands and anions (108). For example the first solid alkali complex of 2,2'-bipyridine (BP) seems to be $(K \cdot BP)^{+}Ph_4B^{-}$, recently isolated by Grillone and Nocilla (109). However, few attempts have been made to study the existence and the stability of such adducts in solutions, and particularly in nonaqueous solutions.

In general alkali cations show a greater tendency to complex with O-donor than with N-donor ligands (110); alkali complexes of 1,10-phenanthroline have received the most attention (107-112). By contrast, 2,2'-bipyridine does not seem to exhibit much complexing ability towards these cations (111,113).

E. Nuclear Magnetic Resonance in Molten Salts

Molten salts differ from conventional nonaqueous solvents in two major respects; high melting point and strong ionic character (114). The latter confers high electrical and thermal conductivity and promotes the solubilization of ionic solutes, e.g., metal oxides. In general molten

salts are better and more versatile solvents than water.

Although molten salts have been studied mostly by electrochemical methods (115-120) it was felt as early as 1958 that NMR techniques might offer valuable information with regard to identifying the species present and determining the small structural changes or the changes in the chemical bonding which accompany a variation in the composition of the melt. Due to the favorable properties of the ^{205}Tl nucleus (spin 1/2, high sensitivity, large chemical shift range), Rowland and Bromberg (121) followed by Hafner and Nachtrieb (122,123) studied solid and molten thallium salts. Except for $Tl(ClO_4)_3$, the ^{205}Tl NMR shift on fusion is in the paramagnetic direction, and the magnitude of the shift is less than the difference between that of the melt and that of an aqueous thallous solution. The direction of the shift was accounted for by overlap effects due to a decrease in the cation-anion distance (122). The authors (122,123) showed that NMR provides a valuable means of exploring deviations from purely Coulombic interactions between ions. The degree of covalency in the cation-anion bond was found to increase with temperature. In Tl^+X^--M^+X^- (M^+ = alkali cation) mixtures, the ^{205}Tl shift varies linearly with the mole fraction of M^+X^- added, and the direction of the shift depends upon the radius of the alkali cation (123). In 1973 Harold-Smith studied the structure of the alkali nitrates by measuring the

spin-lattice relaxation time T_1 of ^{23}Na in $NaNO_3$ (124) and of ^{7}Li in $LiNO_3$ and Li/KNO_3 mixtures of various compositions (125). The quasi-lattice, random-flight model (126,127), which assumes the existence of a pseudo lattice for the liquid, was found to apply to molten $NaNO_3$. Concerning the mixtures, the average Li^+-NO_3^- distance decreases whereas the electric field gradient at the lithium nucleus increases with increasing mole fraction of KNO_3 (125).

Alkali halides and nitrates are typical ionic salts (128). At the other extreme are compounds such as aluminum chloride which undergo only slight dissociation into ions and in which more complex bonding forces operate (115,116). The first attempt to apply NMR methods to the study of the chloroaluminates ($AlCl_3$ - alkali halide mixtures) seems to have been that of Anders and Plambeck (129). These authors measured the ^{23}Na, ^{27}Al and ^{35}Cl line widths in the low melting ternary $AlCl_3$-NaCl-KCl system. The ^{27}Al line width increases with added $AlCl_3$ but the ^{23}Na line remains sharp (9 Hz). In addition there was no detectable ^{23}Na or ^{27}Al chemical shift with changing stoichiometry. The authors concluded that fused alkali chloroaluminates of $Al_2Cl_7^-$ stoichiometry are essentially ionic, the entities in the melt being primarily M^+ and $Al_2Cl_7^-$. The species present in chloroaluminate melts (Cl^-, $AlCl_4^-$, $Al_2Cl_7^-$, $Al_3Cl_{10}^-$, Al_2Cl_6,...) depend on the

composition and are still under debate at the present time (130). Recent developments in molten salt research include ^{1}H and ^{13}C NMR studies of $AlCl_3$-based fused salts that are molten at or near room temperature (131,132).

F. Potassium 39 Nuclear Magnetic Resonance

Three potassium nuclei, ^{39}K, ^{40}K and ^{41}K, possess a magnetic moment (133). Potassium-39 is the most sensitive as well as the most abundant in nature (93.1%). However, the sensitivity of this nucleus is still about 200 times lower than that of the ^{23}Na nucleus, i.e., 5×10^{-4} vs 9.3×10^{-2} with respect to ^{1}H at constant field (61). Consequently ^{39}K NMR studies have been rather sparse even after the development of the Fourier Transform NMR technique and the availability of high field superconducting magnets. Apart from the sensitivity, the general features of ^{39}K NMR are quite comparable to those of ^{23}Na NMR which have been described by several authors (61,34) and which were recently reviewed (57). Several theories have been proposed to calculate the ^{23}Na chemical shifts and quadrupolar coupling constants and to relate these two quantities (61,134). Given the similarities of the two nuclei, only the main features of ^{39}K NMR are mentioned here. For the ^{39}K nucleus:

- The resonance frequency is low (ν = 2.8 MHz in a field of 1.4 Tesla).

- ^{39}K has a spin of 3/2 and it possesses a quadrupole moment of 0.07b (61), smaller than that of ^{23}Na (0.10b). This is a sizeable difference when considering that the linewidths vary as the square of the quadrupole moment.

- The dominant relaxation mechanism is quadrupolar and occurs through molecular reorientation of the solvent.

- The natural line width (narrowest one observed thus far in aqueous solutions) is about 6 Hz (133).

- In solution the chemical shifts range from about -20 ppm to +20 ppm with respect to K^+ at infinite dilution in water (15,135).

- Changes in the paramagnetic screening constant, σ_p, are much larger than changes in the diamagnetic screening constant, σ_d, and thus dominate the chemical shift (61).

- According to Kondo and Yamashita's theory (136), the most important contribution to the chemical shift arises from the overlap repulsive forces between the 3p orbitals of K^+ and the outer s and p orbitals of the neighboring anion(s), ligand(s) and solvent molecule(s).

- The extreme narrowing approximation (137), <u>i.e.</u>, $\omega\tau_c << 1$, where ω is the resonance frequency of the ^{39}K nucleus and τ_c is the correlation time for solvent reorientation, is valid down to the melting point of common

solvents since ω is very small. This implies $T_1 = T_2$.

- The resonance line shape is Lorentzian (FT of an exponential function) and the line width $\Delta\nu_{1/2}$ (full width at half height) equals $1/\pi T_2$.

- Since the magnetogyric ratio γ is small, the contribution from the magnetic field inhomogeneities to the observed line width, $\gamma\Delta H/2\pi$, is small and may often be neglected (see details in the experimental part of Chapter I).

An extensive review of the ^{39}K NMR studies reported up to early 1978 can be found in the Ph.D. thesis of J. S. Shih (15). Very few papers have appeared since then (138-140). A brief review of the ^{39}K NMR work is given below.

The ^{39}K chemical shifts of several potassium salts in aqueous solutions were measured by Deverell and Richards (141) and by Bloor and Kidd (142) who used relatively low fields (<1.3 Tesla) and continuous wave (CW) techniques. The shifts were found to be strongly dependent on the concentration of the potassium salt and the nature of the counterion. Shporer and Luz (48) studied by ^{39}K NMR the kinetics of complexation of K^+ by DB18C6 in methanol. They were using high concentrations (0.5 M), very high field (6.0 Tesla) and extensive signal averaging. Even with these conditions, T_1 measurements were still difficult (48).

Damadian and coworkers (139,143-147) reported a series of T_1 and T_2 measurements in inorganic solutions and ion exchanger resins (144,145) as well as in bacteria (143,144), animal tissues (144-146) and cancer tissues (147). In biological systems, T_1 and T_2 are much shorter than T_1 and T_2 for free K^+ in solution and approach the very short values seen for ^{39}K adsorbed on ion exchanger resins. The authors inferred from this fact that, in cells, K^+ ion is mostly associated with charged groups on macromolecules. For normal tissues the ^{39}K spin lattice relaxation time T_1 is on the average 24% longer than for cancerous tissues (147). Oscillatory T_1 decays found in fast growing tissues (cancer) contrast with smooth exponential T_1 decays observed in most other tissues.

Shih and Popov (135) studied the variation of the ^{39}K chemical shift as a function of concentration and counter-ion in nonaqueous solvents and later extended their ^{39}K NMR investigations to K^+ cryptates (138). The exchange between the solvated and the complexed K^+ was found to be slow (on the NMR time scale) for C222 and C221 but fast for C211. The chemical shift of the C222.K^+ complex is independent of the solvent, thus indicating that K^+ is isolated from the environment by C222. By contrast the ^{39}K signal of C221.K^+ is found in a range of about 3 ppm and on the average appears about 12 ppm downfield from the signal of C222.K^+. Thus K^+ is more tightly embedded in

the C221 than in the C222 cavity but it still can interact with the surrounding solvent molecules.

Until now, very little use has been made of the differences in ^{39}K line width between the solvated and the complexed K^+.

CHAPTER II

EXPERIMENTAL PART

A. Salt and Ligand Purification

Potassium salts were of reagent grade quality. Potassium hexafluoroarsenate (Alfa Inorganics) and potassium hexafluorophosphate (Pfaltz and Bauer) were recrystallized from distilled water. Potassium thiocyanate (Matheson, Coleman and Bell, MCB) and potassium iodide (Mallinckrodt) were recrystallized from water-acetone mixtures. All four salts were dried under vacuum at 110°C for at least one day.

The macrocyclic polyether 18-crown-6 (18C6, Aldrich) was recrystallized from acetonitrile (166) and dried under vacuum at 25°C for 24 hours. The dried 18C6 melted at 36-37°C (lit. m.p. 36.5-38.0°C (167), 39-40°C (4b)). Dibenzo-21-crown-7 (DB21C7, Parish) was obtained from G. Rounaghi (168). Dibenzo-24-crown-8 (DB24C8, PCR Research Chemicals) and Dibenzo-27-crown-9 (DB27C9, Parish) were recrystallized from normal heptane (Mallinckrodt) and their melting points were found to be 102-103°C (lit. 103-104°C (156)) and 107-108°C (lit. 106-107.5°C (156)), respectively. As noted by Pedersen (156), the true value of the m.p. of DB24C8 determined by him is 103-104°C (156) and not 113-114°C (4b) as originally published. Thus the values quoted in References 168 and 169 are probably wrong.

The above three large crowns were dried under vacuum at 60°C for 24 hours. Diaza-18-crown-6 (DA18C6 or [22], Merck) was recrystallized from heptane and dried under vacuum at 25°C. Cryptand 221 (C221, Merck) was dried under vacuum at 25°C for two days. The "conventional" ligand 2,2'-bipyridine (G. F. Smith) was dried under vacuum at 25°C (m.p. 70°C). The purity of all ligands was checked by ^{13}C NMR.

B. Solvent Purification and Sample Preparation

Nitromethane (Mallinckrodt or MCB), nitroethane (City Chemical Corp.), pyridine, tetramethylguanidine (Eastman), dimethylformamide (Mallinckrodt), dimethylsulfoxide (Fisher), propylene carbonate (Aldrich) and formamide (Fisher) were refluxed over calcium hydride under reduced pressure for 12 to 24 hours and then fractionally distilled. Acetonitrile (Mallinckrodt), 1,3-dioxolane (Aldrich) and dichloromethane (Drake brothers) were refluxed over calcium hydride for 12 to 24 hours and then fractionally distilled. 1-Nitropropane (City Chemical Corp.) and toluene (Fisher) were refluxed over phosphorus pentoxide (Fisher) under reduced pressure for 3 hours in a Bantamware apparatus and then fractionally distilled. The same procedure was used for 1,4-dioxane (Baker) and anisole (Aldrich) except for the drying agent which was NaOH (pellets) and barium oxide (Fisher), respectively. Methanol (Mallinckrodt)

was refluxed over Mg turnings and iodine for 12 to 24 hours and then fractionally distilled. Acetone (Mallinckrodt) was purified in the same way but with Drierite as the drying agent. Tetrahydrofuran (MCB) was dried over CaH_2, refluxed over potassium and benzophenone and fractionally distilled. Methyl acetate was washed with a saturated aqueous solution of NaCl, dried over anhydrous $MgSO_4$ and distilled as described by Riddick (170). Ethylene glycol was refluxed over 3Å molecular sieves and then distilled. The Bantamware distillation apparatus was used when the volume of solvent to be distilled did not exceed 70 ml.

All solvents were further dried for 4-12 h over freshly activated 3Å or 4Å molecular sieves. These sieves were washed with distilled water and dried at 110°C for several days. After further heating at 500°C under nitrogen atmosphere for 24 hours, they were stored in a dry box. Solvents such as MeOH (171), DMSO, pyridine and even acetone decompose and turn yellow after a prolonged standing over molecular sieves. The water content of solvents, except acetone, was checked by automatic Karl Fischer titration with an Aquatest II (Photovolt) and was found to be always below 100 ppm. The purity of solvents was checked by ^{13}C NMR.

The deuterated solvents acetone-d_6 (Stohler Isotope Chemicals, SIC), methanol-d_4 (SIC or Aldrich Gold Label)

and THF-d_8 (Aldrich Gold Label) were used directly from the manufacturers sealed vials (45). Chloroform-d (Aldrich Gold Label) and D_2O (SIC) were used as received and methyl iodide (Mallinckrodt) was distilled.

All samples were prepared in a dry box under nitrogen atmosphere. For kinetics studies it is essential to minimize errors in the ligand/salt ratios due to transfers and successive dilutions. In this case each sample was prepared by weighing the desired amounts of ligand and salt in the same 10 ml or 5 ml volumetric flask and immediately transferred to the dry box for subsequent manipulation. In general for mole ratio studies by ^{39}K NMR (or ^{13}C NMR), samples were prepared by diluting appropriate amounts of ligand (or salt) volumetrically with stock solutions of salt (or ligand).

C. Instrumental Measurements and Data Handling

1. Potassium 39 NMR

a. Instrument - Potassium-39 NMR measurements were obtained with a Bruker WH-180 spectrometer operating at a field of 42.3 kG and a frequency of 8.403 MHz in the pulsed Fourier Transform mode. A Nicolet 1180 computer was used to carry out the time averaging of spectra and the Fourier transformation of the data. The low frequency probe has a core diameter of 20 mm.

b. Reference and Corrections - A saturated solution (∿31 molal) of KNO_2 in D_2O at 24°C was used as an external standard (133). The reported chemical shifts are referenced to an aqueous potassium salt solution at infinite dilution ($\delta_{\infty dil} = \delta_{standard} + 3.0$). Due to the difference in deuterium resonance frequency between pure D_2O and D_2O in the standard solution, the observed chemical shift is given by the expression

$$\delta_{obs} = \delta_{standard} + (2.4 \pm 0.1) \qquad (1)$$

where δ is in ppm.

The reported chemical shifts are corrected for the differences in bulk diamagnetic susceptibilities between sample and reference solvent according to the equation of Live and Chan (173) for a cylindrical sample placed in a magnetic field parallel to the main axis of the sample

$$\delta_{corr} = \delta_{obs} - \frac{4\pi}{3} (K_v^{ref} - K_v^{sample}) \qquad (2)$$

where K_v^{ref} and K_v^{sample} are the unitless volumetric susceptibilities (174) of the reference and sample solvent respectively and δ_{corr} and δ_{obs} are the corrected and observed chemical shifts, respectively. It was shown by Templeman and Van Geet (191) that low salt concentrations,

such as were used in this study, the contribution of the added salt to the volumetric susceptibility of the solutions can be neglected. The values of the corrections for various solvents with respect to water are given in Table 6. The paramagnetic shifts from the reference (downfield shifts) are designated as positive. Live and Chan (173) used the opposite convention. Hence the above formula for the correction is different from theirs. The chemical shifts are given in ppm.

c. Field-Frequency Lock and Temperature Control -

(c1) Kinetics Studies - Spinning 20 mm o.d. sample tubes (Wilmad Glass Co.) were used whenever deuterated solvents were available. Each sample (10 ml) contained 2 ml of deuterated solvent which served as an internal lock. 1,3-Dioxolane solutions (5 ml) were contained in 15 mm O.D. tubes (Wilmad) and coaxially mounted with a 20 mm O.D. tube containing Acetone-d_6 as lock, as recommended by Brownstein *et al*. (175). For each sample, the field was locked when the sample temperature was close to the middle of the temperature range studied.

Temperature was controlled with a Bruker B-ST 100/700 temperature control unit and measured to within ±1°C with a calibrated Doric digital thermocouple situated in the probe about 1 cm below the sample. A large flow of N_2

Table 6. Key Solvent Properties and Correction for Magnetic Susceptibility on WH-180.

Solvent	Dielectric Constant	Dipole Moment (D)	Gutmann Donor Number[a]	Volume Suscept. $-K\times10^6$	Correction on WH-180 (ppm)
Pyridine	12.4	2.23	33.1	0.612	-0.452
Water	78.5	1.87	18.0 (33.0)[b]	0.720	0.000
N,N-dimethylformamide	36.7	3.86	26.6	0.573	-0.616
Methanol	32.7	1.70	25.7[b]	0.515	-0.858
Tetrahydrofuran	7.6	1.63	20.0	0.613	-0.448
Acetone	20.7	2.88	17.0	0.460	-1.090
Propylene Carbonate	65.0	5.2	15.1	0.634	-0.360
Acetonitrile	37.5	3.96	14.1	0.534	-0.780
Nitromethane	35.9	3.44	2.7	0.391	-1.378

[a]References 149, 150.

[b]Predicted by ^{23}Na NMR (164).

gas and a spin rate of 10-12 Hz were maintained in order to minimize the temperature gradient across the sample.

(c2) Other Studies - Samples (5 or 10 ml) were contained in 15 mm or 20 mm tubes, depending upon whether D_2O or another deuterated solvent was used as lock. In the latter case the chemical shifts may not be directly compared since the magnetic field has to be adjusted for lock purposes in going from one solvent to another. This arises from the fact that the ^2H resonance frequency varies with the solvent (and also with the temperature). For example at 25°C we found

$$\delta_{\text{Acetone-}d_6} = \delta_{D_2O} + 2.2 \qquad (3)$$

where the subscripts denote the lock solvents. The corrections are about 2 ppm for $C\underline{D}_3OD$ and 2.8 ppm for CD_3CN. These corrections were not systematically applied in the studies at variable temperature.

d. <u>Line Width Measurements</u> - Line width calibrations were made with a 0.25 <u>M</u> solution of KI in a 3:1 (vol.) H_2O-D_2O mixture. The half height line width ($\Delta\nu_{1/2}$) of the ^{39}K NMR signal (25 scans, SW = 5000 Hz, 32 K of memory) of this solution was 7.5 ± 0.3 Hz (corresponding to $T_2 = 1/\pi\Delta\nu_{1/2}$ = 42 ± 2 msec.) before and after each set of

experiments. A comparison of this value with the smallest one reported in the literature (133) for potassium salts at infinite dilution in H_2O, i.e., 5.7 0.6 Hz (T_2 = 56 ± 6 msec.), indicates that the line width contributions from field inhomogeneities range from 1 to 2 Hz at the most despite the large volumes of sample used in this study. This contribution is smaller than, or comparable to, the estimated precision of our measurements which is about 2% for successive runs with the same or different samples. In our kinetics study, rate data were obtained from differences in line widths so that small systematic errors would essentially cancel out. For these reasons, the measured line widths were not corrected for inhomogeneous line broadening. The relaxation rates $1/T_2$ were calculated from the line widths ($1/T_2 = \pi\Delta\nu_{1/2}$) of the absorption spectra.

e. Data Acquisition and Signal Processing - The high quality spectra required for kinetics measurements are particularly difficult to obtain in ^{39}K NMR due to the very low sensitivity of this nucleus. To overcome this problem we used a high magnetic field and a large sample volume, but it was still necessary to carefully optimize every step of the data acquisition in order to obtain spectra with large signal to noise ratio in a reasonable amount of time (<2 h routinely).

Signal Averaging

In dilute solutions (<0.1 M in K^+) ^{39}K signals cannot be detected in 1 scan and extensive signal averaging is necessary. At 25°C the typical numbers of scans (NS) to obtain spectra with a S/N ratio of about 20 for a solution 0.1 M in K^+ (20 mm O.D. tube) are

NS = 2000 if $\Delta\nu_{1/2}$ = 50 Hz and LB = 20 Hz

NS = 50000 if $\Delta\nu_{1/2}$ = 300 Hz and LB = 80 Hz

where LB is the artificial line broadening (see below). Fortunately ^{39}K relaxation times are short so that many signals can be accumulated in a short time. However care must always be taken to avoid both truncation and saturation which distort the line shape and cause erroneous line width measurements (176). All measurements were done in such a manner that the NMR signal decayed completely during the time interval (>5 T_1) between the rf-pulses. Even when this condition applies, a very fast acquisition often leads to some baseline distortion; 1 K was the minimum memory size used in this work.

Zero Filling Technique

The theoretical and practical aspects of this technique were recently reviewed by Lindon and Ferridge (177).

In short, one can increase the point to point resolution and even improve peak lineshapes and positions by adding more than N zeroes to an N-point free induction decay (FID) prior to Fourier transformation. We used this technique for all the kinetics studies except those in acetone and 1,3-dioxolane. Typically the spectra accumulated using 1024 or 2048 points of memory were zero filled to 8192 or 16384 points (177,178). With a spectrum width of 5000 Hz, the chemical shifts were accurate to ±0.3 ppm and the line widths to ±2%. For the low sensitivity nuclei and the broad signals, the zero filling technique brings about a considerable time saving. Furthermore, without it, the acquisition of good quality spectra in unstable super-cooled solutions, e.g., $K^+ \cdot 18C6$ complex in Acetone-THF (80-20% vol.) at -40°C, would have been impossible.

Sensitivity Enhancement

The FID's were multiplied by the universally used negative exponential weighting function, so that the line shape remains Lorentzian after transformation. This method improves the sensitivity and does not introduce any lineshape distortion (177). For each spectrum a compromise must be found between sensitivity enhancement and undesirable line broadening. Typical artificial line broadenings (LB) applied to our spectra were

LB = 5 - 10 Hz for $\Delta\nu_{1/2}$ = 50 Hz

LB = 15 - 50 Hz for $\Delta\nu_{1/2}$ = 100 Hz

LB = 50 - 120 Hz for $\Delta\nu_{1/2}$ = 300 Hz.

For our systems the use of a matched filter (176), i.e., LB = $\Delta\nu_{1/2}$, results in a very broad line especially for K^+-crown complexes and therefore is not recommended.

2. Carbon 13 NMR

a. Instruments - Most ^{13}C NMR measurements were performed on a Varian CFT-20 spectrometer operating at a field of 1.868 Tesla and a frequency of 20.0 MHz. A Bruker WM-250 spectrometer operating at a field of 5.87 Tesla and a frequency of 62.9 MHz was also used. The latter was coupled to an Aspect 2000 computer with 32 K of memory. A large number of measurements were made on both spectrometers.

b. Locking Procedure, Referencing and Corrections - The sample solution was usually contained in an 8 mm o.d. NMR tube (Wilmad) which was coaxially centered by means of teflon spacers in a 10 mm o.d. NMR tube containing dry acetone-d_6 as the lock. The methyl carbon peak of acetone-d_6 was used as the external reference. Carbon-13 chemical shifts were corrected for the differences in bulk diamagnetic susceptibilities between the sample solvent and

acetone according to Equation (2) (WM250) or to Equation (4) (CFT20)

$$\delta_{corr} = \delta_{obs} + \frac{2\pi}{3} (K_v^{ref} - K_v^{sample}) \qquad (4)$$

When values of K_v^{sample} were not available from reference, approximate corrections were obtained by running the same sample on the two spectrometers. The correction in Equation (4) is a third of the difference in the observed chemical shifts between the two spectra. Table 7 gives the corrections for each spectrometer.

c. Temperature - The temperature was measured before and after each experiment with a calibrated Doric digital thermocouple inserted in an NMR tube containing acetone (CFT 20). For temperature measurements on the WM 250, see Paragraph IIIA3.

3. Data Handling

The kinetic parameters and the stability constants of complexes were calculated by fitting the rate-temperature data and the chemical shift-mole ratio data respectively to appropriate equations using a weighted non-linear least-squares program KINFIT (179) on a CDC 7501 computer. Details on the use of this program are given in the Appendices 1 and 2.

Table 7. Diamagnetic Susceptibility Corrections[a] with Respect to Acetone-d6.

Solvent	Correction for Varian CFT-20 and Varian DA-60	Correction for Bruker WH-180 and Bruker WM-250
Acetone	0	0
MeCN	-0.155	+0.310
$CHCl_3$	-0.587	+1.174
CH_2Cl_2	-0.518	+1.036
Formamide	-0.191	+0.382
DMF	-0.237	+0.474
DMSO	-0.304	+0.608
MeOH	-0.116	+0.232
EtOH	-0.242	+0.484
Nitromethane	+0.144	-0.288
Nitroethane	-0.078	+0.156
1-Nitropropane	-0.18[b]	+0.36[b]
Pyridine	-0.319	+0.638
PC	-0.365	+0.730
Tetramethylguanidine	-0.273	+0.546
H_2O	-0.545	+1.09
THF	-0.321	+0.642
1,3-Dioxolane	-0.40[b]	+0.81[b]
Ethylene Glycol	-0.508	+1.016
Toluene	-0.331	+0.662
Anisole	-0.444	+0.888
Methyl Acetate	-0.162	+0.324

[a]in ppm at 25±10°C. [b]This work, approximate values (see text).

CHAPTER III

KINETICS OF COMPLEXATION OF POTASSIUM CATIONS WITH 18-CROWN-6 IN NONAQUEOUS SOLVENTS BY POTASSIUM 39 NUCLEAR MAGNETIC RESONANCE

A. Introduction

It is surprising to note that while hundreds of formation constants of macrocyclic complexes are known, the kinetic properties for the complexation of alkali ions with 18C6, one of the most common and early synthesized crown ethers, have been investigated only in water. Shporer and Luz (48) showed that the exchange of the potassium cation between its solvated site and the K^+•DB18C6 complex is slow enough to be observed by ^{39}K NMR. From these results it was clear that the same technique could be used to study the complexation kinetics of K^+•18C6 in a variety of solvents because the stabilities of the K^+•18C6 and K^+•DB18C6 complexes are comparable (log K_f = 2.03 and 6.05 for K^+•18C6 in H_2O and MeOH respectively vs 1.67 and 5.00 for K^+•DB18C6 (10)) and probably so are the decomplexation rates.

The goal of the work presented in this chapter was to determine if the activation energy for the release of an alkali cation from a small crown molecule (18C6) depends on the solvent or not, since the previous studies concerned with this problem were not conclusive. Spurred by the results of Lin in 1,3-dioxolane and THF (59,148), we were particularly interested in studying the ethereal solvents.

B. Choice of Solvents and Salts

The relatively high concentrations required for detection by ^{39}K NMR (>0.05 M) and the low solubilities of potassium salts and $K^+ \cdot 18C6$ complexes place some restriction on the choice of solvents and salts. Many other factors, which further limited our choice, had to be considered.

The donor abilities of the various solvents used in this study had to be comparable since we wanted to concentrate on the effect of changing the dielectric constant and the solvent structure upon the kinetic parameters. For this reason acetone was chosen as the primary solvent since it has a donor number (149,150) of 17 close to those of THF and 1,3-dioxolane (Table 8). It is a polar solvent in which all the species of interest are sufficiently soluble ($\geq$ 0.1 M) for ^{39}K measurements even at low temperatures. It is miscible in any proportion with the three cyclic ethers used in this study. It has a low melting point as well as a low viscosity so that ^{39}K NMR signals are not too broad in it. Methanol was selected because the only reported kinetics study by ^{39}K NMR (48) was done in this solvent, thus allowing some comparisons to be made. In addition to THF and 1,3-dioxolane, which we used in an attempt to observe with K^+ the slow cation exchange seen with Na^+ (59,148), we chose 1,4-dioxane in connection with its interesting behavior in the propagation of anionic polymerization (76). This reaction involves free ions

such as styrene$^-$(S^-) and ion pairs such as S^-Na^+. The concentration of free ions increases rapidly in THF but slowly in dioxane. The S^-Li^+ ion pair is the most reactive and the S^-Cs^+ the least reactive in THF but the pattern is reversed in dioxane (76). We also resorted to acetone-dioxane and acetone-THF mixtures due to solubility problems. The key properties of the solvents are given in Table 8.

Potassium hexafluoroarsenate is soluble in many organic solvents (151,152), including THF (153) and 1,3-dioxolane. Approximate solubility measurements in these two solvents gave values of 0.18 M and 0.20 M, respectively. Potassium halides are insoluble (KCl $\sim 10^{-4}$ M) in THF even in the presence of DC18C6 (4,154). Even potassium salts with soft anions such as ϕCOO^-, $CH_3CO_2^-$, picrate or $B\phi_4^-$ (153) are insoluble in THF and 1,3-dioxolane. We used $KAsF_6$ for all our measurements except those in MeOH where KI was used.

In most organic solvents, the solubility of 18C6 is greater than 0.1 M (e.g., >0.22 M in MeOH (155)), but the $K^+\cdot$18C6 complex is only sparingly soluble in ethereal solvents. Using $KAsF_6$, we found that, at 25°C, the solubility of $K^+\cdot$18C6 is less than 0.01 M in THF and is about 0.035 M in 1,3-dioxolane, whereas both the free salt and the ligand are soluble (>0.1 M) in both solvents. This is in contrast with the general enhancement of the solubility of inorganic

Table 8. Key Solvent Properties[a] and Corrections[a] for Magnetic Susceptibilities on Bruker WH-180 and WM-250 Spectrometers.

Solvent	Dielectric Constant	Dipole Moment (Debye)	Viscosity (cp)	Donor Number[b] (DN)	m.p. (°C)	b.p. (°C)	Vol. Suscept. $-K \times 10^6$	Correc.[d] Ref. Water (ppm)
Acetone	20.7	2.88	0.304	17.0	-95	56	0.460	-1.09
	29.5(-50°)[e]		0.77(-50°)[e]					
Acetone-1,4-Dioxane 80-20% vol.	∿16[e]		∿0.37[e]					
	2.							
1,4-Dioxane	2.2	0.45	1.087(30°)	14.8	11.8	101	0.606	-0.478
1,3-Dioxolane		1.47		14.7[f]	-95	78		
THF	7.6	1.75	0.460	20.0	-108	65	0.613	-0.448
	11.6(-70°)[e]							
MeOH	32.7	1.66	0.544	25.7[g]	-98	65	0.515	-0.858
	48.5(-50°)[e]		2.19(-50°)[e]					

[a]at 25 5°C unless otherwise indicated. [b]The Gutmann donor number is defined as the negative enthalpy for the reaction $S + SbCl_5 \xrightarrow{1,2\text{-DCE}} S.SbCl_5$. That is $SN = -\Delta H_{S.SbCl_5}$ (149,150). [c]Reference 174. [d]To be introduced in the formula $\delta_{corr} = \delta_{obs} + \text{correction}$. [e]Reference 163. [f]Calculated (see Reference 165). [g]Predicted by ^{23}Na NMR (164).

salts in organic solvents by crowns and cryptands (156). A decrease of solubility upon complexation has already been observed by Wong et al. (55) for several crown complexes of fluorenyl alkali salts in ethereal solvents and by Cambillau et al. (157) for the 18C6 complex of potassium enolate in THF. The poor anion solvating capacity of ethers (150,158) might be responsible for this effect. Complexation of K^+ by 18C6 breaks a large proportion of contact ion pairs (89,159), as shown below. This in turn leads to anion activation (160) and in our case to precipitation of the complex. In MeOH, the $K^+ \cdot 18C6$ complex precipitates if PF_6^- or AsF_6^- is used as the anion but with I^- its solubility is greater than 0.2 M, due probably to the possibility of weak H-bonding with MeOH. It is known that PF_6^- has a poor coordinating ability (161,162); the AsF_6^- anion probably shares this property (151). These results show that any complexation data based on increased solubility of inorganic salts in low polarity media (and also in MeOH) may not yield a clear picture of how effective the various salts complex with crown ethers.

C. Results and Discussion

The kinetics of complexation of 18C6 with potassium cation were studied in five pure or mixed solvents by using ^{39}K NMR line shape analysis. The five solvent systems were acetone, acetone-1,4-dioxane mixture

(80-20% vol.), acetone-THF mixture (80-20% vol.), methanol and 1,3-dioxolane. The structures of the three cyclic ethers are shown below.

THF

1,3-dioxolane

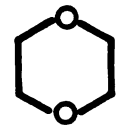

1,4-dioxane

As pointed out in the Introduction, the treatment of kinetics data obtained by alkali metal NMR depends on the differences in chemical shift and line width between the solvated cation and the complexed cation, in the absence of chemical exchange. Therefore it is necessary to characterize the two sites before discussing the kinetics data. In this discussion, site A refers to the solvated site and site B refers to the complexed site.

1. <u>Potassium-39 NMR of the Solvated and Complexed Potassium in the Absence of Chemical Exchange</u>

To obtain the transverse relaxation rates, $1/T_{2A}$ and $1/T_{2B}$, and the chemical shifts, δ_A and δ_B, in the absence of exchange, two solutions in each solvent were prepared. The first contained the potassium salt only

and the second contained equimolar amounts of the potassium salt and of 18C6. Since the $K^+ \cdot 18C6$ complex is quite stable, i.e., $K_A > 10^4$ (10), in all solvents studied and throughout the temperature range considered, the second solution contained only complexed potassium cations. In both solutions chemical exchange is absent.

The temperature dependence of $1/T_{2A}$ and $1/T_{2B}$ is given in Tables 9-13. Figure 3 shows semilog plots of these observed relaxation rates vs reciprocal absolute temperature for all the solvents studied. Figure 4 shows the temperature dependence of the chemical shifts for sites A and B.

Site A

For K^+ ion in solution, we expect to find T_1 to be equal to T_2. This is indeed the case as is shown in Figure 5 where the reported longitudinal relaxation rates $1/T_1$ for a solution of 0.5 M KI in methanol (48), are plotted together with our values of $1/T_2$ for a solution of 0.2 M KI in MeOH. The two solutions differ only by a small change in viscosity and the two sets of data are in good agreement. However, while Shporer and Luz (48) drew a straight line through their data points, our values which are much less scattered clearly show a curvature. Figure 3 also shows some curvature for solvents other than methanol. Therefore the curvature must be real.

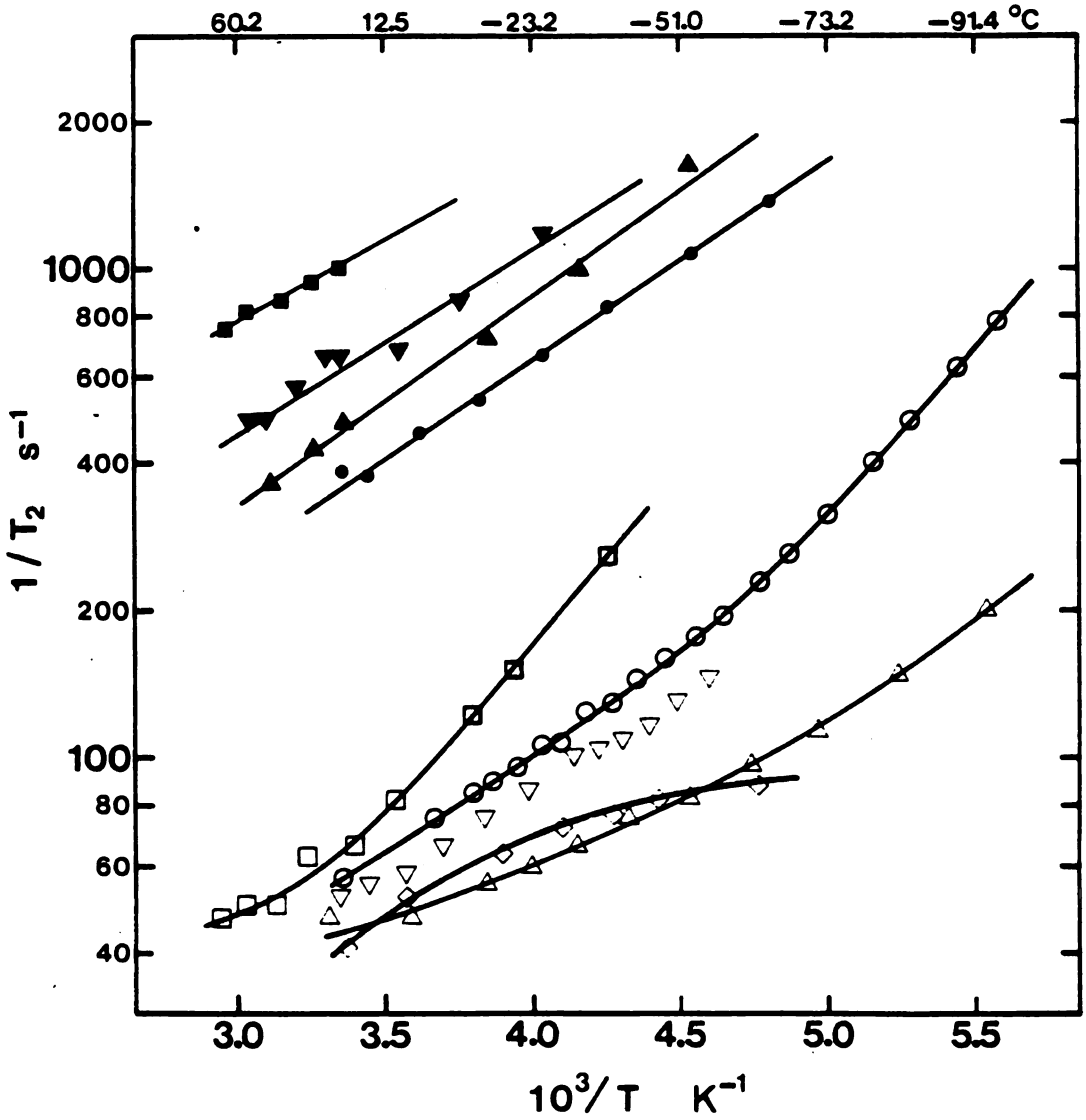

Figure 3. Semilog plots of potassium-39 transverse relaxation rates for the solvated (open symbols) and the complexed (closed symbols) in various solvents. □ Dioxolane; ○ MeOH; ▼ Ac-dioxane; ◇ Ac-THF; △ Acetone.

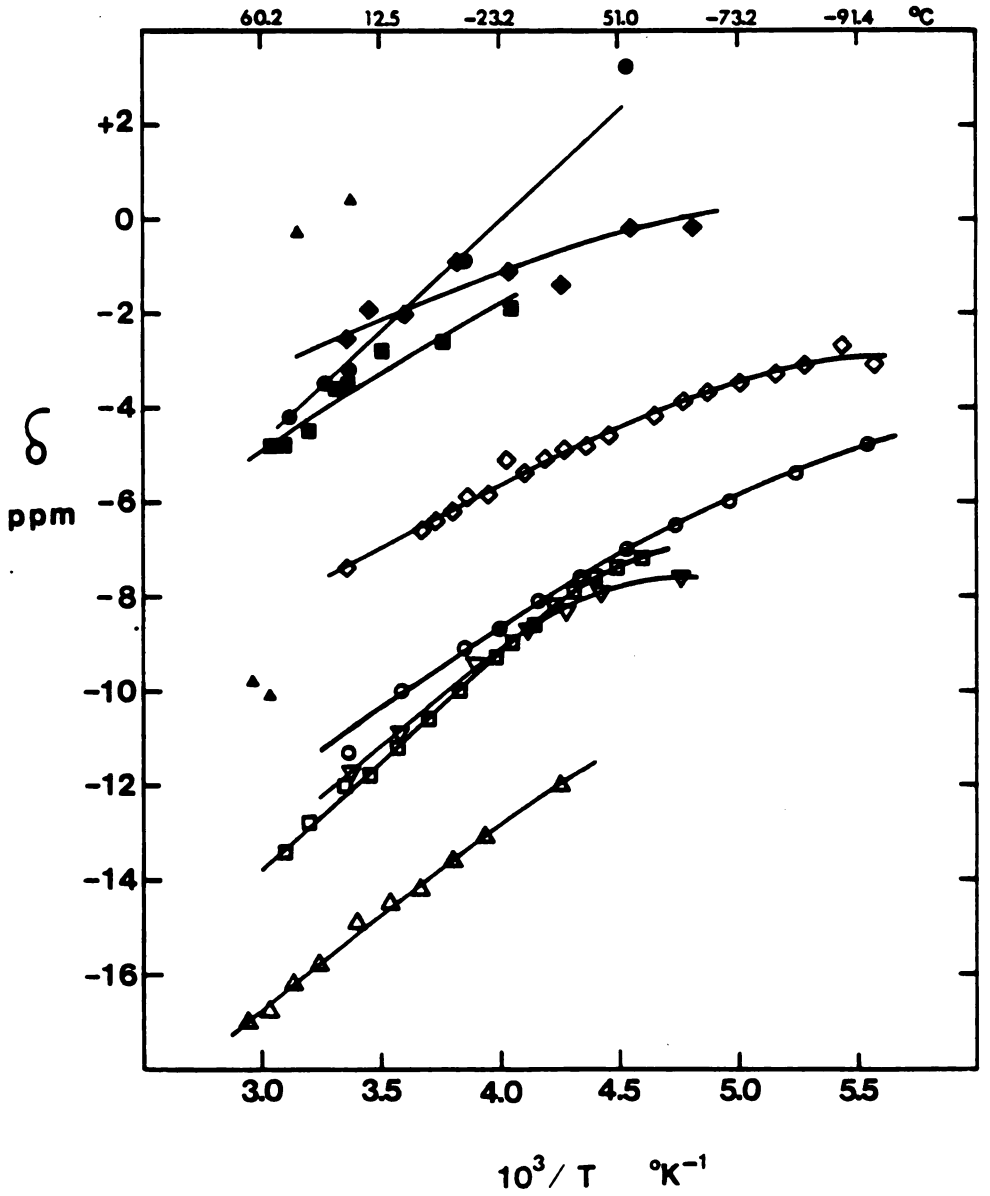

Figure 4. Potassium-39 chemical shifts for the solvated (open symbols) and the complexed (closed symbols) K^+ ion in several solvents. ▲ 1,3-dioxolane; ○ acetone; □ acetone-dioxane (80-20% vol.); ▼ acetone-THF (80-20% vol.); ◇ methanol.

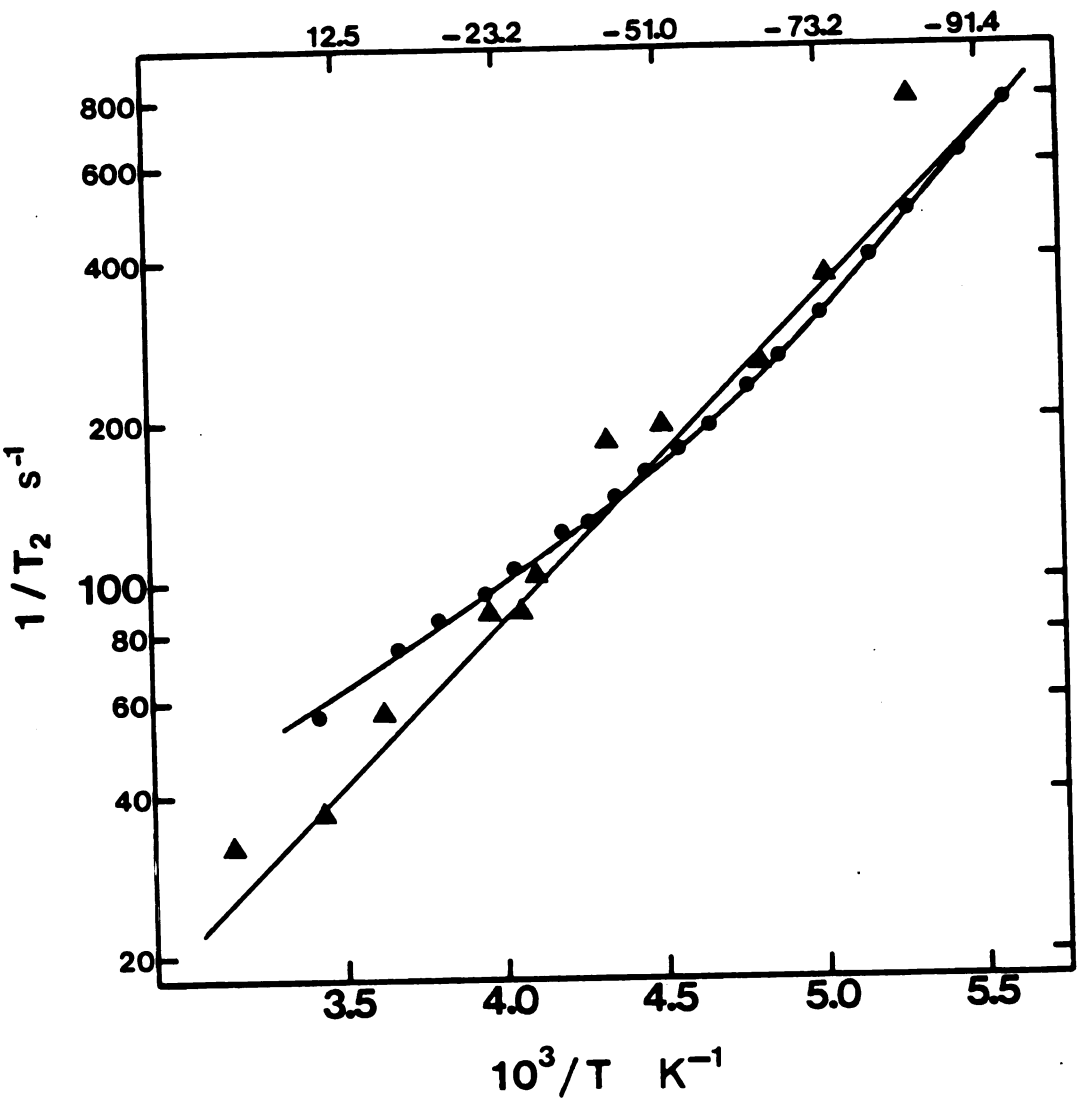

Figure 5. Potassium-39 relaxation rates for solvated K^+ ion in methanol. ▲ 0.5 M KI (Reference 48); ● 0.2 M KI (this work).

Table 9. Potassium-39 NMR Chemical Shifts and Reciprocal Transverse Relaxation Times for Acetone Solutions Containing $KAsF_6$[a] and 18C6 at 18C6/K^+ Mole Ratios of 0, 0.5 and 1.04 and at Various Temperatures.[b]

MR = 0[c]				MR = 0.5[c]				MR = 1.04[e]			
t °C	$10^3/T$ K^{-1}	$1/T_2$ s^{-1}	δ[d] ppm	t °C	$10^3/T$ K^{-1}	$1/T_2$ s^{-1}	δ[d] ppm	t °C	$10^3/T$ K^{-1}	$1/T_2$ s^{-1}	δ[d] ppm
24.0	3.364	47	-11.3	53.0	3.066	242	-8.8	47.5	3.118	365	-4.2
5.3	3.591	47	-10.0	43.5	3.158	261	-8.2	33.2	3.264	430	-3.5
-13.6	3.852	55	- 9.1	24.0	3.365	298	-7.7	23.5	3.370	487	-3.2
-23.0	3.997	60	- 8.7	5.3	3.591	341	-6.5	-13.6	3.851	723	-0.9
-32.9	4.162	66	- 8.1	-13.6	3.852	416	-7.2	-33.0	4.163	1005	(-2.1)
-42.5	4.335	75	- 7.6	-23.0	3.997	415	-6.9	-52.4	4.529	1634	+3.2
-52.4	4.529	83	- 7.0	-33.0	4.163	393	-7.3				
-62.1	4.737	97	- 6.5	-42.4	4.333	298	-7.5				
-71.8	4.965	113	- 6.0	-52.4	4.529	242	-7.0				
-82.5	5.244	148	- 5.4	-61.8	4.730	198	-6.6				
-92.8	5.543	201	- 4.8	-66.3	4.833	192	-6.3				
				-71.8	4.965	204	-5.7				
				-82.5	5.244	251	-5.3				
				-93.0	5.549	361	-5.0				

[a]0.1 M $KAsF_6$. [b]Lock solvent: Acetone-d6. [c]Spectra were accumulated using 8 K or 16 K of memory. [d]Not corrected for the difference in ^2H resonance frequency between D_2O and Acetone-d6. [e]Memory size 4 K or 8 K for these spectra.

Table 10. Potassium-39 NMR Chemical Shifts and Reciprocal Transverse Relaxation Times for MeOH Solutions Containing KI[a] and 18C6 at 18C6/$\overline{K^+}$ Mole Ratio (MR) of 0, 0.5 and 1.02 and at Various Temperatures.[b]

MR = 0				MR = 0.5			
t °C	$10^3/T$ K^{-1}	$1/T_2$ s^{-1}	δ^c ppm	t °C	$10^3/T$ K^{-1}	$1/T_2$ s^{-1}	δ^c ppm
24.7	3.357	56	-7.4	24.7	3.357	217	-5.0
- 0.9	3.672	75	-6.6	14.7	3.473	236	-4.6
- 5.2	3.731	81	-6.4	8.2	3.554	251	-4.5
-10.4	3.805	85	-6.2	3.0	3.621	264	-4.3
-14.9	3.872	90	-5.9	-2.1	3.689	273	-4.1
-19.7	3.945	95	-5.8	-6.5	3.750	283	-4.0
-25.3	4.034	107	-5.0	-11.6	3.823	305	-4.0
-29.5	4.103	107	-5.4	-16.6	3.897	333	-3.7
-34.3	4.186	124	-5.1	-21.6	3.975	355	-3.4
-38.9	4.268	129	-4.9	-26.2	4.049	377	-3.5
-43.8	4.359	144	-4.8	-31.4	4.136	405	-3.5
-48.6	4.452	160	-4.6	-40.7	4.301	418	-3.9
-53.9	4.560	176	-4.3	-45.7	4.396	412	-4.1
-58.1	4.649	195	-4.2	-50.7	4.494	408	-4.3
-63.5	4.769	229	-3.9	-56.2	4.608	377	-4.4
-67.9	4.871	261	-3.7	-60.6	4.704	352	-4.5
-73.5	5.008	314	-3.5	-65.9	4.824	336	-4.0
-79.5	5.163	402	-3.3	-68.6	4.888	342	-4.0
-83.9	5.283	487	-3.1	-70.1	4.924	339	-4.0
-89.4	5.441	628	-2.7	-75.9	5.068	412	-3.3
-94.0	5.580	785	-3.1	-81.5	5.216	487	-3.2

Table 10 - Continued.

MR = 1.02[d]			
t °C	$10^3/T$ K^{-1}	$1/T_2$ s^{-1}	δ^c ppm
24.7	3.357	386	-2.5
17.1	3.445	377	-1.9
2.9	3.622	462	-2.0
-11.8	3.826	540	-2.9
-25.8	4.042	666	-1.0
-38.3	4.257	832	-1.3
-53.2	4.545	1056	-0.2
-65.2	4.808	1366	-0.2

[a]0.2 M KI. Lock solvent:Methanol-d4.

[b]All spectra were accumulated using 1 K or 2 K data points and zero filled to 16 K.

[c]Uncorrected for the differences in ^2H resonance frequencies between D_2O and Methanol-d4 (∿2 ppm).

[d]Number of scans = 6000 (high temp.) to 15000 (low temp.).

Table 11. Potassium-39 NMR Chemical Shifts[a] and Reciprocal Transverse Relaxation Times for Solutions Containing $KAsF_6$ and 18C6 at 18C6/K^+ Mole Ratio (MR) of 0, 0.25, 0.50 and 1.02 in 1,3-Dioxolane and at Various Temperatures.

MR = 0[b,g]				MR = 0.25[b,f]			
t °C	$10^3/T$ K^{-1}	$1/T_2$ s^{-1}	δ ppm	t °C	$10^3/T$ K^{-1}	$1/T_2$ s^{-1}	δ ppm
66.5	2.946	47	-17.0	61.2	2.990	239	-16.3
56.5	3.035	50	-16.8	55.2	3.045	239	-14.7
46.2	3.133	50	-16.2	51.0	3.084	261	-14.4
35.8	3.238	63	-15.8	45.9	3.134	280	-14.9
21.2	3.399	66	-14.9	40.6	3.187	283	-14.6
9.6	3.539	88	-14.5	35.4	3.240	283	-14.6
0.0	3.663	94	-14.2	29.9	3.299	264	-14.8
- 9.8	3.796	122	-13.6	24.6	3.358	229	-15.2
-19.2	3.937	152	-13.1	18.5	3.428	214	-15.0
-38.2	4.255	258	-12.0	14.2	3.480	192	-14.7
				8.6	3.549	160	-14.9
				4.3	3.602	149	-14.7
				- 0.9	3.672	138	-14.6
				- 5.7	3.738	137	-14.2
				-10.3	3.804	135	-13.7
				-14.9	3.872	148	-13.6
				-19.5	3.942	163	-13.2
				-24.2	4.016	188	-13.1
				-29.2	4.098	212	-12.9

Table 11 - Continued.

MR = 0.5[b,g]				MR = 1.02[c,f]			
t °C	$10^3/T$ K^{-1}	$1/T_2$ s^{-1}	δ ppm	t °C	$10^3/T$ K^{-1}	$1/T_2$ s^{-1}	δ ppm
46.2	3.133	477	-10.1	64.2	2.964	754	-9.8±1
35.5	3.241	528	-12.2	56.4[d]	3.036	817	-10.1±1
24.0	3.367	443	-13.8	43.8	3.155	864	-0.3±1
15.0	3.470	320	-14.8	33.4[d]	3.264	942	+1.3±1
9.4	3.541	251	-14.5	23.2[e]	3.374	1005	+0.4±0.5
5.1	3.593	214	-14.6				
0.0	3.660	179	-14.5				
- 9.2	3.788	170	-14.1				
-13.7	3.854	174	-13.8				
-18.7	3.929	190	-13.5				
-23.3	4.002	---	-13.1				

[a]Uncorrected for diamagnetic susceptibilities. Lock Acetone-d6 (see Table 9 footnote d).

[b]0.1 M $KAsF_6$.

[c]0.05 M $KAsF_6$, unless otherwise indicated.

[d]0.04 M $KAsF_6$.

[e]Obtained by extrapolation from data in Acetone-1,3-Dioxolane mixtures (see Table 15).

[f]Memory size 2 K or 4 K. Zero filling to 16 K.

[g]Memory size 8 K or 16 K. No zero filling.

Table 11a. Potassium-39 Chemical Shifts and Line Widths for $KAsF_6$ at Various Concentrations in 1,3-Dioxolane and in THF at 25°C.

1,3-Dioxolane			THF		
$[KAsF_6]$ M	δ[a] ppm	$\Delta\nu_{1/2}$[b] Hz	$[KAsF_6]$ M	δ[a] ppm	$\Delta\nu_{1/2}$[b] Hz
0.0077	-15.99	14.7[c]	0.0070	-16.64	15.0[c]
0.0115	-16.27	15.3	0.0120	-16.68	15.0
0.0145	-16.27	13.7	0.0229	-17.06	21.4
0.0176	-16.48	14.5	0.0386	-17.32	19.8
0.0213	-16.60	15.3	0.0505	-17.50	23.0
0.0293	-16.75	15.1	0.0882	-17.68	23.4
0.0495	-17.10	17.8	0.1186	-17.89	26.8
0.0710	-17.19	19.7	0.158	-17.95	30.0
0.115	-17.44	24.0			

[a] ±0.07 ppm.

[b] ±1 Hz.

[c] For the low concentrations, the reported $\Delta\nu_{1/2}$ values probably exceed by 1 or 2 Hz the real values due to a small instability of the field over the long period of time necessary to obtain these spectra.

Table 12. Potassium-39 NMR Chemical Shifts and Reciprocal Transverse Relaxation Times for Solutions Containing $KAsF_6$[a] and 18C6 at 18C6/K^+ Mole Ratios (MR) of 0, 0.5 and 1.04 in Acetone-1,4-Dioxane (80-20% vol.) and at Various Temperatures.[b,c]

MR = 0				MR = 0.5				MR = 1.04[f]				
t °C	10^3 T K^{-1}	$1/T_2$ s^{-1}	δ[d,e] ppm	t °C	$10^3/T$ K^{-1}	$1/T_2$ s^{-1}	δ[d,e] ppm	Conc. M	t °C	$10^3/T$ K^{-1}	$1/T_2$ s^{-1}	δ[d,e] ppm
49.8	3.096	46	-13.4	45.6	3.137	278	-9.0		55.7	3.040	487	-4.8
39.4	3.199	49	-12.8	35.2	3.242	308	-8.7	0.10	49.7	3.097	487	-4.8
25.5	3.348	52	-12.0	24.5	3.359	346	-8.2	0.05	49.7	3.097	471	-4.3
16.5	3.452	55	-11.8	17.7	3.438	358	-8.1	0.025	49.7	3.097	433	-3.7
				12.7	3.498	380	-8.2		39.3	3.200	569	-4.5
6.6	3.574	58	-11.2	7.0	3.569	388	-7.9		28.7	3.312	653	-3.6
				2.7	3.624	399	-7.8	0.10	24.4	3.360	657	-3.5
- 2.8	3.698	66	-10.6	-2.5	3.694	421	-8.1	0.05	23.5	3.370	594	-3.2
				-7.0	3.757	430	-7.9	0.025	23.5	3.370	578	-3.1
-12.4	3.834	75	-10.0	-12.1	3.830	412	-8.9		12.0	3.506	675	-2.8
				-16.8	3.900	391	-8.9		-7.0	3.757	854	-2.6
-21.9	3.979	85	- 9.3	-21.7	3.976	339	-9.0		-26.1	4.047	1178	-1.9
-26.1	4.047	91	- 9.0	-26.6	4.055	276	-9.4					
-31.7	4.141	100	- 8.6	-31.5	4.137	220	-9.1					
-36.4	4.223	104	- 8.2	-36.5	4.225	166	-8.6					
-41.1	4.308	108	- 7.9	-40.8	4.303	138	-8.4					
-46.0	4.401	118	- 7.6	-45.6	4.394	129	-8.1					
-50.5	4.490	127	- 7.4	-50.7	4.494	124	-7.6					
-55.6	4.596	144	- 7.2									

Table 12. Continued.

[a] 0.10 M $KAsF_6$ unless otherwise indicated.

[b] The lock solvent is Acetone-d_6.

[c] 1 K points zero-filling to 8K at low temperatures. 2K points zero-filling to 16 K at high temperatures (see Experimental Part).

[d] δ's are corrected assuming that the diamagnetic susceptibility of the mixture is the same as that of acetone.

[e] δ's are not corrected for the differences in ^2H resonance frequencies between D_2O and Acetone-d_6.

[f] A slight excess of 18C6 was added to ensure that all the potassium cations are complexed.

Table 13. Potassium-39 NMR Chemical Shifts and Reciprocal Transverse Relaxation Times for Solutions Containing $KAsF_6$[a] and 18C6 at 18C6/K^+ Mole Ratio (MR) of 0, 0.5, and 1.02 in Acetone-THF (80-20% vol.) and at Various Temperatures.

MR = 0				MR = 0.5[d]			
t °C	$10^3/T$ K^{-1}	$1/T_2$ s^{-1}	$\delta^{b,c}$ ppm	t °C	$10^3/T$ K^{-1}	$1/T_2$ s^{-1}	$\delta^{b,c}$ ppm
23.0	3.376	41	-11.7	53.6	3.060	213	-9.3
6.6	3.574	52	-10.9	46.7	3.126	242	-9.0
-16.3	3.893	64	- 9.4	40.5	3.188	234	-8.5
-29.8	4.108	73	- 8.7	33.3	3.263	259	-8.5
-39.3	4.275	76	- 8.3	25.6	3.347	283	-7.9
-47.4	4.429	83	- 7.9	20.7	3.403	277	07.8
-63.3	4.764	88	- 7.6	18.3	3.430	298	-8.1
				14.4	3.477	283	-8.4
				9.8	3.534	302	-7.5
				7.1	3.568	300	-7.5
				3.7	3.611	313	-7.6
				0.3	3.656	336	-7.2
				-2.3	3.691	346	-7.0
				-5.8	3.740	334	-7.4
				-11.2	3.817	368	-6.8
				-15.5	3.880	364	-7.4
				-21.8	3.978	360	-7.8
				-25.6	4.039	342	-7.9
				-29.6	4.105	336	-8.1
				-33.5	4.172	278	-8.1
				-36.0	4.216	261	-8.3
				-38.0	4.252	248	-8.1
				-43.0	4.344	191	-7.7
				-46.6	4.413	163	----
				-48.0	4.440	166	-7.8

Table 13. Continued.

MR = 1.02			
t °C	$10^3/T$ K^{-1}	$1/T_2$ s^{-1}	$\delta^{b,c}$ ppm
53.6	3.060	422	-4.7
43.5	3.158	427	-4.4
33.2	3.264	479	-3.6
23.4	3.374	487	-2.3
12.0	3.506	543	-3.1
4.3	3.604	622	-3.0

[a]0.1 M $KAsF_6$. Lock solvent:Acetone-d6.

[b]Corrected by assuming that the difference in diamagnetic susceptibility between the solvent mixture and pure acetone is negligible.

[c]Uncorrected for the difference in ^2H resonance frequency between D_2O and Acetone-d_6.

[d]Below -21°C, the solubility of the complex is less than 0.1 M, and all the measurements were done (with 1 K of memory) on the unstable supercooled solution. Once the probe is at -40°C, it takes ∿15 minutes to bring the sample temperature from +25°C to -40°C with a large flow of N_2 (gas). About 10 minutes were then available for the measurement before the first crystals appear in the sample. The absence of crystals was checked after each run.

It is interesting to speculate if this phenomenon is indeed predicted by the theory.

The quadrupolar relaxation rate for ^{39}K in solutions and in the absence of chemical exchange is given by (137):

$$\frac{1}{T_1} = \frac{1}{T_2} = \frac{3}{40} \frac{2I+3}{I^2(2I-1)} \left(1 + \frac{v^2}{3}\right) \left(\frac{eQ}{\hbar} \frac{\partial^2 V}{\partial z^2}\right)^2 \tau_c \qquad (1)$$

where I is the spin of the nucleus, v is the asymmetry parameter ($v = 0$ for a symmetric field gradient, $0 \leq v \leq 1$) Q is the quadrupole moment of the nucleus, $\partial^2 V/\partial z^2$ is the z component of the electric field gradient at the nucleus produced by solvent fluctuations and τ_c is the correlation time which characterizes these fluctuations. For a simple reorientation process, τ_c may be expressed by (61)

$$\tau_c = A' \, e^{-\frac{E_r}{RT}} \qquad (2)$$

where E_r is an activation energy for solvent reorganization. We prefer to use this general expression rather than Debye's formula $\tau_c = 4\pi\eta a^3/3kT$ (η = viscosity) which has been found to give too large τ_c values for solvated species (151) as well as for complexes (60). Besides, the macroscopic viscosity does not adequately describe

the frictional forces acting on a solute molecule (180). If the nuclear quadrupole coupling constant (NQCC) $eQ/\hbar \times \partial^2V/\partial z^2$ is assumed not to change with temperature, then the relaxation rate will vary exponentially as a function of temperature. Figure 3 shows that in all the solvents studied this behavior is observed for the bound site but not for the solvated site. Large deviations of the semilog plots from linearity have been observed by ^{23}Na NMR for Na^+ in pyridine (34), DMF (46) and methanol (20) at various temperatures. The Debye formula predicts that $1/T_2$ is proportional to η/T. Deviations from this behavior have been reported, e.g., for Na^+ in THF (49). In some cases, the line width increases, instead of decreasing, with the temperature, e.g., for $Na^+BPh_4^-$ in 1,3-dioxolane (148). For all these cases, either the NQCC changes with temperature or τ_c does not behave as predicted by expression 2.

The two species capable of producing field gradients at the potassium nucleus are solvent dipoles and anions. Consequently in low polarity media, e.g., 1,3-dioxolane, a change in contact ion-pair formation with temperature might account for the observed curvature. However this explanation does not hold for methanol which has a high dielectric constant, especially at low temperatures (ε = 59 at -70°C (181)). The ion pair formation constant of KI in methanol is about 10 at 25°C (182,183), but this

value refers to solvent-separated ion pairs. There are virtually no K^+I^- contact ion pairs throughout the temperature range under study. Thus in methanol, the large increase of $1/T_2$ at low temperature is due to a large increase of viscosity, because the solvent dimers tend to form networks of polymers (181). From the slope of the tangent to the relaxation curve in MeOH (Figure 3) we calculated that the activation energy for solvent reorientation increases from 1.7 $kcal.mol^{-1}$ at 10°C to 3.2 $kcal.mol^{-1}$ at -90°C.

For acetone solutions the curvature of the plot in Figure 3 is significant but smaller than that for methanol solutions. Two solvent mixtures, both of which contain acetone, show abnormal behavior. In particular, acetone-THF gives a curvature opposite to that of acetone. We do not have an explanation for this observation, but it must be related to a change in the solvent structure between acetone and acetone-THF mixture. The convergence of the curves at high temperature is also remarkable and it is only seen for the solvated sites. It is interesting to note that the solvent effect on the relaxation rate of the solvated potassium is important only at low temperatures, at least for the few solvents investigated. A variation of the NQCC with the temperature might also explain the curvatures of the relaxation curves for the site A.

Site B

The situation is different for the bound site. The relaxation rates of site B are much larger than those of site A (Table 14). This is caused by the asymmetry of the electric field at the potassium nucleus due to the planar structure of the crown. The plots of $1/T_2$ are linear and almost parallel to each other. The disappearance of both the convergence and the curvature upon complexation points to a rather weak cation-solvent interaction in the complex.

Kolthoff and Chantooni (184) measured the transfer activity coefficients in various solvents of several univalent cations complexed with DB18C6. In particular they observed that the solvation of K^+ ion in these complexes is weak and that the K^+•DB18C6 complex is less strongly solvated in methanol than in acetonitrile, PC, DMF and DMSO. In connection with this work, it is interesting to note that the relaxation rate of K^+ ion complexed by 18C6 is smaller in methanol than in the other solvents studied. The relaxation rates decrease in the order, dioxolane > methanol > acetone-dioxane > acetone, for site A whereas the order is dioxolane > acetone-dioxane > acetone > methanol for site B. This last order is also the order of solubilities of the complexes. The change seen for methanol is surprising. We observed a large increase in the relaxation

rate of site A in acetone upon addition of 18C6 (see below) or 1,4-dioxane (Figure 16). Thus the presence of these ethers markedly increases the viscosity of acetone solutions. This is not so for MeOH. The $K^+ \cdot 18C6$ complex is probably more solvated in methanol than in other solvents and there is some experimental evidence that a stronger solvation results in a smaller NQCC (172). However, we can neither measure nor calculate the NQCC or τ_c to evaluate their relative contributions to $1/T_2$.

Kintzinger and Lehn (60) obtained the ^{23}Na quadrupolar coupling constants of four sodium cryptates by calculating τ_c from the ^{13}C relaxation times T_1 of the CH_2 carbons of the cryptates and introducing τ_c in Equation (1). They made the assumption that τ_c (from ^{13}C data) also represents the reorientational motions which modulate the ^{23}Na quadrupole interaction. This assumption, probably valid for the rigid cryptates, may not be reliable for crown ether complexes due to the fluctuation of the coordinating sphere. Thus we cannot obtain the NQCC.

The weak solvation of the complex is also indicated by the small solvent dependence of the resonance frequencies of the complexed potassium cation. The chemical shifts measured by Shih (15) are given in Table 14 along with our results. While the chemical shifts of the solvated K^+ ion vary over a range of more than 22 ppm, the signals of the bound site are found between -3.8 ppm and

Table 14. Potassium-39 Chemical Shifts and Transverse Relaxation Rates for the Solvated (Site A) and the Complexed (Site B) K^+ Ions in Various Solvents at 25°C.

Solvent	δ_A ppm	δ_B ppm	$\delta_A-\delta_B$ ppm	$\nu_A-\nu_B$ Hz	$1/T_{2A}$ s^{-1}	$1/T_{2B}$ s^{-1}	T_{2A}/T_{2B}
Acetone	-11.3	-3.2	8.1	68	80	487	6.1
Acetone-1,4-Dioxane 80/20 v/v %	-12.0	-3.5	8.5	71	52	657	12.6
Acetone-THF 80/20 v/v %	-11.8	-2.3	9.5	80	50	487	9.7
1,3-Dioxolane	-15.2	+0.4	15.6	131	80	1000	12.5
MeOH	- 7.4	-2.5	4.9	41	65	386	5.9
DMF[b]	∿-6	-3.8	∿2.2	∿18		∿560	
DMSO[b]	∿+7	-0.6	∿7.6	∿64			
H_2O[b]	+0.5	-1.6	2.1	18			

[a]Extrapolated from the low temperature $1/T_2$ values (see text).

[b]Data from Reference 15.

+0.4 ppm. It is noticeable that the extent of variation of δ with the solvent is about the same for $K^+ \cdot 18C6$ and $K^+ \cdot C221$ (138). The potassium cation fits nicely into the 18C6 cavity (82), so that only a small portion of its surface is exposed to the solvent (184). The X-ray crystallographic data show that in the $K^+ \cdot C221$ complex, K^+ also lies in the cavity of the 18-membered ring (92). Therefore, K^+ may also interact with the solvent, at least in one direction. Further details are given in Chapter IV. For site B as for site A, the signal is shifted in the paramagnetic direction in all solvents and at a rate of 3-5 ppm/100°C.

Dioxolane exhibits a behavior different from the other solvents. First, the relaxation rate of site B is large, i.e., $1/T_{2B} = 1000$ at 25°C. Second, the chemical shift of site B is the largest downfield shift of the $K^+ \cdot 18C6$ complexes at 25°C whereas the signal of K^+ solvated (or ion paired) in dioxolane is the most upfield one (Table 4). Third, between 44°C and 56°C, the chemical shift of site B drops by about 10 ppm while, in other solvents, δ_B decreases steadily with increasing temperature (Figure 4). The low solubility of the $K^+ \cdot 18C6$ complex in dioxolane (0.035 M at 25°C) precluded a direct measurement of δ and $\Delta\nu_{1/2}$. As shown in Figure 6, we obtained the values of these parameters at 23°C (Table 14) by extrapolating to pure dioxolane the values measured in acetone-dioxolane

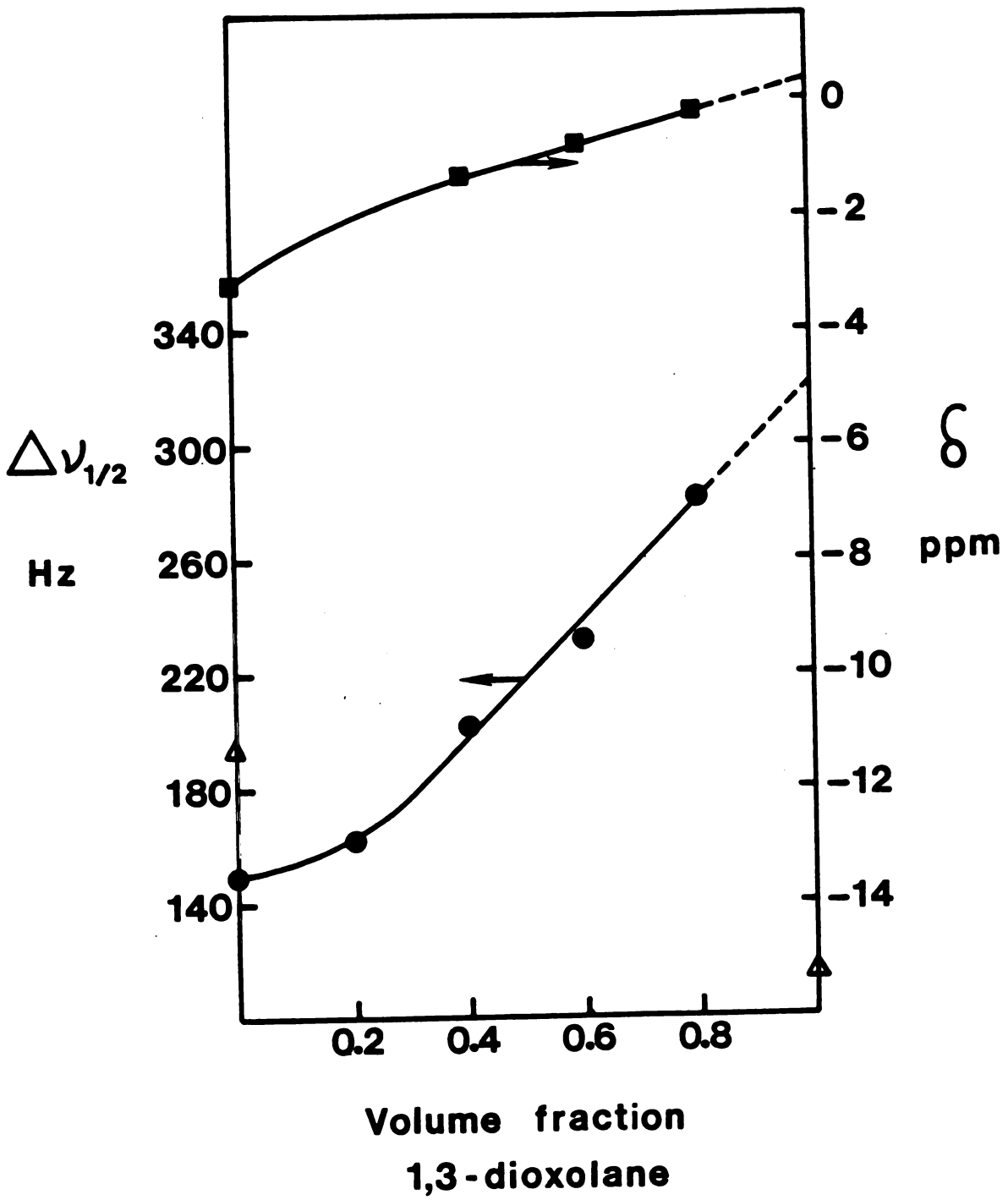

Figure 6. Potassium-39 chemical shifts and line widths for the $K^+ \cdot 18C6$ complex in acetone-1,3-dioxolane mixtures.

Table 15. Potassium-39 NMR Chemical Shifts and Line Widths for Acetone-1,3-Dioxolane Mixtures[a] Containing 0.05 M $KAsF_6$ and 0.05 M 18C6 at 23 1°C.

Acetone Vol %		1,3-Dioxolane vol %	δ^b ppm	$\Delta\nu_{1/2}$ Hz	$1/T_2$ s^{-1}
100	-	0	-3.5	149	468
80	-	20	(-4.5)	162	509
60	-	40	-1.3	202	635
40	-	60	-0.8	232	729
20	-	80	-0.2	281	883
0	-	100	+0.4[c]	320[c]	1005

[a]Lock Acetone d6. See Table 9 footnote d.

[b]Uncorrected for diamagnetic susceptibilities.

[c]Extrapolated. The $K^+ \cdot 18C6$ complex is soluble less than 0.05 M in 1,3-Dioxolane. See Figure 6.

mixtures (Table 15). Both δ and $\Delta\nu_{1/2}$ vary continuously from pure acetone to acetone-dioxolane (80-20% vol.) and there is no appreciable preferential solvation of the complex (185-187,153), as far as the concept of preferential solvation may be applicable to complexes. The extrapolated values of δ and $\Delta\nu_{1/2}$ in dioxolane are in accordance with the values measured directly at slightly higher temperatures where the $K^+\cdot 18C6$ complex is more soluble (see the points corresponding to $1/T_2$ and δ for $K^+\cdot 18C6$ in dioxolane at the highest $10^3/T$ in Figures 3 and 4 respectively).

The simplest way to determine if complexed ion pairs are responsible for the broad line and the large shift observed is to study the concentration dependence of δ and $1/T_2$ of site B. Unfortunately the present instrumentation does not allow us to use concentrations of less than 0.05 M when the signal is broad. Ion pairing may, however, be studied for the pure salt at low concentration since the signal of the solvated site is narrow (Table 11a). Figure 7 shows the variation of δ and $\Delta\nu_{1/2}$ of K^+ as a function of the $KAsF_6$ concentration in THF and dioxolane solutions. As the concentration increases, the signal broadens and shifts upfield, thus indicating increasing contact ion pairing. In solutions $\sim$0.05 - 0.1 M in both solvents, a large fraction of the salt is associated, as shown by the leveling off of the chemical shift. The very small

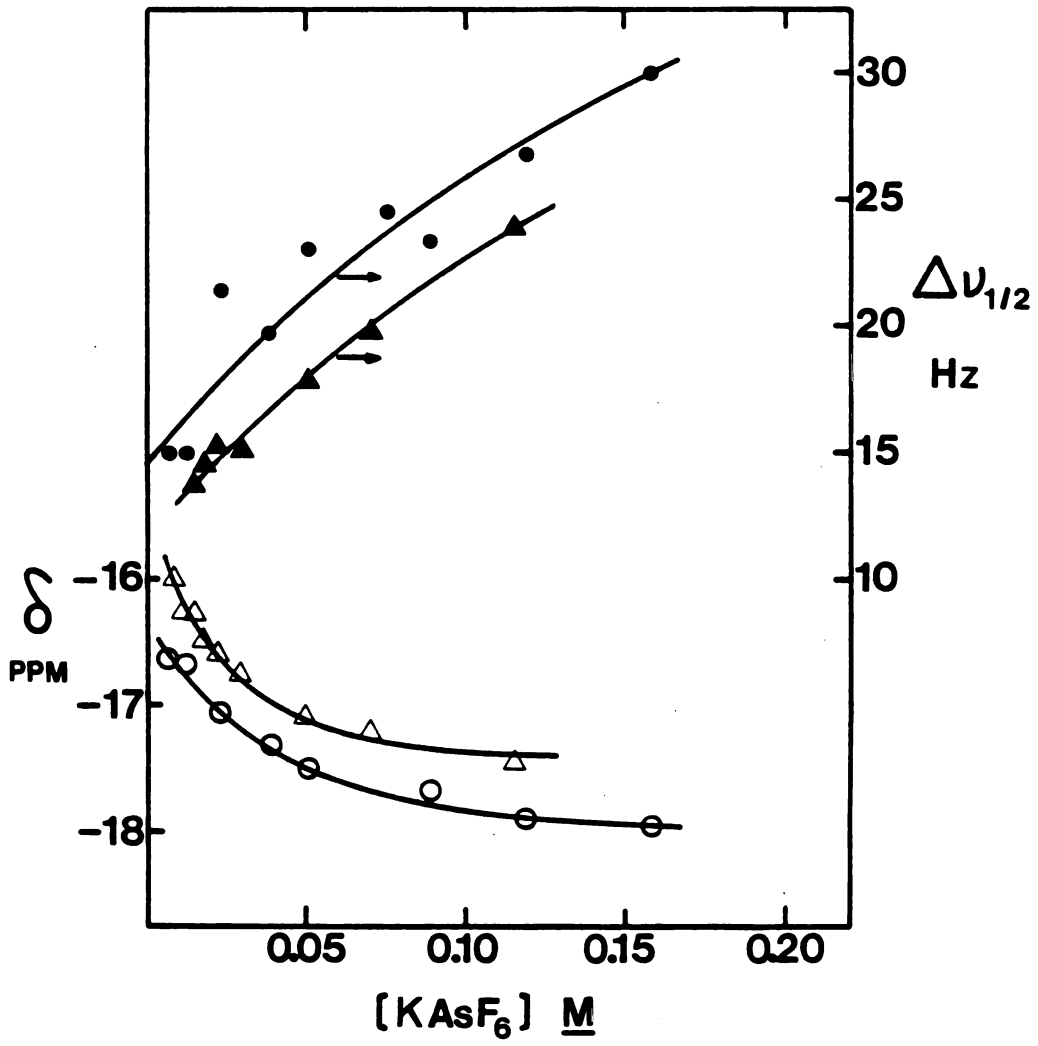

Figure 7. Concentration dependence of the potassium-39 chemical shift and line width for $KAsF_6$ in THF (circles) and 1,3-dioxolane (triangles).

difference in δ and $\Delta\nu_{1/2}$ between THF and dioxolane shows that these solvents provide similar environments for the potassium cation.

Judging from the large upfield shifts in the concentration range 0.007 M - 0.15 M, it can be said that the donor ability of these solvents with respect to K^+ is weak. To be more precise, the signal of K^+ at the lowest concentration studied (0.007 M) in THF is only 4.5 ppm downfield (-16.6 ppm vs -21.1 ppm) from the infinite dilution chemical shift of K^+ in the very weak donor nitromethane (DN = 2.7). The Gutmann donor number of THF is 20.0 (149,150). That of dioxolane has not been measured but a value of 14.7 has been calculated to Griffiths and Pugh (165) from the frequency shift of the O-D vibrational band of methanol-d (188). A lower D.N. for dioxolane than for THF is consistent with the decrease of the basicity of the coordinated oxygen atom due to the presence of a second oxygen in the ring. However, the extent of the decrease seems to depend on the cation considered because steric factors are important for small cyclic ethers (49,55).

Chan et al. (49) found the ratio of the solvent-separated to contact fluorenyl lithium ion pairs to be about 50 times larger in THF than in dioxolane. The authors attributed this behavior to the lower basicity of dioxolane although they pointed out that other factors, such as the stability of the contact ion pair, steric hindrance, and

repulsion between the two oxygen atoms, might be important. Shatenstein et al. (190) measured the concentrations of radical anions, e.g., lithium and sodium biphenyl and sodium naphthalene, formed in a series of ethers. They observed that in going from Li^+ to Na^+ the solvating power of dioxolane increases with respect to THF and 1,4-dioxane. For the sodium salt, 1,3-dioxolane and 1,3-dioxane have the same solvating power which is intermediate between that of THF and that of THP (190).

Our results indicate that the donating abilities of THF and dioxolane for the K^+ ion are comparable and relatively weak. Steric hindrance may indeed explain the low solvating power of dioxolane for the Li^+ ion since it appears that the solvating power of dioxolane increases with respect to THF as the cation size increases.

The chemical shifts of K^+ at infinite dilution, δ_{lim}, in THF and 1,3-dioxolane cannot be obtained from Figure 7, being given the steepness of the curves at low concentration. Several potassium salts soluble up to 0.1 M minimum are needed to calculate δ_{lim} (75). If, as we expect, δ_{lim} is several ppm downfield from -16 ppm (see Figure 7 and Chapter V), the breaking of contact ion pairs should result in a large downfield shift. In this case breaking of contact ion pairs upon complexation by 18C6 could explain the large downfield shift found for the $K^+ \cdot 18C6$ complex in dioxolane at room temperature (Figure 4).

It would also explain the apparent abnormality of the temperature dependence of δ_B in this solvent (Figure 4). As the temperature increases, contact ion pairing in the complex causes a large upfield shift as is found for the uncomplexed salt. This happens only at high temperature probably because the AsF_6^- anion is bulky ($r_{AsF_6^-} \simeq 3$ Å (172)) and cannot easily come into contact with K^+ complexed by 18C6.

2. Kinetics Study in Pure and Mixed Solvents

Kinetics data for the exchange of potassium ions between the solvated site and the $K^+ \cdot 18C6$ complex were obtained from the temperature dependence of the ^{39}K transverse relaxation rates of solutions containing both species. In each solvent a solution containing $KAsF_6$ (or KI) and 18C6 with a $18C6/K^+$ mole ratio (MR) of 0.5 was prepared. Due to the large formation constant of the complex in all the solvents studied, the concentration of the complex was equal to that of the 18C6 added to the salt.

Under our experimental conditions, only one ^{39}K resonance was observed throughout the temperature range covered. This is seen in the middle part of Figure 8 where typical spectra obtained in acetone-1,4-dioxane mixture of the solvated form, the complexed form and the mixture are shown on the left, on the right and in the middle, respectively. Figure 9 shows a typical semilog plot of $1/T_2$

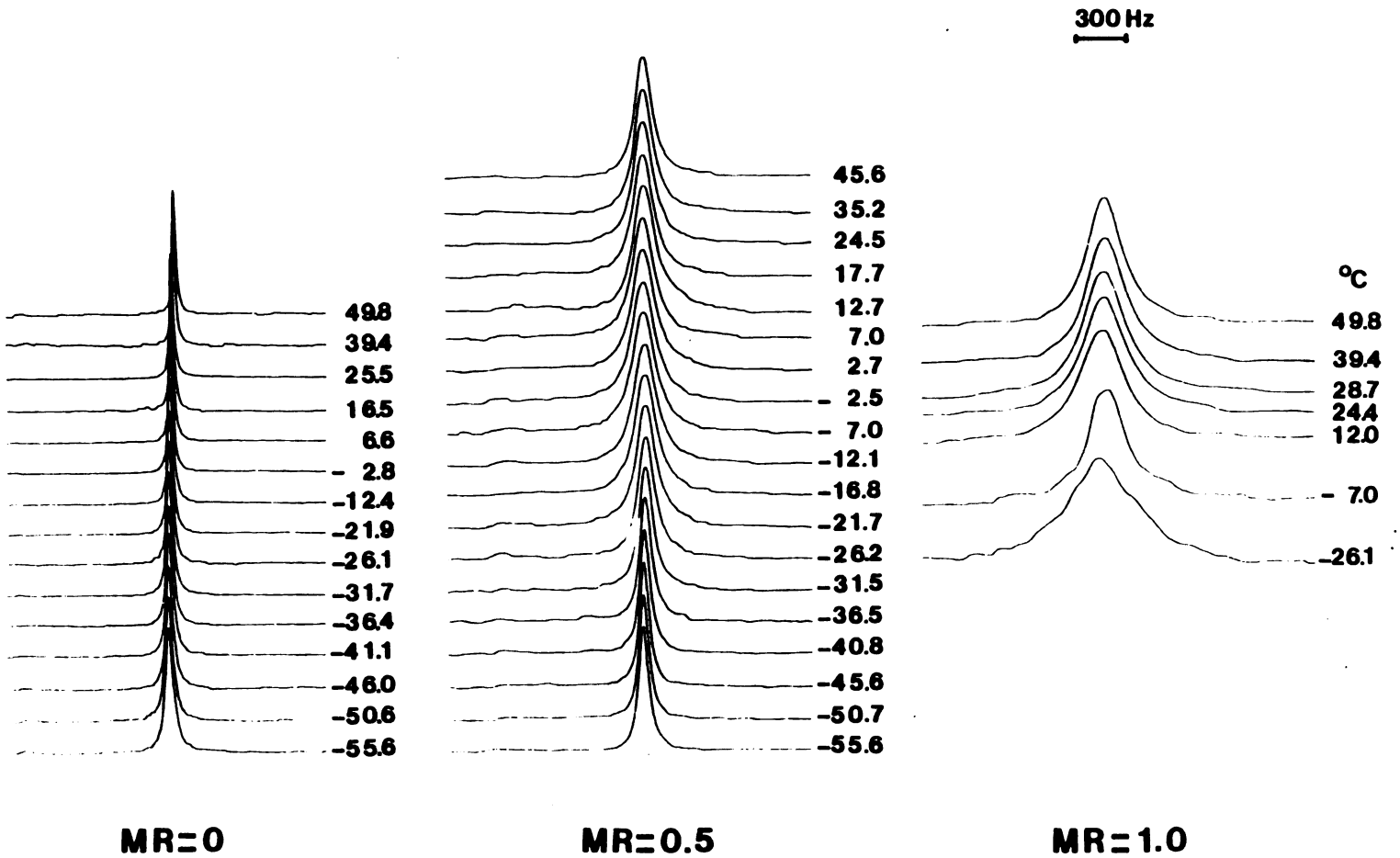

Figure 8. Potassium-39 NMR spectra for solutions containing $KAsF_6$ and 18C6 at various 18-Crown-6/K^+ mole ratios (MR) in acetone-1,4-dioxane (80-20% vol.) at various temperatures.

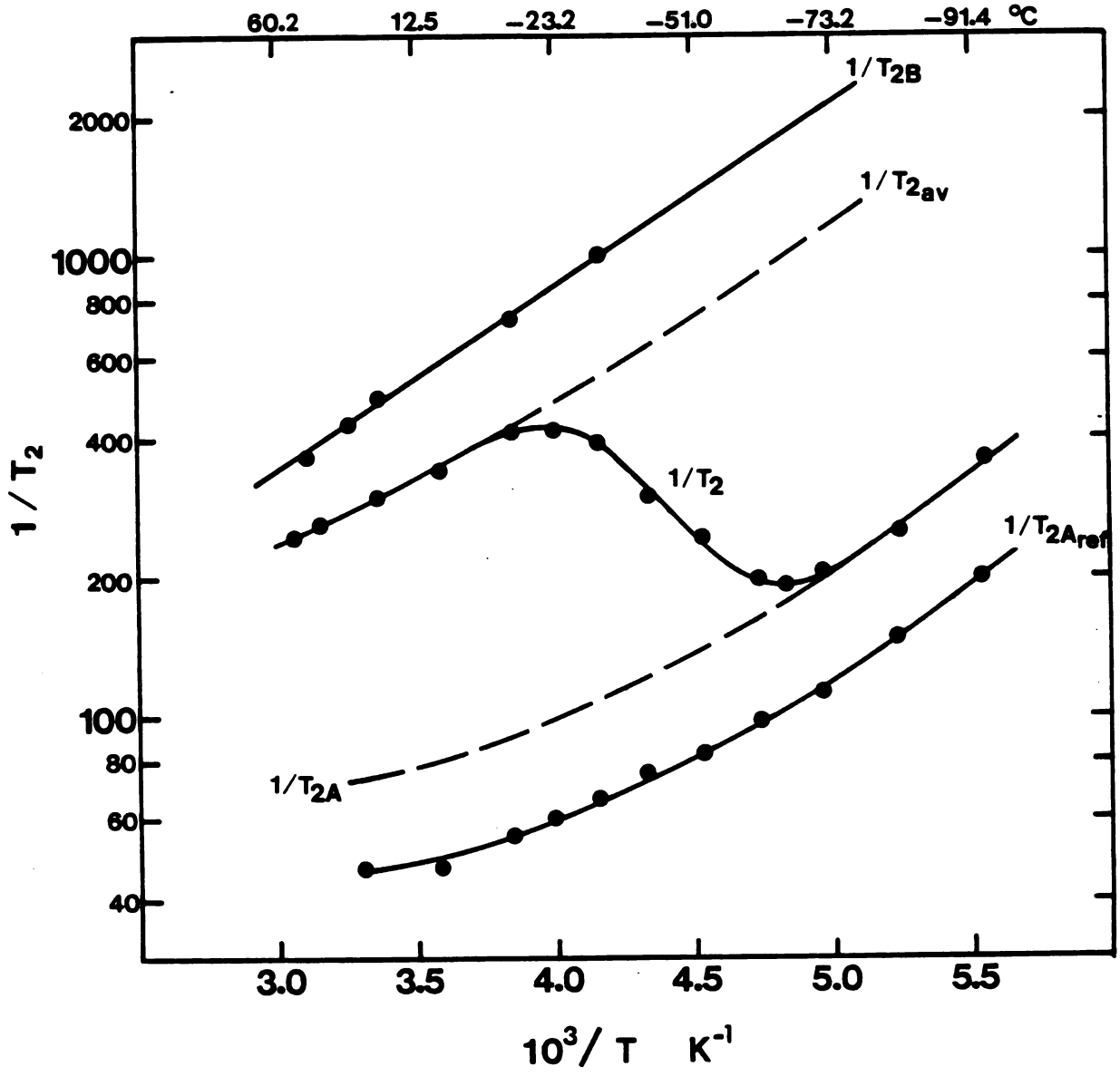

Figure 9. Semilog plots of $1/T_2$ vs $1/T$ for acetone solutions containing $KAsF_6$ and 18C6 at ligand/K^+ mole ratio of 0 ($1/T_{2Aref}$), 0.5 ($1/T_2$) and 1.0 ($1/T_{2B}$).

vs reciprocal absolute temperature for an acetone s lution containing 0.10 M $KAsF_6$ and 0.05 M 18C6. With increasing temperature, $1/T_2$ first decreases then passes through a minimum at ∿-65°C, a maximum at ∿-23°C and again decreases at high temperatures. This behavior indicates a kinetic process in which potassium cations exchange between the solvated (or ion paired) site and the complexed site. Below -70°C the exchange is slow; only one narrow resonance corresponding to the solvated K^+ cation is observed since the signal of the bound site is too broad to be detected. On the other hand, above -10°C the exchange is fast; the NMR spectrum still consists of a single peak, but the observed relaxation rate is the average of the relaxation rates in the two sites. In the intermediate region, from -70 to -10°C, the exchange rate is of the order of the relaxation rates and the kinetic parameters can be derived from the NMR data by line shape analysis. We have seen earlier (Table 14) that at 25°C the difference in chemical shift between site A and site B (40 to 130 Hz) is small or negligible with respect to the relaxation rate of the complexed potassium (400 to 1000 Hz). This is even more so at the low temperatures where the kinetic processes occur.

It is seen from the data collected in Table 16 that the product $(\nu_A - \nu_B)\ T_{2B}$ does not exceed 0.1 in any solvent system studied. In this case the relaxation rate

Table 16. Potassium-39 Chemical Shifts and Transverse Relaxation Rates for the Solvated (Site A) and the Complexed (Site B) K^+ Ions in Various Solvents at the Temperatures Corresponding to the Middle of the Intermediate Region in Each Solvent.

Solvent	t_M[a] °C	t_m[a] °C	$10^3/T$ K^{-1}	δ_A ppm	δ_B ppm	$\nu_A-\nu_B$ Hz	T_{2A}/T_{2B}	$(\nu_A-\nu_B)T_{2B}$
Acetone	-23	-65	4.4	-7.5	∿+2	80	9.5	0.06
Acetone-1,4-Dioxane 80-20 v/v %	- 7	-51	4.1	-8.8	-1.9	58	13.0	0.05
Acetone-THF 80-20 v/v %	-17	?	4.3	-8.3	∿-1	61	∿15	0.05
MeOH	-40	-69	4.6	-4.2	-0.2	34	5.5	0.03
1,3-Dioxolane	+35	- 9	3.5	-14.5	∿0	122	13.2	0.09

[a] t_M and t_m are the temperatures corresponding to the maximum and to the minimum of the $1/T_2$ curve, respectively.

data can be treated by use of relations which omit the chemical shift, which simplifies greatly the data analysis. If the product $(\nu_A - \nu_B)\ T_{2B}$ were large, both the nuclear transfer and the chemical shift would affect the relations describing the transverse relaxation rate $1/T_2$, and make the data treatment more complex. In fact it would have been necessary to measure by a pulse sequence the longitudinal relaxation times which are not affected by the chemical shift. This would have required an enormous amount of time given the low concentrations of solutions used in this study.

A theoretical description of the effects of nuclear transfer on apparent relaxation times has been given by Woessner (62). The actual derivation of the kinetic parameters, which has been done by Shchori et al. (46) for our relatively simple case, is outlined below.

In the absence of a chemical shift between the two magnetic environments the T_2 relaxation curve F(t) is a sum of two exponential functions

$$F(t) = P'_A \exp\left(-\frac{t}{T'_{2A}}\right) + P'_B \exp\left(-\frac{t}{T'_{2B}}\right) \qquad (3)$$

where P'_A, P'_B and T'_{2A}, T'_{2B} are the apparent population fractions and transverse relaxation times, respectively.

The Fourier transform of F(t) is a superposition of two Lorentzian functions

$$I(\omega) = \frac{P'_A\ T'_{2A}}{1 - \omega^2 T'^2_{2A}} + \frac{P'_B\ T'_{2B}}{1 - \omega^2 T'^2_{2B}} \tag{4}$$

where ω is the Larmor frequency of the two sites. The apparent intensities (P'_A, P'_B) and widths ($1/T'_{2A}$, $1/T'_{2B}$) of the two Lorentzian curves are functions of the transverse relaxation rates in the absence of chemical exchange ($1/T_{2A}$, $1/T_{2B}$) and the mean lifetimes of the two species (τ_A, τ_B).

$$P'_A = 1 - P'_B \tag{5}$$

$$P'_B = \frac{1}{2} - \frac{1}{2}\,\frac{(\frac{1}{\tau_B} - \frac{1}{\tau_A})(\frac{1}{T_{2A}} - \frac{1}{T_{2B}}) + \frac{1}{\tau_A} + \frac{1}{\tau_B}}{[(\frac{1}{T_{2A}} - \frac{1}{T_{2B}} + \frac{1}{\tau_A} - \frac{1}{\tau_B})^2 + \frac{4}{\tau_A\tau_B}]^{1/2}} \tag{6}$$

$$\frac{1}{T'_{2A}} = \frac{1}{2}[\frac{1}{T_{2A}} + \frac{1}{T_{2B}} + \frac{1}{\tau_A} + \frac{1}{\tau_B} - [(\frac{1}{T_{2A}} - \frac{1}{T_{2B}} + \frac{1}{\tau_A} - \frac{1}{\tau_B})^2 + \frac{4}{\tau_A\tau_B}]^{1/2}] \tag{7}$$

$$\frac{1}{T'_{2B}} = \frac{1}{2}[\frac{1}{T_{2A}} + \frac{1}{T_{2B}} + \frac{1}{\tau_A} + \frac{1}{\tau_B} + [(\frac{1}{T_{2A}} - \frac{1}{T_{2B}} + \frac{1}{\tau_A} - \frac{1}{\tau_B})$$

$$+ \frac{4}{\tau_A \tau_B}]^{1/2}] \qquad (8)$$

The fractional populations of each site, P_A and P_B, are related to τ_A and τ_B by the equations

$$P_A = \frac{\tau_A}{\tau_A + \tau_B} \quad \text{and} \quad P_B = \frac{\tau_B}{\tau_A + \tau_B} \qquad (9)$$

so that the equilibrium condition may be written as

$$\frac{P_A}{\tau_A} = \frac{P_B}{\tau_B} \qquad (10)$$

For our system T_{2A} is much larger than T_{2B} and P_A is equal to or larger than P_B. It follows from Equations (5-8) that $P'_A T'_{2A} >> P'_B T'_{2B}$. Hence the observed signal $I(\omega)$ given by Equation (4) is a single Lorentzian curve (see Figure 8) with a line width $1/T_2 = 1/T'_{2A}$. It is the apparent resonance of the solvated site. In our experiments, the free induction decay following the pulse was recorded after a time delay of 1200 to 1500 μs in order to allow for a nearly complete decay of the intensity of the broad line due to the complexed potassium. Rearrangement

of Equation (7) (see the derivation in Appendix 3) based on the equilibrium condition (Equation (10)) leads to the following expression for $1/\tau_A$ in the intermediate region

$$\frac{1}{\tau_A} = \frac{(1/T_{2B} - 1/T_2)(1/T_2 - 1/T_{2A})P_B}{1/T_{2av} - 1/T_2} \tag{11}$$

where

$$1/T_{2av} = P_A/T_{2A} + P_B/T_{2B} \ . \tag{12}$$

In the fast exchange region, $1/T_2$ is given by (46),

$$1/T_2 = P_A/T_{2A} + P_B/T_{2B} + P_A P_B(\omega_A - \omega_B)^2\tau \tag{13}$$

where τ is the mean lifetime of the interaction; that is $\tau = \tau_A\tau_B/\tau_A + \tau_B$. In our case the difference $(\tau_A - \tau_B)$ is small so that $1/T_2 = 1/T_{2av}$ at high temperature as seen in Figure 9.

The parameters necessary to compute $1/\tau_A$ can all be read off plots of the type shown in Figure 9. The values of $1/T_{2A}$ in the intermediate region were obtained by the extrapolation of the low temperature values of $1/T_2$ assuming that $1/T_{2A}$ and $1/T_{2Aref}$ have the same temperature dependence. A direct verification of the validity of this assumption was possible at high temperatures where the

values of $1/T_{2B}$ were obtained directly from the spectra. The values of $1/T_{2A}$ calculated from Equation (12) were the same as the extrapolated ones, thus validating our assumption. In general, we did not rely on any other extrapolation than that mentioned above. Unlike Shchori et al. (46,47) and Shporer and Luz (48), we were able to detect the signal of the bound site, due to the following reasons.

(1) The signal of the K^+•18C6 complex is narrower than that of the Na^+ or the K^+.DB18C6 complex, which might be due to the absence of benzene rings that increase the asymmetry of the electric field at the metal nucleus.
(2) We accumulated a very large number of scans - up to 100000 - to obtain certain spectra for the complex. The direct measurement of $1/T_{2B}$ increases the overall reliability of the results since the extrapolation of the high temperature values of $1/T_2$ in order to obtain $1/T_{2av}$ in the intermediate region is no more necessary. In fact this extrapolation is subject to large errors in those solvents where the low and high temperature values of $1/T_2$ do not fall on parallel straight lines due to the curvature of the $1/T_{2A}$ curve (an example is shown in Figure 10).

The procedure used in this kinetics study consists of four steps:

- measurement of the line widths in a large temperature range;

- calculation of $1/\tau_A$ from the relaxation rates with Equation (11);
- computer fitting of the Arrhenius or the Eyring plots to obtain the activation parameters; and
- determination of the exchange mechanism.

We will examine successively the results for the pure solvents and for the mixed solvents.

Pure Solvents

Four pure solvents, acetone, methanol, 1,3-dioxolane and DMF, were investigated. In DMF the ratio T_{2A}/T_{2B} is not large enough to allow quantitative rate data to be obtained. The values of $1/T_2$ measured in the three other solvents are presented in Tables 9-11. Figures 9-11 illustrate the temperature variation of $1/T_2$ for acetone, methanol, and 1,3-dioxolane, respectively. For each solvent the $1/T_{2B}$ and $1/T_{2Aref}$ curves were reproduced from Figure 3. In addition, the temperature dependence of the chemical shift for the samples with a ligand/K^+ ratio of 0.0, 0.5 and 1.0 in methanol is shown in Figure 12. The pattern observed for the chemical shifts closely resembles that for the relaxation rates. In particular, at high temperature the signal for the solution with a mole ratio of 0.5 is half way between the two signals of the solvated and the complexed potassium. This clearly confirms that the

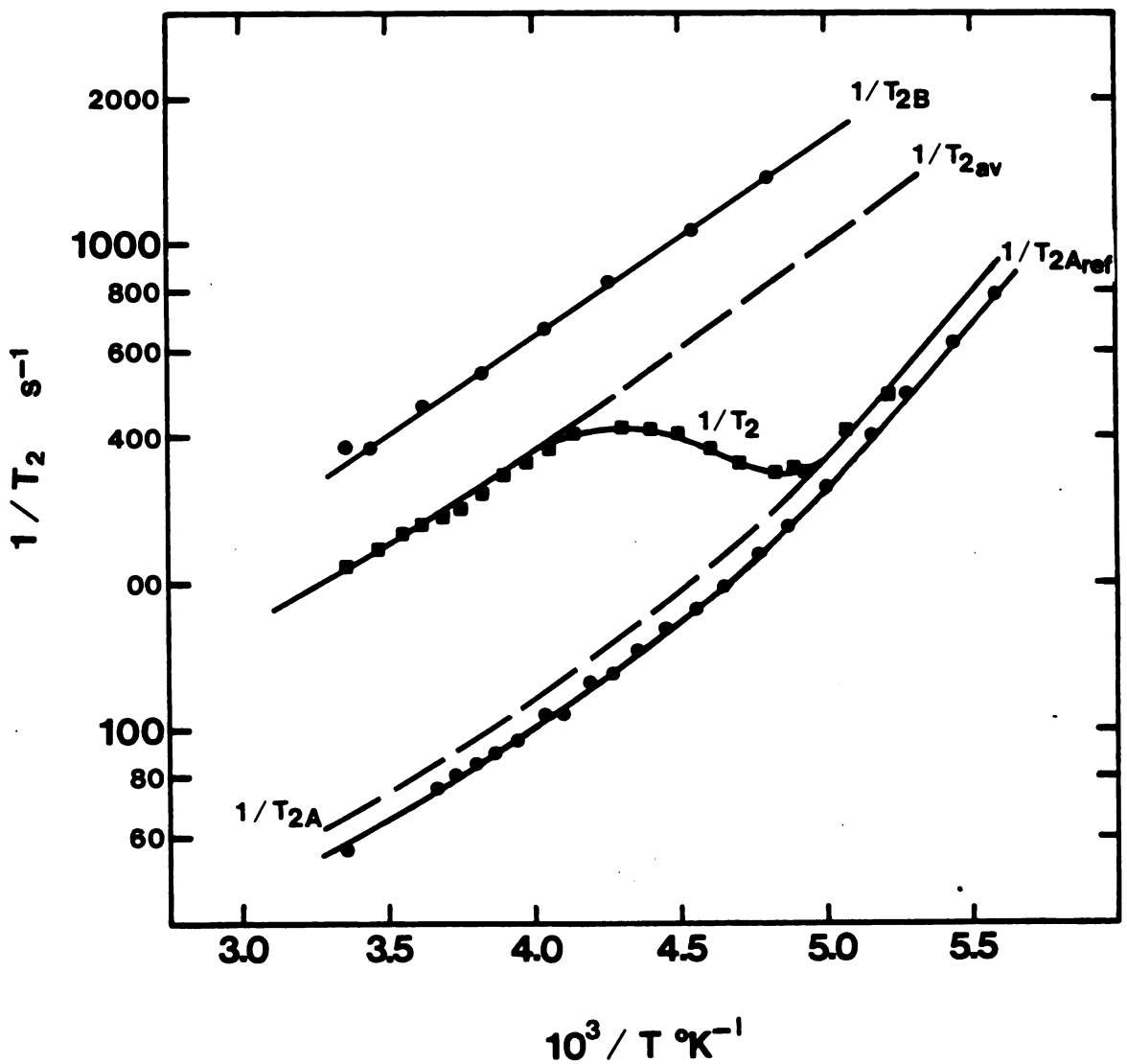

Figure 10. Semilog plots of $1/T_2$ vs $1/T$ for methanol solutions containing KI and 18C6 at ligand/K^+ mole ratio of 0 ($1/T_{2Aref}$), 0.5 ($1/T_2$) and 1.02 ($1/T_{2B}$). The extrapolations of $1/T_{2A}$ and $1/T_{2av}$ are described in the text.

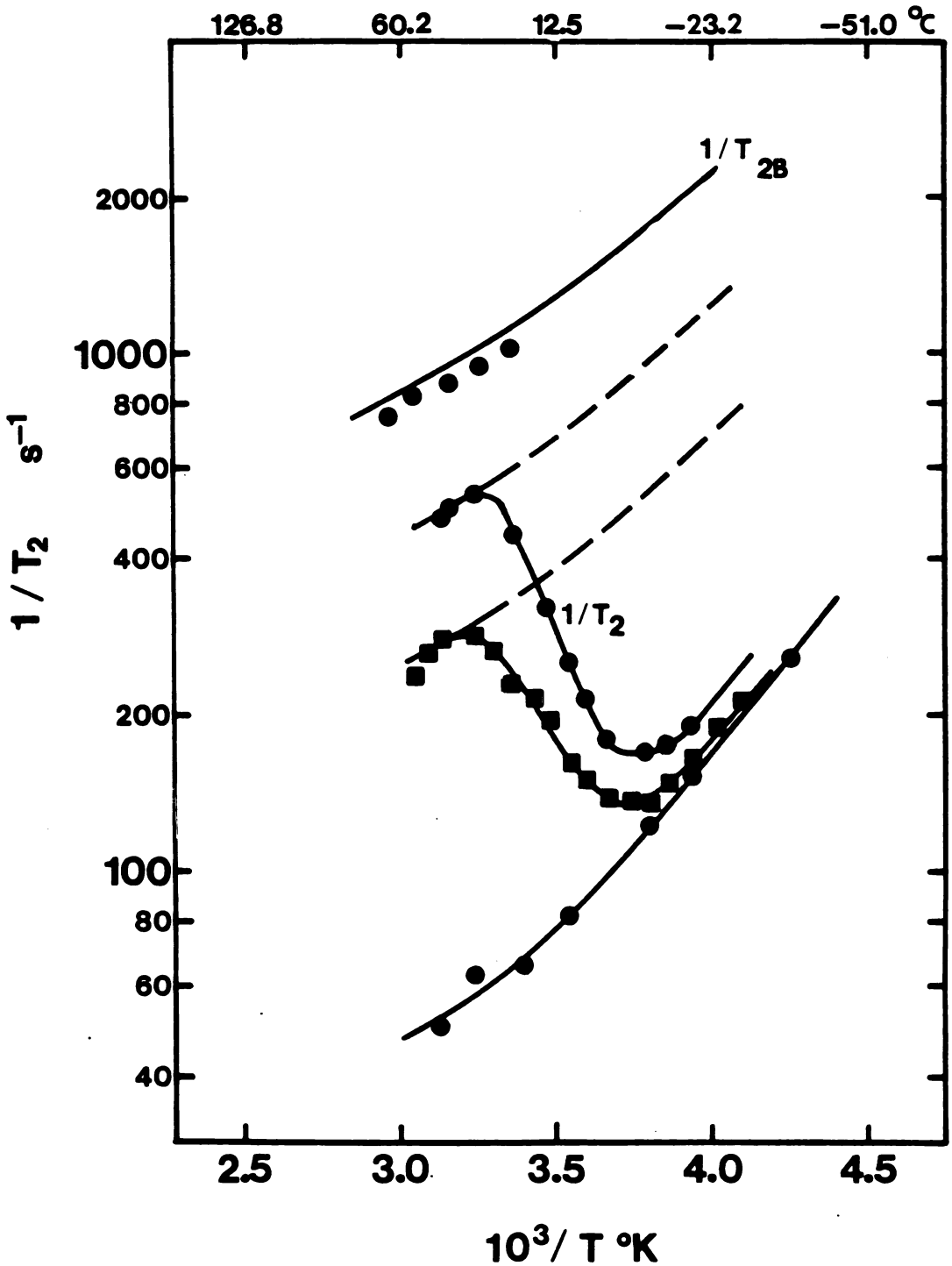

Figure 11. Semilog plots of potassium-39 relaxation rates vs 1/T for 1,3-dioxolane solutions. -Top curve: K^+ 18C6 complex (0.05 M); -Middle full curves: (●) 18C6/K^+ = 0.5 (■) 18C6/K^+ = 0.25; -Lower curve: $KAsF_6$ (0.1 M); -dashed curves: extrapolations of $1/T_{2av}$ (details in the text).

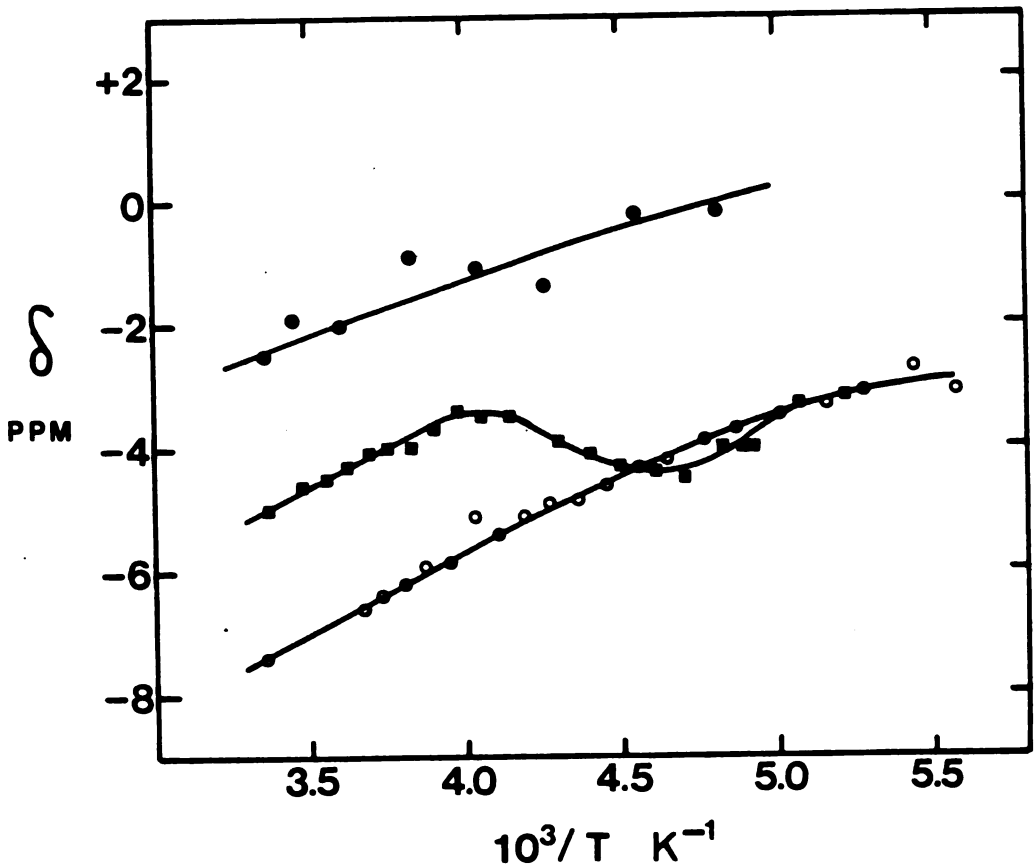

Figure 12. Temperature dependence of the ^{39}K chemical shift in methanol solutions with $18C6/K^+$ ratios of 0 (o), 0.5 (■) and 1.02 (•).

observed kinetic process involves potassium cations exchanging between sites A and B.

The temperatures corresponding to the maximum and the minimum of the $1/T_2$ curve respectively appear in Table 16. Going from acetone or methanol to 1,3-dioxolane the active temperature range is shifted to higher temperatures by about 60°C. With AsF_6^- as the anion, the exchange of K^+ between sites A and B is observable at room temperature in 1,3-dioxolane. This result allows us to propose an explanation for the anion effect reported by Lin and Popov (59).

As mentioned in the historical part, it is observed that in 1,3-dioxolane solutions of $NaBPh_4$ at 25°C, the exchange of Na^+ ions between sites A and B is slow (i.e., the ^{23}Na NMR is not affected by the exchange). It is fast however with perchlorate or the iodide as the anion (59, 148). The formation constant of the $K^+ \cdot 18C6$ complex is between one and two orders of magnitude larger than that of the $Na^+ \cdot 18C6$ complex in H_2O and MeOH (10) and most likely in other solvents too. Bearing in mind that the formation rates of crown ether complexes do not vary to a large extent in going from Na^+ to K^+ (40) we would expect to find the decomplexation rates to be smaller for potassium than for sodium complexes. This is indeed observed with $NaClO_4$ and NaI, but the reverse is found with $NaBPh_4$.

The above behavior is probably due to the difference

in the types of ion pairs formed by sodium salts. We have shown previously that, in 1,3-dioxolane and in THF, $KAsF_6$ forms a tight ion pair. The same observation probably holds for $NaClO_4$ (77) and NaI salts in these solvents. In these cases the anions compete with the ligand 18C6 for the cation, and therefore the complexes are destabilized. This destabilization apparently manifests itself by a marked increase in the decomplexation rates. Conversely, in THF solutions, $NaBPh_4$ is believed to form solvent-separated ion pairs (76,193) which would result in a more stable $Na^+ \cdot 18C6$ complex and in smaller decomplexation rates. The increase of 60°C in the coalescence temperature, T_c, when ClO_4^- or I^- is replaced by BPh_4^- (148) is consistent with this model. The fact that T_c increases by the same amount in THF and in 1,3-dioxolane probably indicates that in both solvents the solvation state of the ion pair for each salt is the same. However it should be noted that differences in specific solvation between Na^+ and K^+ ions may account for some variation in the exchange rates. The THF binds more strongly to Na^+ than to K^+ (55,194). It is noticeable that in 1,3-dioxolane the ^{23}Na NMR signal of the solvated Na^+ ion is several ppm downfield from that of the complex (whatever the salt used), whereas the corresponding ^{39}K NMR peaks are in the reverse order (Table 14). The change in the chemical shift of the complex rather than of the solvated species is responsible for this. The

smaller extent of overlap between the outer orbitals of the Na^+ ion and those of the oxygen atoms of the crown probably accounts for the large upfield shift of the ^{23}Na resonance in the $Na^+ \cdot 18C6$ complex (See Chapter V).

Due to the poor solubility of the $K^+ \cdot 18C6$ complex in 1,3-dioxolane the values of $1/T_{2B}$ were measured in solutions which were 0.05 or 0.04 M whereas the other parameters were measured with solutions containing 0.1 M $KAsF_6$ and various amounts of 18C6. Hence the $1/T_{2B}$ curve, calculated from Equation (12), lies slightly above the experimental points (Figure 11).

The values of $1/\tau_A$ for the three solvents are collected in Tables 17-19. Semilog plots of $1/\tau_A$ vs $1/T$, shown in Figure 13, give straight lines. Activation energies, E_a, are obtained from the slope of these plots (Table 20, first column). The data of Liesegang et al. (42) for the same system in water are inserted in Table 20 for comparison.

The important result is the very strong solvent dependence of the activation energy E_a which varies between 9.2 kcal mol^{-1} and 16.8 kcal mol^{-1}. The lower value found in acetone and methanol solutions slightly exceeds that reported (38) for the $Cs^+ \cdot 18C6$ complex in pyridine (Table 5). It also compares well with the activation energies (Table 5) found for the release of Cs^+ ion from DC18C6 in PC (38) and for the release of Na^+ ion from DC18C6 in methanol (47). The energy barrier to decomplexation is

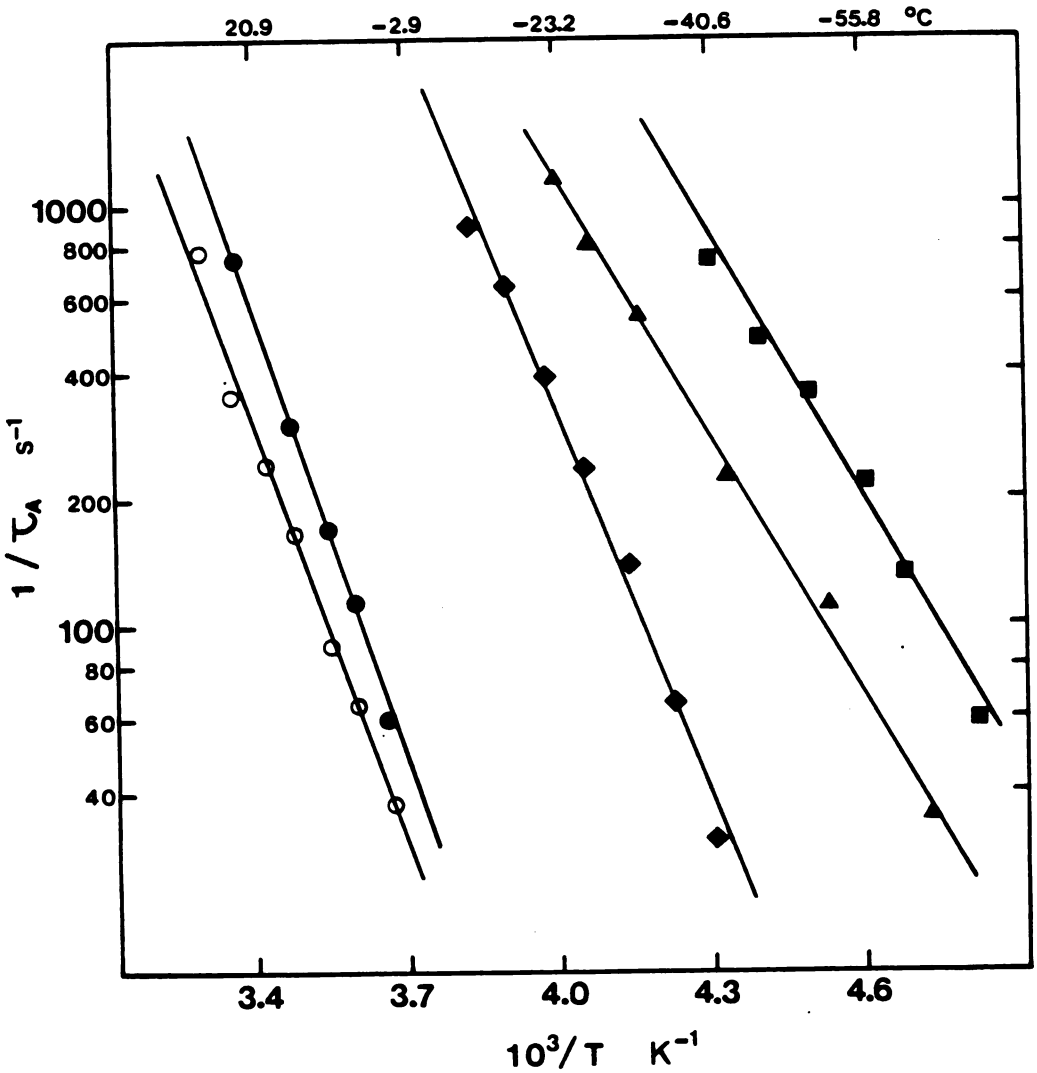

Figure 13. Semilog plots of $1/\tau_A$ vs $1/T$ in various solvents.

- ○ 1,3-dioxolane (sample with $18C6/K^+$ = 0.25);
- ● 1,3-dioxolane (sample with $18C6/K^+$ = 0.50);
- ◆ acetone-1,4-dioxane (80-20% vol.);
- ▲ acetone;
- ■ methanol.

Table 17. Values of $1/\tau_A$ and $1/\tau_A \times [K^+ \cdot 18C6]$ in Acetone in the Intermediate Temperature Region.[a]

$10^3/T$ K^{-1}	$1/T_{2B}$[b] s^{-1}	$1/T_{2A}$[b] s^{-1}	$1/T_2$ s^{-1}	$1/\tau_A$[c] s^{-1}	$1/\tau_A \times [K^+ \cdot 18C6]$ $\underline{M}^{-1}\ s^{-1}$	Sr[d] T
3.997	850	100	415	1142	22840	13
4.163	990	110	393	538	10760	7
4.333	1150	122	298	222	4440	5
4.529	1385	140	242	112	2240	9
4.730	1660	164	198	35	700	22

[a] $[K^+ \cdot 18C6] = 0.05\ \underline{M}$.

[b] These values were interpolated or extrapolated from the values measured at other temperatures (see Table 9 and Figure 9).

[c] Calculated with Equation (11).

[d] Calculated relative standard deviation on $1/\tau_A$ or $1/\tau_A \times [K^+ \cdot 18C6]$ (see Appendix 4).

Table 18. Values of $1/\tau_A$ and $1/\tau_A \times [K^+ \cdot 18C6]$ in Methanol in the Intermediate Temperature Region.[a]

$10^3/T$ K^{-1}	$1/T_{2B}$ s^{-1}	$1/T_{2A}$[b] s^{-1}	$1/T_2$ s^{-1}	$1/\tau_A$[c] s^{-1}	$1/\tau_A \times [K^+ \cdot 18C6]$ $\underline{M}^{-1}$ s^{-1}	Sr[c] %
4.301	840	150	418	734	7340	15
4.396	925	165	412	476	4760	10
4.494	1010	184	408	357	3570	7
4.608	1125	209	377	217	2170	7
4.704	1230	238	352	131	1310	8
4.824	1380	280	336	59	590	15

[a] $[K^+ \cdot 18C6] = 0.1$ $\underline{M}$.

[b] These values were interpolated or extrapolated from data given in Table 10. See extrapolations in Figure 10.

[c] See Table 17 for details.

Table 19. Values of $1/\tau_A$ and $1/\tau_A \times [K^+ \cdot 18C6]$ in 1,3-Dioxolane in the Intermediate Temperature Region.[a]

$10^3/T$ K^{-1}	$1/T_{2B}$[b] s^{-1}	$1/T_{2A}$[b] s^{-1}	$1/T_2$ s^{-1}	$1/\tau_A$[c] s^{-1}	$1/\tau_A \times [K^+ \cdot 18C6]$ $\underline{M}^{-1}\ s^{-1}$	Sr[c] %
$18C6/[K^+] = 0.5$						
3.367	1140	82	443	749	14980	12
3.470	1250	93	320	300	66000	10
3.541	1335	103	251	171	3420	13
3.593	1410	110	214	114	2280	18
3.660	1515	122	179	60	1200	29
$18C6/[K^+] = 0.25$						
3.299	1070	64	264	782	31280	
3.358	1130	68	229	347	13880	
3.428	1200	74	214	244	9760	
3.480	1260	79	192	166	6640	
3.549	1350	87	160	89	3560	
3.602	1420	93	149	64	2560	
3.672	1530	103	138	38	1516	

[a] $[KAsF_6] = 0.1\ \underline{M}$.

[b] Values interpolated or extrapolated from data given in Table 11. See extrapolations in Figure 11.

[c] See Table 17 for details.

Table 20. Activation Parameters and Exchange Rates for K^+ 18C6 Complexes in Various Solvents.

	E_a[a] kcal mol^{-1}	$\Delta H^{\neq}$[b] kcal mol^{-1}	$\Delta S^{\neq}$[b] cal K^{-1} mol^{-1}	$\Delta G^{\neq}$[c] kcal mol^{-1} (298K)	k[d] $\underline{M}^{-1}$ sec^{-1}	Mech.[e]
Acetone	9.2±0.5[f]	8.6±0.5	-4 2	9.8±0.1[g]	(4.1±0.9)x10^5	I
Acetone-1,4-dioxane	13.8±0.5	13.2±0.5	12±2	9 6±0.1	(5.7±1.1)x10^5	I
Methanol	9.2±0.7	8.6±0.7	-3±3	9.5±0.2	(6.8±2.7)x10^5	I
			-8±3	10.9±0.2	(6.8±2.7)x10^4[h]	II
H_2O[i]	10.8	10.2	+3.1	9.3	3.7 x 10^6[h]	II
1,3-dioxolane	16.8±0.3	16.2±0.3	15±1	11.70±0.01	(1.65±0.04)x10^4	I
	15.5±0.7	14.9±0.7	11±2	11.67±0.03	(1.74±0.09)x10^4	I

[a]Arrhenius activation energy. [b]$\Delta H^{\neq}$ and $\Delta S^{\neq}$ are the activation enthalpy and entropy, respectively. [c]$\Delta G^{\neq} = \Delta H^{\neq} - T\Delta S^{\neq}$. [d]$k = 1/\tau_A \times [K^+ \cdot 18C6]$. The values were either directly calculated or extrapolated from the values measured in the active temperature range. [e]See text for description of I and II. [f]Standard deviation estimated by KINFIT. [g]The standard deviation calculated by using the approximate equation $\sigma(\Delta G^{\neq}) \approx |\sigma(\Delta H^{\neq}) - T\sigma(\Delta S^{\neq})|$ (See Reference 54). [h]Units s^{-1}. [i]Reference 42.

somewhat larger in water (10.8 kcal mol^{-1}) although this solvent exhibits a stronger donor character (195). The result obtained in 1,3-dioxolane is the most striking. In this solvent the activation energy is almost twice that found in acetone and methanol solutions. Two different samples (MR = 0.25 and MR = 0.50) gave the two values, 15.5 and 16.8 kcal mol^{-1}, which are in fair agreement considering the narrow temperature range accessible to study in this solvent. The activation energy in 1,3-dioxolane is comparable to the E_a values reported for some very stable cryptates such as Li^+•C211 (35) and Na^+•C222 (34) in various solvents (Table 4). It also approaches the high E_a value of 18 ± 1 kcal mol^{-1} found for the decomplexation of $tBuNH_3^+$ from 18C6 in $CDCl_3$ (51).

The exchange of K^+ ion between sites A and B may proceed via two mechanisms: the bimolecular exchange process (I) and the dissociative mechanism (II).

$$*K^+ + K^+\cdot 18C6 \underset{k_{-1}}{\overset{k_1}{\rightleftarrows}} *K^+\cdot 18C6 + K^+ \qquad \text{I}$$

$$K^+ + 18C6 \underset{k_{-2}}{\overset{k_2}{\rightleftarrows}} K^+\cdot 18C6 \qquad \text{II}$$

Since these two mechanisms may contribute to the overall potassium ion exchange, the general expression for

the reciprocal mean lifetime of the solvated species (46) is:

$$1/\tau_A = k_1[K^+\cdot 18C6] + k_{-2}[K^+\cdot 18C6]/[K^+] \qquad (14)$$

The contributions of mechanisms I and II may be determined by plotting $1/\tau_A[K^+\cdot 18C6]$ vs $1/[K^+]$. This was done for 1,3-dioxolane. The values of $1/\tau_A$ were measured for two samples with $18C6/K^+ = 0.25$ and 0.5 respectively (see Figure 11 and Table 11). The ionic strength was kept constant (0.1 M), since rates of reactions between ionic species may be strongly affected by the ionic strength of the solution; there is also a small ionic strength effect on the rates of reactions between ions and neutral molecules (196a). The values of $1/\tau_A$ were not obtained exactly at the same temperatures in the two samples; therefore they were read from the computer fitted Arrhenius plots shown in Figure 13, at several temperatures. The plot of $1/\tau_A[K^+\cdot 18C6]$ vs $1/[K^+]$ is shown in Figure 14. The values of $1/\tau_A[K^+\cdot 18C6]$ are constant within experimental error. This indicates that the contribution of mechanism II to the exchange is negligible (any contribution of mechanism II would show as a positive slope in the plot). Hence the Arrhenius plots of Figure 13 yield the activation energy for the exchange and not for the release of K^+ ion from 18C6.

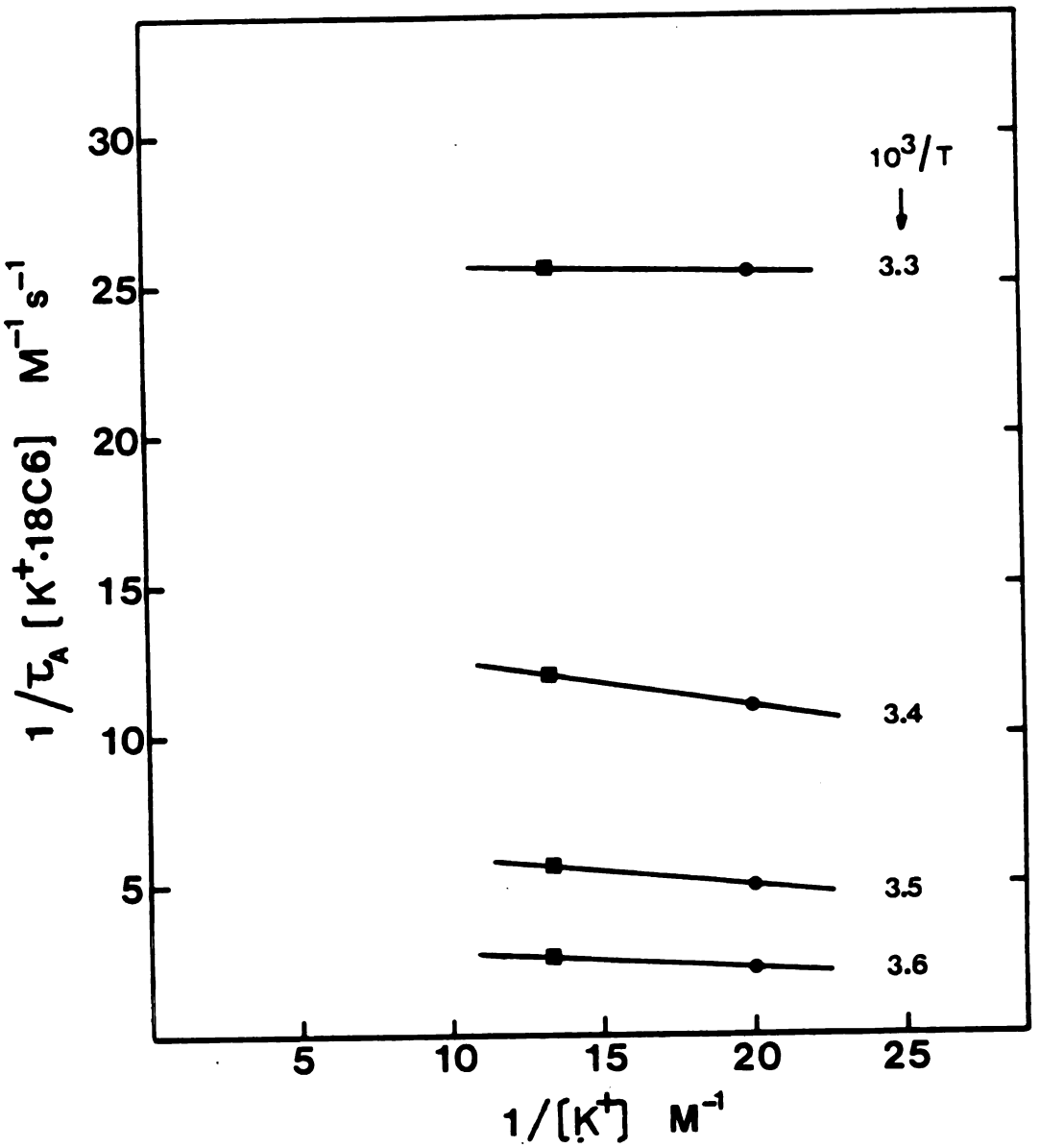

Figure 14. Plot of $1/\tau_A$ x [K^+·18C6] vs $1/[K^+]$ in 1,3-dioxolane at various temperatures.

This result was unexpected because for all alkali crown ether complexes for which it has been tested the cation exchange proceeds via the dissociative mechanism II (89). For example Liesegang et al. (42) reported that for the $K^+ \cdot 18C6$ complex in water, where the decomplexation rates are much faster than in 1,3-dioxolane (Table 20), mechanism II - coupled with a conformational rearrangement of the crown - best fits their ultrasonic relaxation data. Thus the solvent effect is two fold. In comparison with water, 1,3-dioxolane considerably reduces the dissociation rates and changes the mechanism.

In this respect it is interesting to note that for the system $tBuNH_3^+ \cdot 18C6/CDCl_3$ already mentioned (51) mechanisms I and II both contribute to the exchange but at 20°C the decomplexation rate, k_{-2}, is very small ($60 \pm 10\ s^{-1}$) while the exchange rate k_1 is large ($1.5 \times 10^6\ \underline{M}^{-1}\ s^{-1}$). Also, in the case of the system $Fl^- Na^+ \cdot$dimethyl-DB18C6/ THF-d_8, Wong et al. (55) postulated that the mechanism I is operative and calculated the exchange rate to be $3200\ \underline{M}^{-1}\ s^{-1}$ at 2°C. Other workers (45) observed that the exchange rates are small in ethereal solvents and in $CDCl_3$.

The two aspects of the solvent effect on the complexation kinetics are probably related in the following way; when the energy barrier to decomplexation becomes very large it may eventually reach a point where lower energy pathways become available. In our case the lower energy

route is the bimolecular exchange with a symmetrical energy profile.

This last mechanism was not encountered for cryptates even when the activation energy for the release of the metal ion from the ligand molecule is very large. However, the mechanism does not seem to have been tested in THF and pyridine in which solvents the decomplexation rates are small (34) and mechanism I is the most likely to participate to the cation exchange. It could be argued that even in these solvents the contribution of mechanism I is probably small because one cation must leave the cryptand cavity before another one can move in.

The case of 18C6 is different. The molecule is symmetrical and the probabilities of access of the cation to the 18C6 binding sites from the "top" and from the "bottom" of the molecule are identical. This might favor mechanism I. However, this mechanism is not favored on electrostatic grounds since it requires a collision between like charges.

The mechanism was tested in acetone by the same method. The measurements at a mole ratio of 0.25 were not as accurate as those at a mole ratio (MR) of 0.50. A rough calculation for the former sample yielded an activation energy of 10.6 kcal mol^{-1}. This value is larger by 1.4 kcal mol^{-1} than the value obtained with MR = 0.5. We feel that the value of E_a reported in Table 20, 9.2 kcal mol^{-1}, is the more reliable. As in 1,3-dioxolane, our data

strongly favor mechanism I.

The mechanism was not tested in methanol. It would be rather difficult to do so because the ratio T_{2A}/T_{2B} is not very large in this solvent (Figure 10 and Table 10). For a sample at MR < 0.5 the differences of relaxation rates involved in Equation (11) would be small and therefore subject to a large relative error. Besides, the active temperature range is quite narrow. We can, however, speculate on the mechanism. Assuming that the measured activation energy, 9.2 kcal mol^{-1}, is for the decomplexation step (mechanism II), we can calculate the rate of release of K^+ from 18C6 at 25°C by extrapolation of the low temperature values. Using k_{-2} = 131 s^{-1} at -60.6°C (Table 18) with E_a = 9.2 kcal mol^{-1}, we obtain k_{-2} = 6.8 x 10^4 s^{-1} at 25°C. This value combined with Lamb's (197) complexation constant $K_f = 10^{6.05}$ yields k_2 = 7.6 x 10^{10} $\underline{M}^{-1}$ s^{-1} which is about one order of magnitude larger than the theoretical value for a diffusion-controlled reaction in methanol (22,39). There are two plausible explanations. As noted by Liesegang <u>et al</u>. (39) in a similar case, the k_{-2} and E_a values may not lend themselves to an extended extrapolation (-61 → +25°C in our case). In other words E_a may vary with temperature. Another possibility is that mechanism I contributes to the exchange. Both factors may act in the same direction.

It seems reasonable to say that in general the slower

the dissociation of the complex, the more likely the contribution of mechanism I to the cation exchange. The results of the kinetics study in mixed solvents will shed some light on the behavior of ethereal solvents.

Mixed Solvents

The spectra obtained in acetone-dioxane (80/20 v/v%) and acetone-THF (80/20 v/v %) are shown in Figures 8 and 15, respectively. For the latter mixture the signal-to-noise ratios are relatively low, since only a few minutes were available for the measurement before the complex precipitates (see Table 13, Footnote d). The relaxation rates and chemical shifts appear in Tables 12-13. Semi-log plots of $1/T_2$ vs $1/T$ for each mixture are shown in Figures 16 and 17 where the results in pure acetone are reproduced for comparison.

In both cases the presence of ethereal solvent in the mixture shifts the kinetic process to higher temperatures and increases the activation energy, which is related to the absolute slope of the $1/T_2$ curve in the intermediate region. These effects are more pronounced with 1,4-dioxane than with THF.

Due to the precipitation of the complex, the low temperature portion of the $1/T_2$ curve for the THF containing mixture could not be obtained. As a result the $1/T_{2A}$ values are missing. This precludes the calculation of

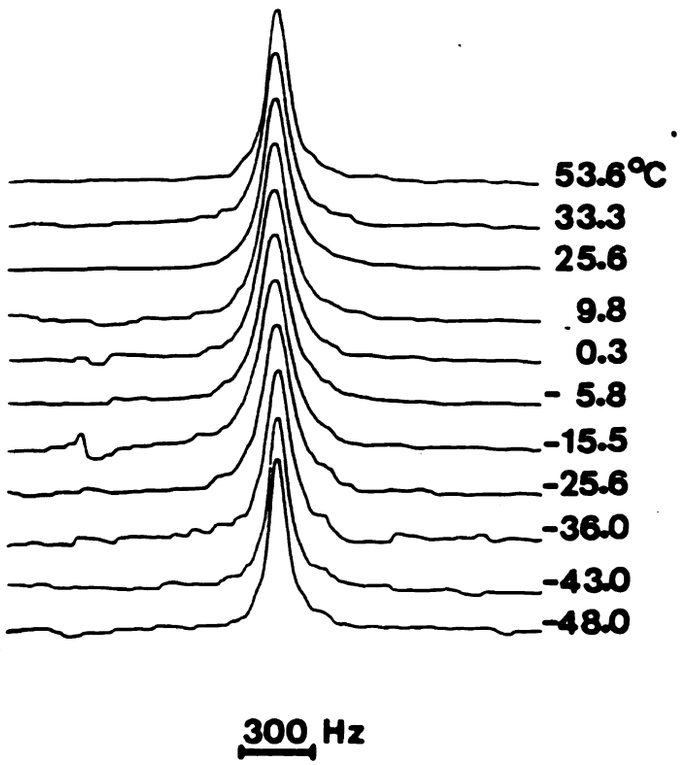

Figure 15. Potassium-39 NMR spectra for solutions containing 0.10 M $KAsF_6$ and 0.05 M 18C6 in acetone-THF (80-20% vol.) at various temperatures.

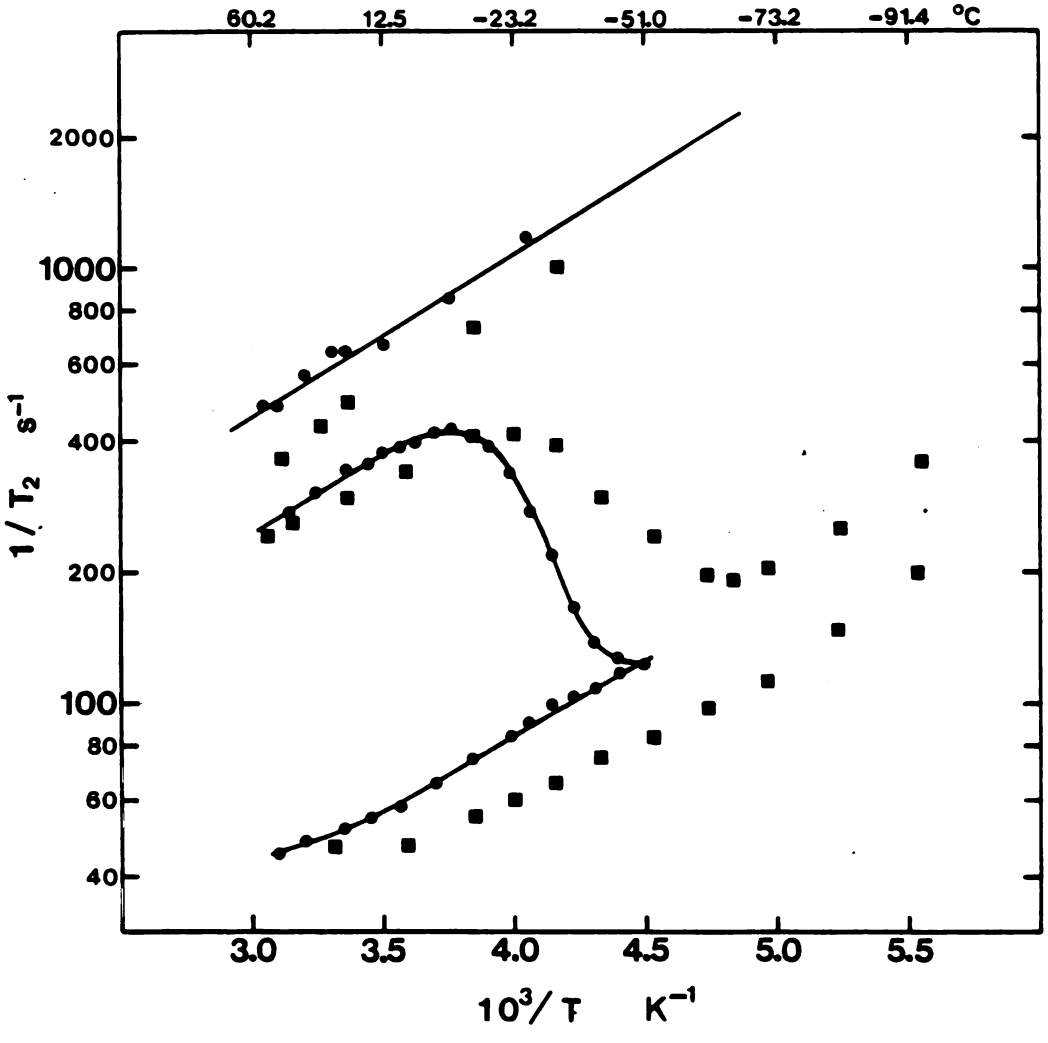

Figure 16. Semilog plots of $1/T_2$ vs $1/T$ for (■) acetone and (●) acetone-dioxane (80-20% Vol.) solutions containing 0.1 M $KAsF_6$ (bottom curves), 0.1 M $KAsF_6$ + 0.05 M 18C6 (middle curves), 0.1 M $KAsF_6$ + 0.1 M 18C6 (top curves).

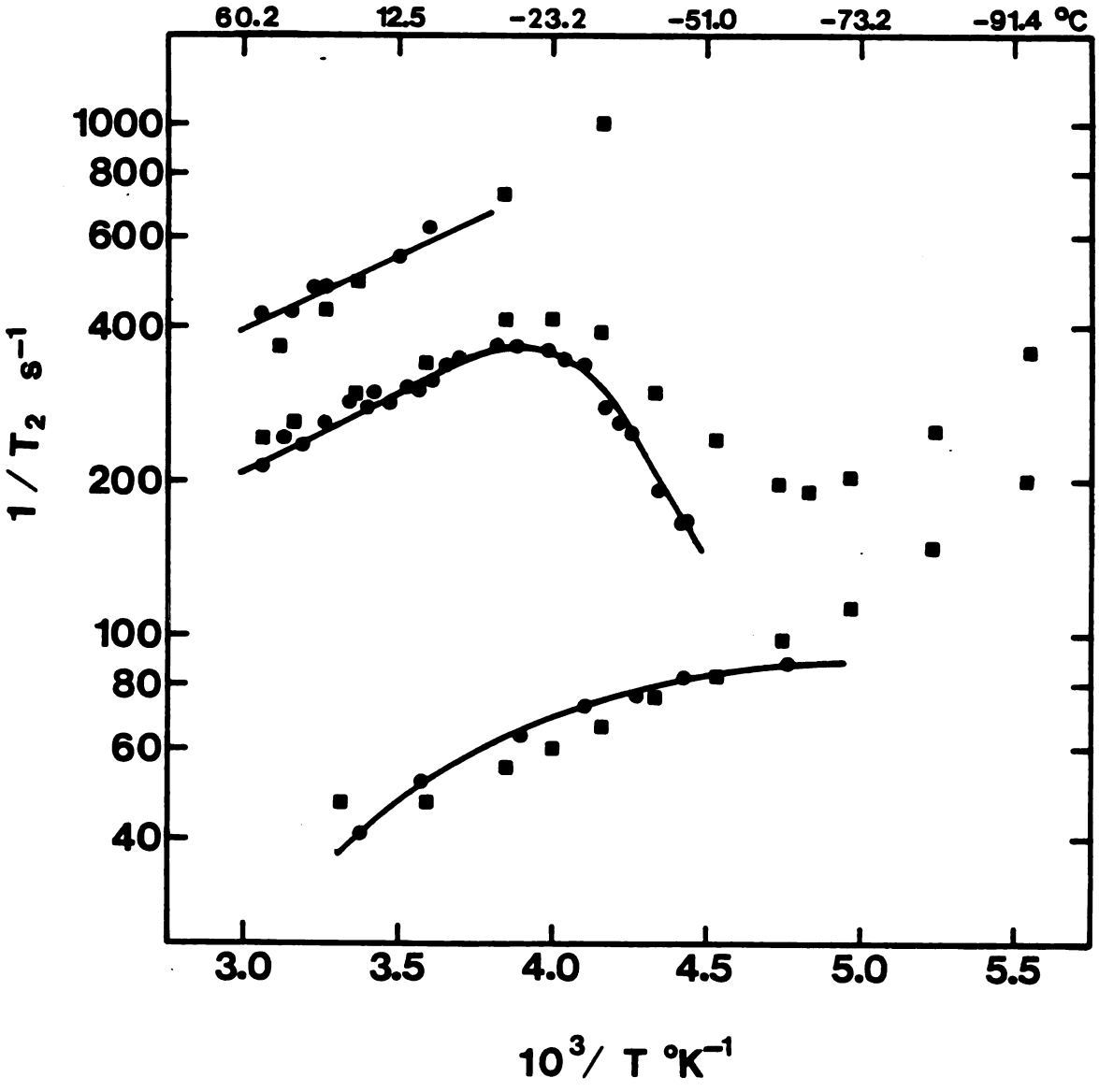

Figure 17. Semilog plots of $1/T_2$ vs $1/T$ for (■) acetone and (●) acetone-THF (80/20% vol.) solutions containing 0.1 M $KAsF_6$ (bottom curves), 0.1 M + 0.05 M 18C6 (middle curves), 0.1 M $KAsF_6$ + 0.1 M 18C6 (top curves).

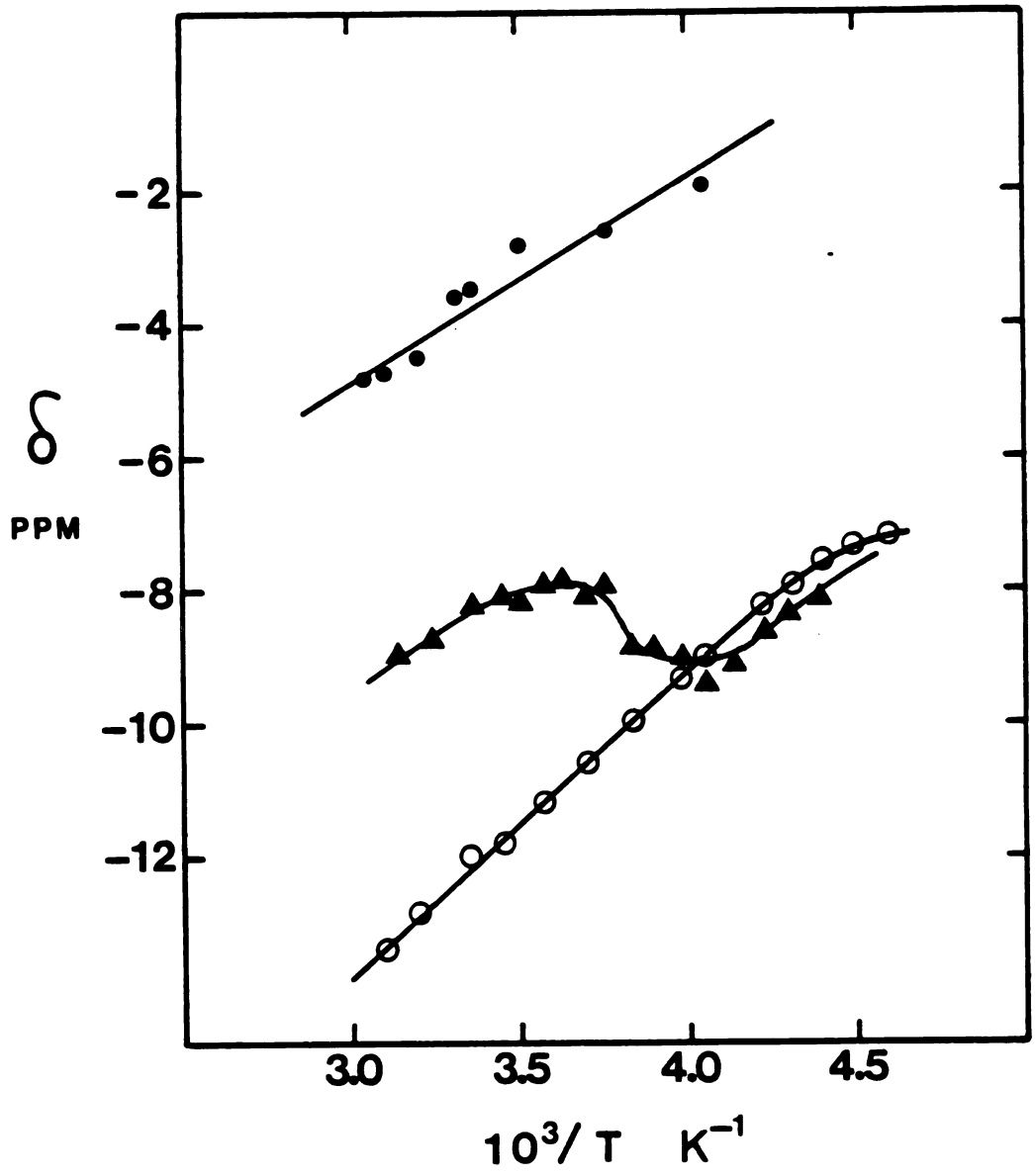

Figure 18. Temperature dependence of the ^{39}K chemical shifts in acetone-dioxane (80/20% vol.) solutions.
○ $18C6/K^+ = 0$;
▲ $18C6/K^+ = 0.5$;
● $18C6/K^+ = 1.0$.

Table 21. Values of $1/\tau_A$ and $1/\tau_A \times [K^+ \cdot 18C6]$ in Acetone-1,4-Dioxane (80/20% vol.) in the Intermediate Temperature Region.[a]

$10^3/T$ s^{-1}	$1/T_{2B}$[b] s^{-1}	$1/T_{2A}$[b] s^{-1}	$1/T_2$ s^{-1}	$1/\tau_A$[c] s^{-1}	$1/\tau_A \times [K^+ \cdot 18C6]$ $\underline{M}^{-1}\ s^{-1}$	S_r[d] %
3.757	890	71	430	1635	32700	23
3.830	955	75	412	888	17760	11
3.900	1005	79	391	634	12680	7
3.976	1075	85	339	388	7760	5
4.055	1150	91	276	235	4700	5
4.137	1230	98	220	139	2780	6
4.225	1330	104	166	65	1300	10
4.303	1420	108	138	31	620	16

[a] $[K^+ \cdot 18C6] = 0.05\ \underline{M}$.

[b] These values were interpolated or extrapolated from the values measured at other temperatures (see Figure 16).

[c] Calculated with Equation (11).

[d] Calculated relative standard deviation on $1/\tau_A$ or $1/\tau_A \times [K^+ \cdot 18C6]$. (See Appendix 4.)

the activation energy for this solvent system.

The dioxane-containing mixture is more amenable to a quantitative study since the values of $1/T_2$ could be measured down to the minimum of the $1/T_2$ curve. It is noticeable that the two curves $1/T_2$ and $1/T_{2Aref}$ meet at this minimum. This is not found in acetone (Figure 16) which is the only solvent studied in which the addition of 0.05 M 18C6 markedly increases the relaxation rates of the solvated K^+ cations. The temperature dependence of the chemical shifts in the mixture is illustrated in Figure 18. The variation of δ is steeper for site A than for site B ($\sim$6 ppm vs $\sim$4 ppm/100°C); for each site it is steeper than the corresponding variation in methanol (Figure 12). The values of $1/\tau_A$ and $1/\tau_A[K^+\cdot 18C6]$ are given in Table 21. The semilog plot of $1/\tau_A$ vs $1/T$, shown in Figure 13, yields an activation energy E_a of 13.8 kcal mol^{-1}. Thus E_a increases by 4.6 kcal mol^{-1} between acetone and the acetone-dioxane mixture. This is a very large increase if we consider that the mole fraction of dioxane is only 0.18. It confirms the results obtained in dioxolane that the presence of ethereal solvents drastically increases the activation energy. The dielectric constant of the mixture is about 16 instead of 20.7 for pure acetone. Besides, 1,4-dioxane is a poor donor solvent so that we can expect a larger population of contact ion pairs (for the uncomplexed potassium) in the mixture than in acetone. The

ion pairing would tend to destabilize the complex and, as seen earlier, to increase the decomplexation rates. On the other hand, the lower donicity of dioxane as compared to acetone would tend to stabilize the complex and perhaps to reduce the decomplexation rates. Thus, the two factors are competing. However, what is observed by NMR is the exchange process not the decomplexation step so that we cannot use these arguments to interpret the kinetic parameters.

General Discussion

The treatment of the exchange rates with the absolute rate theory of Eyring (198, 64) yields the activation parameters given in Table . The expression used for the exchange rate is

$$k_1 = \frac{k_B T}{\hbar} e^{-\frac{\Delta G^{\neq}}{RT}} \qquad (15)$$

where k_B is the Boltzmann constant, $\hbar$ is the Planck constant and $\Delta G^{\neq} = \Delta H^{\neq} - T\Delta S^{\neq}$. The other symbols have their usual meaning. It was assumed that mechanism I is operative in all solvents except methanol. In this solvent the activation parameters calculated assuming mechanism I or mechanism II are given in Table 20.

Inspection of Table 20 reveals that the large

differences in activation energy of exchange between acetone-dioxane and 1,3-dioxolane on one hand, acetone and methanol on the other hand, are not reflected in the free activation energies which are all close to 10 kcal mol^{-1}. Hence the exchange rates vary only by a factor 50 at room temperature. Differences in activation entropies account for this fact. While the activation entropy is -4 cal mol^{-1} deg^{-1} in acetone and -3 cal mol^{-1} deg^{-1} in methanol, it is +12 cal mol^{-1} deg^{-1} in acetone-dioxane and +15 cal mol^{-1} deg^{-1} in 1,3-dioxolane. Thus the effect on $\Delta S^{\neq}$ of adding 20% dioxane to acetone is almost as large as that of replacing acetone by 1,3-dioxolane. Between acetone and acetone-dioxane, the compensation of the difference in $\Delta H^{\neq}$ by the difference in $\Delta S^{\neq}$ is total. Such a compensation effect is not uncommon (65). For example, it had been observed (35) in the case of the $Li^{+}\cdot$C211 cryptates in various solvents.

The activation entropy for the release of K^{+} ion from 18C6 (mechanism II) is positive in water (3.1 cal mol^{-1} deg^{-1}). A similar value was found in the case of Li^{+} and Na^{+} cryptates; it probably reflects a participation of the solvent in the transition state (34,35). More interesting are the large positive activation entropies found in 1,3-dioxolane and in acetone-dioxane. For macrocyclic complexes in nonaqueous solvents, such large values have only been encountered for the release of Cs^{+} from

C222 in DMF and C222B in PC (37). Since mechanism I is applicable to our system, the overall entropy change is zero, so that we cannot relate the $\Delta S^{\neq}$ values to the corresponding thermodynamic parameters.

The activation enthalpies are a little more tractable, since they are related to the interactions between the species present. In reactions between ions, the electrostatic interactions predominate. In our system, changes in the enthalpies of solvation of the reactant cations from one solvent to another should not affect the reaction rates significantly, because the solvent systems used exhibit relatively poor donor character as seen from the upfield shifts of the solvated K^+ ions (Figure 4). We have seen earlier that the complexation of K^+ with 18C6 in dioxolane involves the breaking of contact ion pairs (below $\sim$40°C). The most likely transition state for mechanism I is the symmetrical "complex" represented by $K^+ \cdot 18C6 \cdot K^+$. If the ion pairs are broken in the transition state, a large amount of Coulombic interaction has to be spent in going from the reactants to this transition state. This would account for the large $\Delta H^{\neq}$ in 1,3-dioxolane. The same explanation probably holds for the acetone-dioxane mixture. In addition, in these two cases where the uncomplexed potassium salt exists as a contact ion pair, the solvent does not assist the exchange. The increase in $\Delta H^{\neq}$ due to this second factor may even be predominant. The large $\Delta H^{\neq}$ values point to a

"loose" transition state, as pictured below. Since the exchange mechanism resembles the SN2 type mechanism, this "looseness" implies that bond-breaking must occur prior to bond-forming (199).

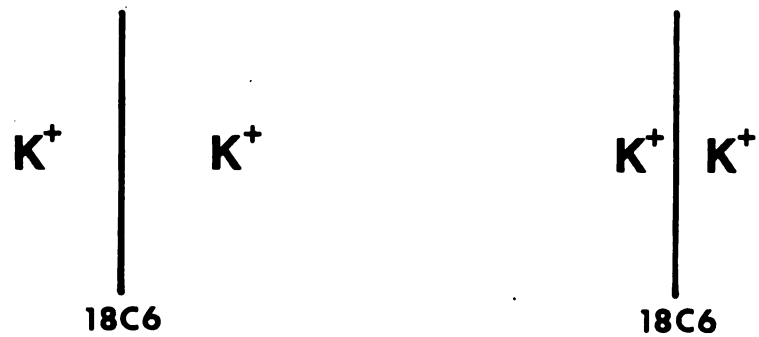

"loose" transition state "tight" transition state

In the low polarity solvents, strong Coulombic forces such as cation-cation repulsion and cation-anion attraction would tend to favor such a "loose" transition state. However, the large repulsive forces between the two like charges in the transition state are likely not to change in a large extent from one solvent to another, since the local dielectric constant is expected to vary much less than the bulk dielectric constant. The large $\Delta S^{\neq}$ value associated with a "loose" transition state might arise partly from the ligand conformational entropy. If the cations are not tightly bound to the ligand in the transition state, the faster segmental motion of the ether

fragments as compared to that in the complex (45) should increase the conformational entropy.

D. Conclusion

The kinetic parameters for the $K^+ \cdot 18C6$ complex are very sensitive to the solvent medium. In ethereal solvents and probably also in acetone and methanol, the cation exchange between the solvated and the complexed forms proceeds via a bimolecular process. The very large activation energies found in the former solvents are compensated by differences in activation entropies. As a result the exchange rates at 25°C do not vary in a large extent. Changes of solvent exert their influence on $\Delta H^{\neq}$ in a rather complex manner although ion pairing effects seem to be predominant. The variations in $\Delta S^{\neq}$ are difficult to interpret and quite generally follow the variations in $\Delta H^{\neq}$ so as to minimize $\Delta G^{\neq}$. Kinetics studies in solvent mixtures offer an interesting perspective for studying the various factors responsible for the solvent effect.

CHAPTER IV

MULTINUCLEAR NMR STUDY OF THE FREE CRYPTAND C221 AND OF THE C221·K^+ CRYPTATE

A. Carbon-13 NMR Study of the Solvation and the Conformation of Cryptand 221

I. Introduction

The solvation of ligands is generally believed to be much less important than ionic solvation (222). As a result, the former has received less attention than the latter. However, in the case of tetraaza ligands, Hinz and Margerum (223,224) proposed that the "macrocyclic effect" (225) is due to the weaker solvation of the macrocyclic ligands as compared to open-chain ligands with the same donor groups. In protic solvents, hydrogen bonding is likely to play an important role in the solvation of basic ligands such as tetraaza ligands and cryptands (106,224). The situation is far from clear in the dipolar aprotic solvents. Conformational entropy as well as solvent ordering differ from solvent to solvent and can alter the "enthalpic" selectivity.

The negative entropy associated with the formation of most cryptates in nonaqueous solvents is composed of several terms, such as the release of solvent molecules from the cation and the ligand solvation shells (entropy increase), changes in the ligand conformational

entropy (entropy decrease). Therefore it was of interest to us to study these two somewhat related factors. Several techniques must be used to collect the conformational information and the thermodynamic parameters.

The purpose of this study was to investigate by ^{13}C NMR the interaction of the free and the complexed cryptand 221 with a large number of solvents.

2. Results and Discussion

The cryptand C221 has three sets of $O\underline{C}H_2$ carbons in the 38-42 ppm region and two sets of $N\underline{C}H_2$ carbons in the 24-29 ppm region (with respect to the methyl carbons of acetone-d6). In this discussion we will be mostly interested in the $N\underline{C}H_2$ carbons (C(4) and C(5)) since the assignment of the $O\underline{C}H_2$ peaks is not definitive yet.

The spectrum of the C221·K^+ cryptate (Figure 19), which is virtually identical in all solvents studied, shows the $N\underline{C}H_2$ carbons of the short bridge, C(5), about 4.7 ppm upfield of the $N\underline{C}H_2$ carbons of the long bridges, C(4). In contrast, in the C221·Na^+ cryptate, the C(5) resonance is downfield of the C(4) resonance by about 0.5 ppm (Figure 19,20). When it is complexed, the ligand is assumed to be in the in-in form (Chapter I, Part C) to allow the two nitrogen atoms to contribute to the complex stability. Since the in-in form should dominate in both cryptates,

Figure 19. Carbon-13 spectra of (a) the C221·K^+ cryptate in methanol (S = solvent peak) and (b) the C221 Na^+ cryptate in pyridine (small peaks). The large peaks in spectrum b are those of the uncomplexed cryptand.

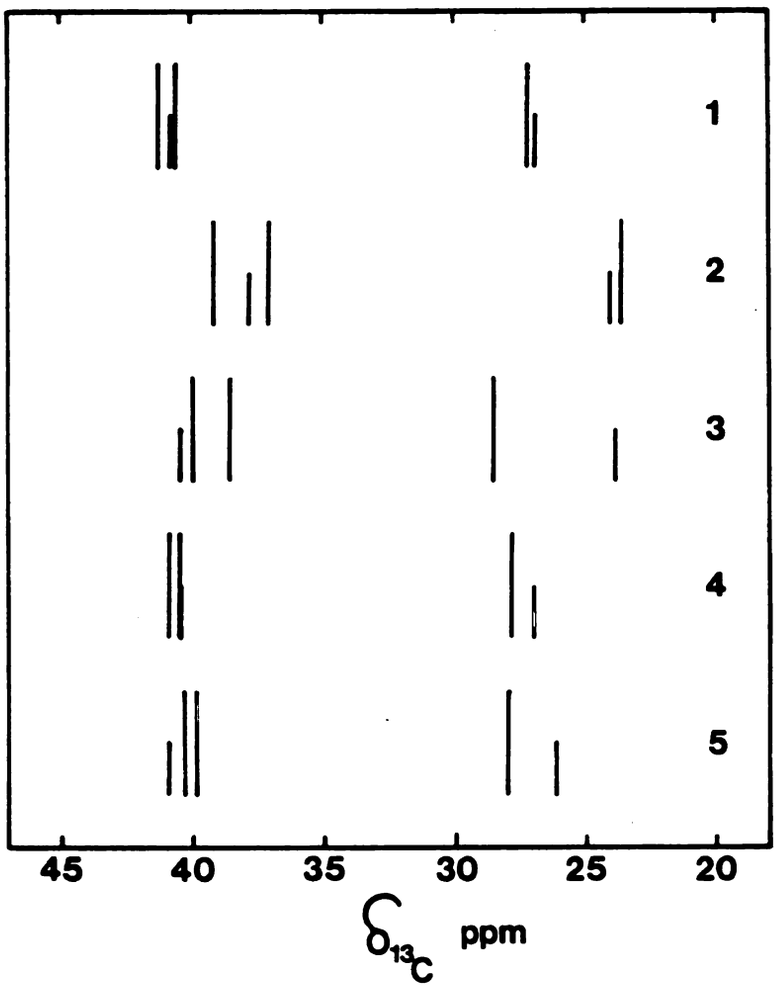

Figure 20. A comparison of the patterns observed in the Carbon-13 spectra of C221 and of its cryptates with the Na^+ and the K^+ ion.

1 C221 in MeOH.

2 C221 Na^+ in pyridine.

3 C221 K^+ in methanol.

4 C221 in nitromethane (+25°C).

5 C221 in nitromethane (-20°C).

the patterns observed in the ^{13}C spectra are not simply related to the in-in form of the ligand. The differences in the patterns reflect changes in the conformation of the bridges of the macrobicyclic ligand. The C221·Cs^+ cryptate gives the same pattern as the C221·K^+ cryptate (97).

The change in pattern observed when Na^+ ions are replaced by K^+ or Cs^+ ions may be attributed to two factors: First, the larger sizes of the latter ions might force the cryptand to increase its cavity size by taking a different conformation than the one it has in the C221·Na^+ cryptate; second, the electric field around the Na^+ ion is larger than that around the larger K^+ and Cs^+ ions.

The first factor should affect each resonance in a different extent, while the second one should shift all resonances by approximately the same amount. Crystallographic data (92) indicate that several torsional angles about the N-C segments and the corresponding conformations (anti or gauche) are changed when the Na^+ ion is replaced by the K^+ ion in the C221 cavity. In solution, what is observed by NMR is an average of various conformations and torsional angles. Although the effect of the two factors mentioned above cannot be isolated at the present time, it can be said that the ^{13}C spectra indicate large changes in torsional angles.

In going from C221·K^+ to C221·Na^+, the chemical shift of the C(5) carbons is virtually unchanged while the C(4)

resonance shifts upfield by about 5 ppm (Table 22). If the γ effect (226) is operative here, the shielding of C(4) would indicate that the C(4)-N bond changes from the anti to the gauche conformation with respect to the C(5)-C(3) bond. Since the γ effect is a mutual effect, the C(3) carbons should also be shielded. Indeed the C(3) resonance shifts upfield by 2.7 ppm, which is more than the upfield shift observed for the corresponding $O\underline{C}H_2$ carbons of the long bridges. An even larger upfield shift could be expected for C(3) since there are one short bridge and two long ones and, on the average, the C(5)-C(3) bond should be in the "gauche" conformation longer than each of the two C(4)-N bonds.

The above discussion may not be carried very far until the field effect is precisely evaluated. This effect, which consists of shifting upfield the ^{13}C resonances of the ligand molecule when a cation is introduced in the cavity, is quite small when the K^+ (or Cs^+) ion is involved. In this case, the conformational effects dominate the changes in chemical shifts between the free and the complexed ligand. For example, in methanol, the C(5) and the C(2) resonances shift upfield by 3.01 and 2.22 ppm, respectively, (Tables 22 and 23, Figures 19 and 20) upon formation of the complex C221·K^+. This strongly indicates that the C(5)-N and the C(2)-C(4) segments switch from the anti to the gauche conformation with respect to each other. The

Table 22. Carbon-13 Chemical Shifts of the Sodium and Potassium Cryptates.

	δ^a (ppm)		
	C221•Na^+ (pyridine)[b]	C221•K^+ (methanol)[b]	Diff. (Na^+-K^+)
1[c]	39.13	39.95	-0.82
2[c]	37.07	38.51	-1.44
3	37.78	40.45	-2.67
4	23.58	28.54	-4.96
5	24.02	23.86	+0.16

[a]Reference: Methyl carbons of acetone-d6.

[b]The chemical shifts are virtually solvent-independent.

[c]The assignment of these peaks is tentative and the respective position of peaks 1 and 2 is assumed to be identical in the two cryptates.

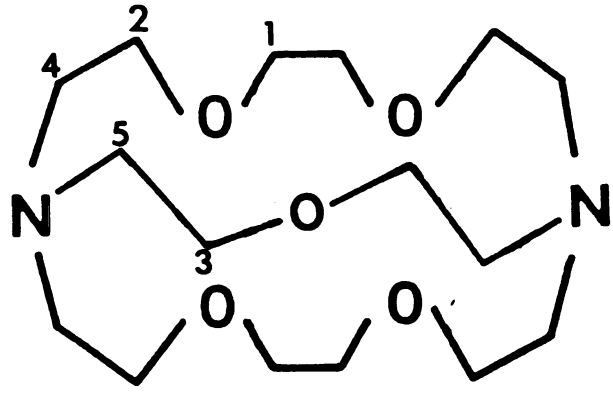

Table 23. Carbon-13 Chemical Shifts of the Free C221 Cryptand in Various Solvents and at Several Temperatures.

Solvent (m.p.°C)	ε	t(°C)	δ (ppm) 1	2	3	4	5	$\delta_4-\delta_5$ (ppm)
Formamide (2)	109	34	40.71	39.47	40.71	28.13	25.81	2.32
Water (0)	78	30	70.59	69.69	70.59	57.03	54.93	2.10
Nitromethane	35.9	25	40.87	40.46	40.46	27.80	26.96	0.84
(-29)		-20	40.31	39.84	40.90	27.94	26.16	1.78
Nitroethane	28	38				27.85	27.76	0.09
(-89)		-37				27.28	26.60	0.68
		-70				27.38	25.89	1.49
1-Nitropropane (-104)	23	23	41.57	41.02	41.02	27.90	27.90	0
		-20	41.24	40.53	40.71	27.53	27.33	0.20
		-80	40.50	39.65	40.50	26.24	25.50	1.26
Ethylene Glycol (-13)	37.7	24	41.41	40.64	40.74	27.04	26.67	0.37
Acetonitrile-d_3	37.5	55	70.15	69.67	69.67	56.69	56.41	0.28
(-45)		24	69.83	69.28	69.40	56.43	55.96	0.47
		-42	68.79	68.15	69.14	56.37	54.73	1.64
Methanol	33	44	41.53	41.02	41.02	27.57	27.35	0.22
(-98)		34	41.42	40.86	40.86	27.41	27.16	0.25
		24	41.24	40.59	40.73	27.17	26.87	0.29

Table 23. Continued.

Solvent (mp °C)	ε	t(°C)	δ (ppm) 1	2	3	4	5	$\delta_4-\delta_5$ (ppm)
Methanol		-43	40.75	39.79	40.43	26.69	25.77	0.92
(-98)		-80	40.26	39.15	40.26	26.58	24.88	1.70
Ethanol	24.5	23	41.42	40.80	40.80	27.48	27.48	∿0
(-114)		-33	41.01	40.18	40.42	26.98	26.54	0.44
		-84	40.57	39.51	40.16	26.72	25.57	1.15
Dichloromethane	8.0	25	41.56	41.00	41.00	27.88	27.88	∿0
(-97)		-42	40.82	40.06	40.82	27.27	26.21	1.06
		-90	40.03	39.29	40.47	26.9	25.0	∿1.9
Pyridine	12.4	24	41.35	40.88	40.68	27.69	27.62	0.07
(-42)		-39	40.67	40.05	40.05	26.88	26.88	∿0
Tetramethylguan-	11.0	24	41.56	41.02	40.75	27.97	27.92	0.05
idine (∿-80)		-25	41.48	40.77	40.77	27.76	27.76	∿0
Acetone-d_6	20.7	34	41.52	41.07	40.81	27.92	27.92	∿0
(-95)		24	41.48	40.99	40.76	27.86	27.82	0.04
		-65	40.79	40.05	40.20	26.95	26.95	0
		-90	40.42	39.59	40.06	26.60	26.60	0

Table 23. Continued.

Solvent (mp °C)	ε	t(°C)	δ (ppm) 1	2	3	4	5	$\delta_4-\delta_5$ (ppm)
DMF	36.7	34	41.53	41.10	40.85	28.04	28.04	0
(-61)		24	41.50	41.01	40.82	27.87	27.79	0.08
		-53	40.76	40.24	40.32	27.04	27.04	0
Chloroform-d	4.7	21	-6.35	-7.18	-7.07	-20.54	-20.54	0
(-64)		-25	-6.65	-7.76	-7.26	-21.12	-21.12	0
		-60	-6.85	-8.29	-7.44	-21.73	-21.73	0
THF	7.6	24	41.58	41.09	41.09	27.99	27.95	0.04
(-109)		-65	41.03	40.33	40.33	27.22	27.22	0
		-88	40.86	40.15	40.15	27.07	27.07	0
1,3-dioxolane		24	41.53	41.05	40.86	27.91	27.86	0.05
(-95)		-93	40.18	39.62	40.18	26.71	26.71	0
Toluene	2.4	23	41.42	40.91	40.64	27.78	27.78	0
(-95)		-30	40.98	40.39	40.39	27.30	27.30	0
		-80	40.60	39.98	39.98	26.72	26.72	0
Anisole	4.3	38	41.45	40.97	40.72	27.82	27.82	0
(-37.5)		-37	40.79	40.15	40.15	27.03	27.03	0
Methyl Acetate (-98)	6.7	34	41.64	41.23	40.93	28.07	28.07	0

same behavior is observed in other solvents (see below).

In the case of sodium, the field effect is much larger, and the whole spectrum of C221·Na^+ complex is shifted up-field with respect to that of C221·K^+ (Figure 20); the chemical shifts are difficult to rationalize without an estimation of the field effect.

The solvent dependence and, whenever possible, the temperature dependence of the ^{13}C spectrum of the free cryptand 221 were studied in 20 solvents. The chemical shifts are listed in Table 23. No change in chemical shift was observed when the concentration was varied between 0.05 and 0.25 M, indicating that, in this concentration range, intermolecular interactions are negligible.

The ^{13}C spectra of the free C221 in various solvents and of the C221·K^+ cryptate are shown in Figure 21. Table 23 gives the difference in chemical shift between the C(4) and the C(5) resonances in all solvents studied. At room temperature, this difference varies between -0.1 ($CDCl_3$) and 2.3 ppm (Formamide). When the difference (δ_4-δ_5) is large, the spectrum shows a pattern similar to that observed for the C221·K^+ cryptate (Figures 20,21); we will say that the spectrum is of the "K^+-type".

On lowering the temperature, the difference (δ_4-δ_5) increases in solvents such as nitromethane and acetonitrile (Table 22 and Figure 22) whereas in other solvents peaks 4 and 5 remain superimposed down to the melting point. The two

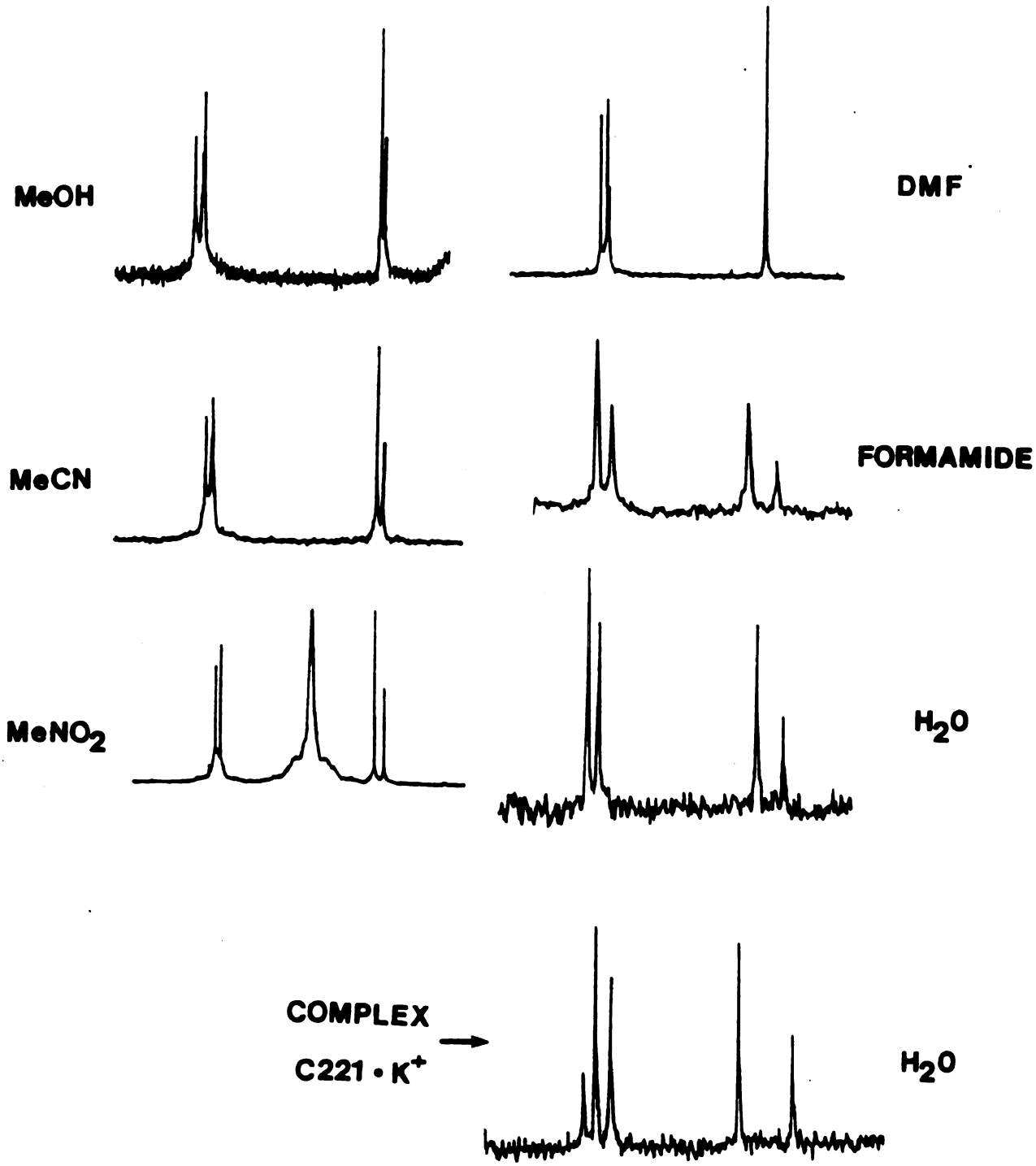

Figure 21. Carbon-13 spectra of the free C221 cryptand in various solvents and of the C221·K^+ cryptate in water.

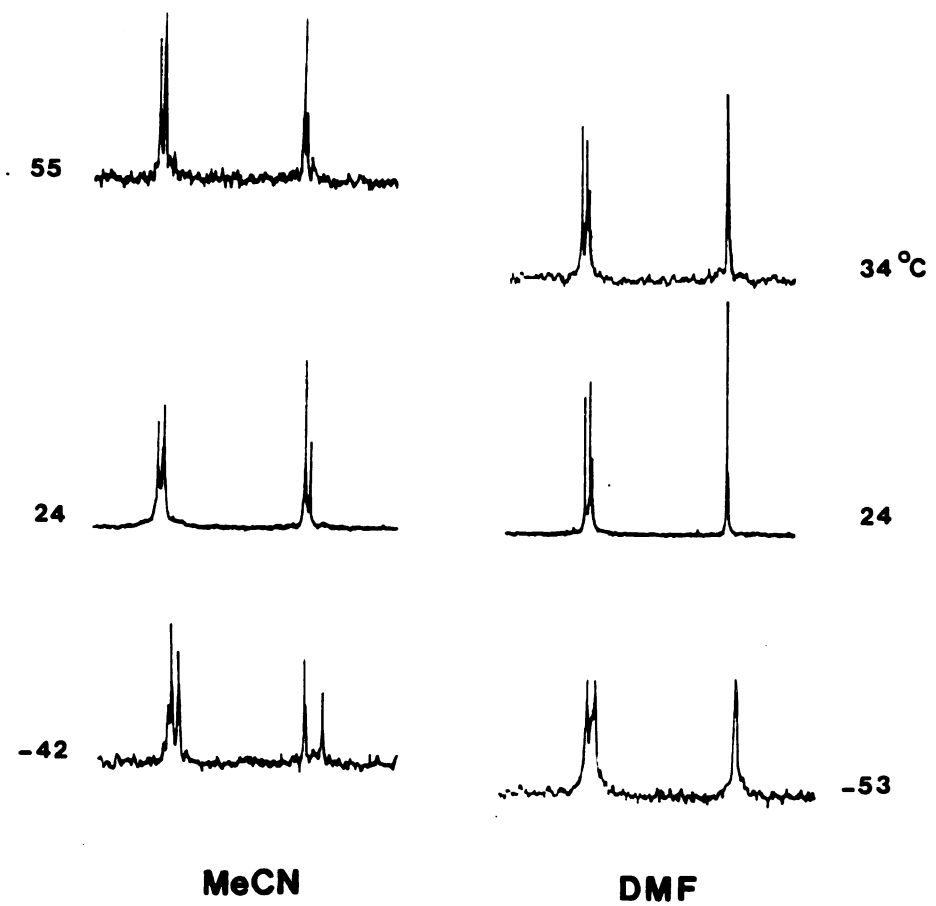

Figure 22. Carbon-13 spectra of the free cryptand 221 in acetonitrile and DMF at various temperatures.

types of behavior are illustrated in Figure 22 for acetonitrile and DMF, respectively. It is clear that certain solvents interact with the C221 molecule while others do not.

This interaction may be simply represented by

$$C221 + nS \rightleftarrows C221 \cdot S_n \qquad \Delta S^\circ < 0$$

where S stands for a solvent molecule. Due to the negative entropy associated with this "complexation" reaction, the equilibrium is shifted to the right at low temperature (ΔH° is independent of temperature), which explains the evolution of the spectra seen for example in acetonitrile (Figure 22). In this solvent and in all the solvents which give a separation of the peaks 4 and 5, which we will now call A-type solvents, the low temperature spectra are of the K^+-type.

A similarity in pattern does not necessarily imply a similarity in conformation. However, in the case of potassium, the field effect is small. Also the data given in Table 23 indicate that in A-type solvents and with decreasing temperature the C(4) and C(5) resonance signals tend toward the corresponding signals in the $C221 \cdot K^+$ cryptate (Figure 20). This behavior suggests that indeed A-type solvents force the C221 cryptand to take a conformation similar to that observed in the $C221 \cdot K^+$ cryptate.

It is not surprising that water, methanol and formamide interact with C221 since these solvents can form hydrogen bonds with the bridgehead nitrogen atoms. The oxygen atoms may also participate in H-bonding with the solvent molecules; however, according to Lord and Siamwiza (227), they probably interact, at best, to a very limited extent. These authors studied by IR the interaction between C222 and $CDCl_3$ and concluded that the six oxygen atoms appear to be inaccessible to the chloroform-d. Their conclusions should be valid for the case of C221 in various solvents. An exception could be water. Water molecules are only slightly larger than K^+ ions (2.9 vs. 2.66 Å) so that they can probably penetrate into the C221 cavity as do K^+ ions. In this case they may have access to the oxygen atoms.

It is noticeable that A-type solvents are all acidic even if some of them, e.g., CH_2Cl_2, are very weakly acidic. Methanol probably interacts via the O-H group and formamide via the NH_2 group. Both acetonitrile and nitromethane have an electron withdrawing group and most likely interact via the positively charged methyl group. In order to verify this hypothesis, we studied the spectral changes along the series nitromethane, nitroethane and 1-nitropropane, in a large temperature range (Figure 23). The differences (δ_4-δ_5) are plotted as a function of the temperature in Figure 24. It is seen that, at a given temperature, the quantity (δ_4-δ_5) decreases as the methyl group is removed further from the

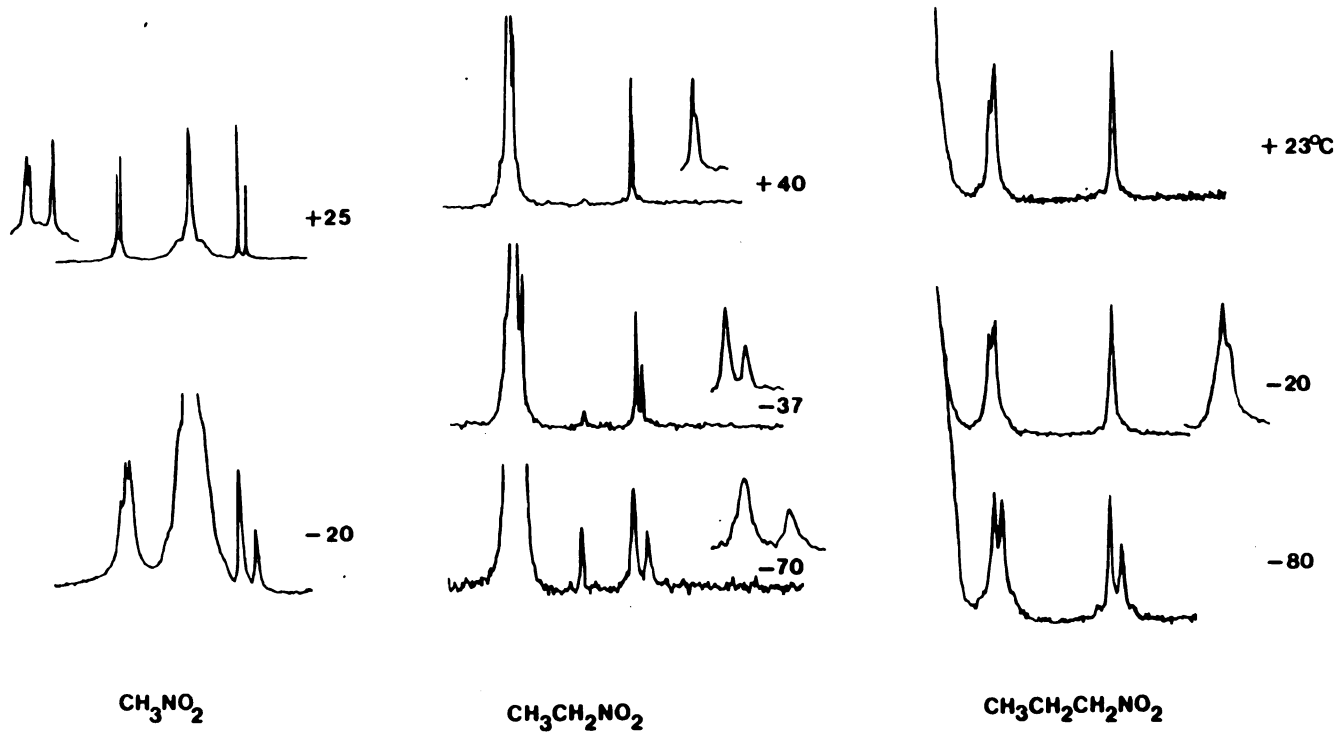

Figure 23. Carbon-13 spectra of the free cryptand 221 in nitromethane, nitroethane and 1-nitropropane at various temperatures. In each spectrum the broad peak is the solvent peak.

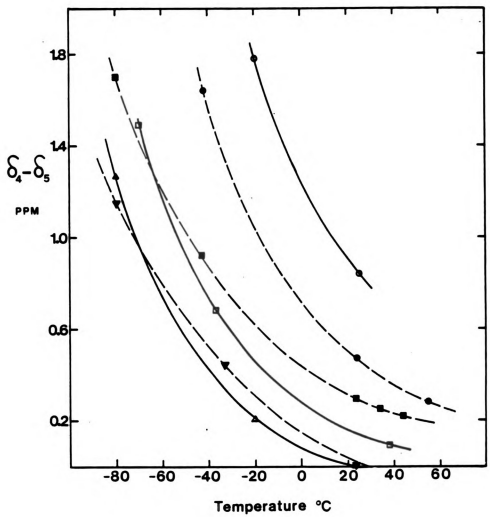

Figure 24. A plot of the difference in chemical shift between the two $N\underline{C}H_2$ resonances of the free cryptand 221 as a function of temperature in several solvents. (○) nitromethane; (□) nitroethane; (△) 1-nitropropane; (●) acetonitrile; (■) methanol; (▼) ethanol.

electron withdrawing group; the largest decrease occurs, as expected, between nitromethane and nitroethane.

Consequently the methyl group of these solvents appears to be responsible for the interaction with the C221 ligand. A decrease of (δ_4-δ_5) was also observed in going from methanol to ethanol (Figure 23). This result does not indicate that the methyl group is responsible for the interaction; it simply shows that the interaction is weaker in the case of ethanol. It should be noted that, within a series of solvents, the differences (δ_4-δ_5) are about the same when calculated at the same $T/T_{m.p.}$ ratio.

Ethylene glycol, which is an H-bonding solvent, gives a difference (δ_4-δ_5) of 0.37 ppm at 24°C. The high melting point of this solvent precludes a low temperature study. Toluene and anisole gave about the same chemical shifts, indicating that the methyl group of anisole is not acidic enough to interact noticeably with C221 even at low temperature.

Perhaps the best evidence that the solvent acidity (defined in terms of acceptor ability) is responsible for the solvent - C221 interaction is provided by the drastic spectral change observed between C221 in DMF and C221 in formamide (Figure 21). At 34°C, peaks 4 and 5 are superimposed in DMF whereas they are separated by 2.32 ppm in formamide. The substitution of two methyl groups by two hydrogen atoms increases the acidity. Formamide is

capable of H-bonding and its acidity is comparable to that of the lower aliphatic alcohols (150). The spectrum of C221 in formamide is about the same as that observed in water, which indicates a relatively strong C221-formamide interaction.

The only acidic solvent, or acceptor solvent in the Gutmann sense (150), which does not seem to interact with C221 is chloroform-d. Dichloromethane, which is much less acidic than chloroform, gives a 4-5 split of about 1 ppm at -42°C while chloroform-d does not split the two peaks at all, even at -60°C. The latter solvent has been shown by IR (227) to form hydrogen bonds with the nitrogen atoms of C222, the ligand being presumably in the in-out or the out-out form. Chloroform-d probably behaves in the same way with C221. However, the interaction is not detected by ^{13}C NMR, which indicates that either the interaction is too weak to affect the spectrum or the conformation of C221 hydrogen-bonded to chloroform-d is the same as that of C221 in non acidic solvents such as ethers. The C221-dichloromethane interaction might be favored by the presence of two acidic hydrogen atoms and by the larger dipole moment of dichloromethane as compared to chloroform-d (1.55 vs. 1.0 Debye (165)).

Ethers such as THF and 1,3-dioxolane, which are poor acceptor solvents (150), appear not to interact with C221, even at -90°C (Table 22). Tetramethylguanidine is capable

of hydrogen-bonding (228); however no interaction can be detected. Steric hindrance due to the four methyl groups of the TMG molecule may prevent the acidic hydrogen from gaining access to the nitrogen atoms of C221.

It is noticeable that solvents possessing two or three acidic hydrogen atoms appear to interact with C221 stronger than solvents having only one acidic hydrogen atom. For example, formamide gives a much larger 4-5 split than methanol and ethanol although, as previously mentioned, these solvents have similar acidities. The same holds for dichloromethane and chloroform-d. A solvent molecule with two hydrogen atoms may be able to bind the two nitrogen atoms of C221 at the same time if the cryptand is in the in-in conformation and if the solvent molecule is small enough to penetrate into the ligand cavity. Water is probably the only solvent which meets the last condition. It is unlikely that other solvents form 1:1 "complexes" with C221 because the entropy associated with the complexation reaction would be very small and spectral changes with decreasing temperature would also be very small.

3. Conclusion

In solvents which exhibit well developed acceptor properties, the free cryptand 221 appears to have the same conformation as the one it has in the $C221 \cdot K^+$ and $C221 \cdot Cs^+$

cryptates. This conformation is favored at low temperature. Hydrogen-bonding between the acidic hydrogen atoms of the solvent molecules and the nitrogen atoms of the cryptand is probably responsible for the solvent-C221 interaction which forces the cryptand to take the conformation of the C221·K^+ cryptate.

In a series of solvents with the same functional group, the strength of the C221-solvent interaction follows the order of the acidities. However if solvents with different functional groups are considered, not only the acidity but also the number of acidic hydrogen atoms, the size of the solvent molecule and the steric hindrance around the acidic group seem to play a determining role in the C221-solvent interaction. Dr. J. P. Kintzinger (Université Louis Pasteur, Strasbourg, France) is now completing a study of the same system by using ^1H NMR, ^{13}C relaxation measurements and calorimetric techniques.

B. Potassium-39 NMR Study of the C221·K^+ Cryptate

1. Introduction

The size of the K^+ ion is a little smaller than the cavity size of C221, 2.2 Å (229) vs. 2.66 Å (202). In the similar case of Cs^+ ion and C222, Kauffmann et al. (97) found that the Cs^+ ion can form two kinds of complexes with

C222, an inclusive and an exclusive complex. Therefore it was of interest to continue the studies of Shih and Popov (138) in order to determine if one or two modes of complexation exist for C221·K^+.

2. Results and Discussion

The ^{39}K chemical shifts and line widths of the C221·K^+ cryptate in various solvents are given in Table 23. Corrections due to the use of different lock solvents were not applied in this table. The corrected values are given in the footnotes.

The chemical shifts of C221·K^+ range from 10.2 to 15.2 ppm. The variation of 5 ppm, which roughly corresponds to that found in the case of 18C6·K^+ (Chapter III), shows that the K^+ ion is not completely isolated from the surrounding solvent molecules. A chemical shift range of about 50 ppm was reported by Gudlin and Schneider (230) for the ^{205}Tl chemical shift of the C221·Tl^+ cryptate. Considering that the chemical shift ranges for the free ion via common solvents are about 40 and 500 ppm for the K^+ and Tl^+ ion, respectively, the variations seen for the cryptates are comparable. This is expected since the K^+ and the Tl^+ ion have similar sizes and have the same area of their surface exposed to the solvent molecules. Although the chemical shift range is quite small, it can be said that the C221·K^+ cryptate is an exclusive complex.

Table 24. Potassium-39 NMR Chemical Shifts[a] and Line Widths of $K^+ \cdot C221$ Cryptates[b] in Several Solvents and at Various Temperatures.

Solvent	Lock Solvent	Salt	δ(ppm)	$\Delta\nu_{1/2}$[c] (Hz)	t[d] (°C)
Acetone	D_2O	KPF_6	10.2±0.6	64	22
	Ac-d6	KSCN	13.9±0.6[f]	58	22
			13.4±0.6	83	0
			12.8±0.6	87	-10
			13.4±0.6	146	-31
			13 ±1	302	-51
Acetonitrile[e]	CD_3CN	$KAsF_6$	16.2±0.3[f]	91	24
			15.6±0.3	165	-22
			14.5±0.3	220	-40
Methanol	CD_3OD	KSCN	13.3±0.3[f]	60	22
			13.6±0.6	112	-15
			13.0±0.6	170	-33
			14 ±1	280	-46
	CD_3OD	KI	13.9±0.3	44	50
			13.3±0.3	56	22
			14.2±0.6	233	-46
			13 ±1		

Table 24 - Continued.

Solvent	Lock Solvent	Salt	δ(ppm)	$\Delta\nu_{1/2}$[c] (Hz)	t[d](°C)
DMSO	D_2O	KPF_6	14.3±0.3	109	50
			13.4±0.6	156	22
Pyridine	D_2O	KSCN	15.2±0.3	101	22
		KPF_6	14.0±0.3	111	22
			15.8±0.6	375	-36
PC	D_2O	KPF_6	15 ±1	160	61
THF	THF-d8	$KAsF_6$	10.2±0.3	71	59
			10.5±0.3	78	50
			10.6±0.3	96	34
			11.1±0.3	107	23
			11.4±0.3	126	0
			(9.4±0.6)	195	-20
			11 ±1	240	-40
			11 ±1	350	-60
				~700	-85

Table 24 - Continued.

[a] A comparison of chemical shifts obtained in different solvents can only be made if the lock solvents are the same (See Chapter II).

[b] $[K^+ \cdot C221] = 0.05$ M.

[c] ±5% if $\Delta\nu_{1/2}$ <200 Hz, ±5-10% if $\Delta\nu_{1/2}$ >200 Hz.

[d] ±1°C.

[e] $[K^+ \cdot C221] = 0.075$ M.

[f] To obtain the corrected chemical shifts, subtract 2.2 ppm, 2.8 ppm, and 2.0 ppm when the lock is Acetone-d_6, CD_3CN and $C\underline{D}_3OD$, respectively.

The large paramagnetic shift (the central value is about 13 ppm) is similar to that found in the case of the DB18C6·K^+ complex (Chapter V). It indicates a strong overlap of the orbitals of the donor atoms of the ligand with the outer p orbitals of the cation. Such an overlap would not be possible if the K^+ ion were displaced from the center of the 18-membered ring of C221 towards the outside of the cavity as the crystallographic data indicate (92). Also a larger solvent dependence would be observed in this case. Therefore the K^+ ion appears to lie inside the ligand cavity although it is able to come into contact with the solvent molecules.

When KPF_6 is replaced by KSCN, the cryptate signal shifts downfield by 1.5 ppm in acetone and 1.2 ppm in pyridine (Table 23). The direction of the shift is that found in the absence of C221 (135), which could indicate some extent of ion pairing in the cryptate. However, the magnitude of the shift is almost within experimental error and does not give a conclusive evidence for ion pairing. In methanol the results obtained for KSCN and KI are about the same.

The ratio of the K^+ ion size over the C221 cavity size, 2.66/2.2 = 1.21, is virtually identical to the corresponding ratio for the Cs^+ ion and C222, 3.34/2.8 = 1.19. Two kinds of complexes, one inclusive and one exclusive, were found in the case of C222·Cs^+ (97). However, in the

case of C221·K^+, the quasi invariance of the ^{39}K resonance frequency in a large temperature range (Table 23) shows that there is only one mode of complexation for the K^+ ion. The invariance of the ^{13}C spectrum of C221·K^+ with the solvent and with the temperature (Part A) supports the above conclusion.

The invariance of the ^{39}K shift with increasing temperature is in contrast with the large upfield shift observed with 18C6·K^+ (Chapter III) in all solvents studied. It probably indicates a weaker K^+-solvent interaction in the cryptate as compared to the crown complex. Such a weak interaction in turn suggests that the K^+ ion is closer to the center of the C221 cavity than crystallographic data indicate. However, the invariance of the shift could also arise from the compensation of two effects, e.g., weaker solvation (→ upfield shift) and stronger cation-ligand overlap (→ downfield shift). At low temperature the ^{39}K chemical shifts do not converge towards a solvent independent shift, indicating that the K^+ ion remains exposed to the solvent molecules.

3. Conclusion

The large paramagnetic shift of the C221·K^+ cryptate shows that the K^+ ion is tightly embedded in the cryptand cavity. The relatively small solvent dependence of the

shift and its quasi invariance with temperature clearly indicate that in solution there is only one kind of C221·K^+ cryptate in which the K^+ ion is closer to the center of the C221 cavity than it is in the solid state.

CHAPTER V

MULTINUCLEAR NMR STUDY OF THE COMPLEXATION OF POTASSIUM IONS WITH CROWN ETHERS AND WITH "CONVENTIONAL" LIGANDS

A. Potassium Cation Interaction with Crown Ethers

Introduction

The complexation reactions of the K^+ ion with the crown ethers 12C4, 15C5, B15C5, 18C6 and DB18C6 were investigated in several nonaqueous solvents by Shih (15) using ^{39}K and ^{13}C NMR. A number of formation constants were reported for the smaller crowns and the presence in solution of "sandwich" 2:1 (ligand : K^+) complexes with 15C5 and MB15C5 was detected. Broad signals precluded a quantitative study for 18C6 and DB18C6.

In this part, the above study was extended to other ligands such as dithia-18C6 and to large members of the crown family such as DB21C7, DB24C8 and DB27C9 (Figure 1).

Results and Discussion

Potassium-39 NMR Studies

The ^{39}K chemical shifts were measured as a function of the ligand/K^+ mole ratio. The concentration of the salt, $KAsF_6$ or KI, was held constant at 0.05 or 0.075 M and the ligand concentration was varied. In all cases the exchange rate of the K^+ ion between the solvated and the complexed site was fast on the ^{39}K NMR time scale and only one

population-averaged line was observed. If only a 1:1 complex is present and if ion pairing is negligible, the observed chemical shift, δ_{obs}, is then given by

$$\delta_{obs} = X_{M^+} \quad \delta_{M^+} + X_{M^+L} \; \delta_{M^+L} \tag{1}$$

where δ_{M^+} and δ_{M^+L} are the chemical shifts of the solvated and complexed cation and X_{M^+} and X_{M^+L} are the respective mole fractions of the two species, respectively. The concentration equilibrium constant for the formation of the complex is,

$$K_f = \frac{C_{M^+L}}{C_{M^+} \; C_L} \tag{2}$$

where C_{M^+L}, C_{M^+} and C_L denote the equilibrium molar concentrations of the complex, the cation and the ligand, respectively.

By combining Equations (1) and (2) with the mass balance equations it can be shown that

$$\delta_{obs} = K_f C_M^t - K_f C_L^t - 1) + K_f^2 C_L^t + K_f^2 C_M^{t^2} - 2K_f^2 C_L^t C_M^t$$

$$+ (2K_f C_L^t + 2K_f C_M^t + 1)^{1/2} \; \frac{\delta_M - \delta_{ML}}{2K_f C_M^t} + \delta_{ML} \quad . \tag{3}$$

In Equation (3) the total concentrations of the cation and

the ligand (C_M^t and C_L^t, respectively) are known and δ_M is determined by measuring the cation chemical shift in the absence of the ligand. The two unknown quantities, K_f and δ_{ML}, can be evaluated by a non-linear least-squares procedure starting with reasonable estimates of K_f and δ_{ML}. The program KINFIT (179) was used to perform the iterations and to obtain statistical information regarding the unknowns. Details about the use of this program can be found in the Appendix 1.

The systems investigated were (i) dithia-18C6 (DT18C6) + $KAsF_6$ in acetone, (ii) DB21C7 + $KAsF_6$ in acetonitrile, (iii) DB24C8 + $KAsF_6$ in nitromethane, acetonitrile, pyridine and methanol (KSCN was used in the last solvent), (iv) DB27C9 + $KAsF_6$ in acetonitrile and pyridine.

The chemical shifts and the line widths as a function of the ligand/K^+ molar ratio are given in Table 25 and plotted in Figure 25 for the system involving DT18C6. In this case, the quite narrow signal gradually shifts in the paramagnetic direction with increasing ligand/K^+ mole ratio: The chemical shift does not reach a limiting value (δ_{ML}) up to a mole ratio of 2.17, the highest one which could be obtained due to the low solubility of the ligand. This behavior is indicative of a rather weak K^+·DT18C6 interaction.

A data analysis using KINFIT yielded a value of 2.8±0.8 (log K_f = 0.45±0.12) for the association constant K_f. It

Table 25. Potassium-39 Chemical Shifts and Line Widths in Acetone Solutions Containing $KAsF_6$[a] and Dithia-18C6 at Various Mole Ratios and at 25°C.[b]

$\frac{[DT18C6]}{[K^+]}$	δ[c] (ppm)	$\Delta\nu_{1/2}$[d] (Hz)
0	-13.1	12
0.42	-12.0	18
0.42[e]	- 8.7	41
0.65	-11.0	20
0.90	-10.2	22
1.00	-10.2	24
1.10	- 9.8	25
1.25	- 9.6	25
1.72	- 8.5	27
2.17	- 7.5	33

[a] $KAsF_6$ = 0.075 M.

[b] Unless otherwise indicated.

[c] ±0.2 ppm.

[d] ±1-2 Hz depending on the line width.

[e] t = -42°C.

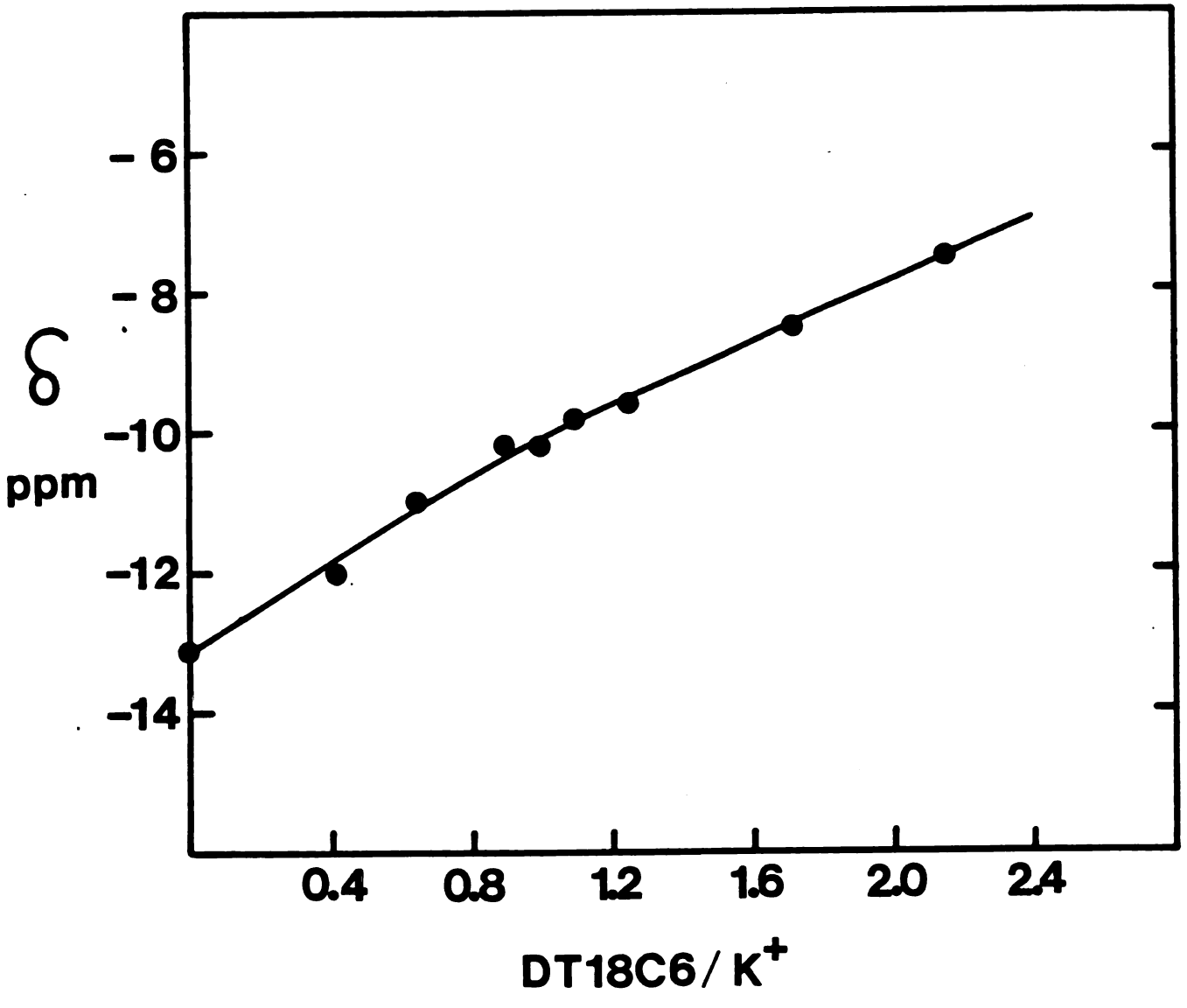

Figure 25. Potassium-39 chemical shifts as a function of the DT18C6/K^+ ratio in acetone solutions.

should be noted that this value roughly corresponds to the lower limit of the range of reliable values measurable by ^{39}K NMR with our method. Since ion pairing was not considered in the calculation of δ_{obs}, the actual value of K_f is probably larger than 2.8. A K_f value of 14 (log K_f = 1.15) was reported (200) for the K^+•DT18C6 complex in methanol. Considering that the formation constants of M^+•crown complexes are of the same order of magnitude in methanol and in acetone (15), our result is in the expected range. Reported (201) log K_f values for M^+•DT18C6 complexes in acetone include 0.61±0.09 ($M^+ = Cs^+$) and 2.98± 0.01 ($M^+ = Tl^+$). Although the sizes of Tl^+ and K^+ are comparable (1.40 and 1.33 Å, respectively (202)), the former cation gives a much more stable complex than the latter. This is expected since there must be some covalent interaction between the "soft" acid (203) Tl^+ ion and the "soft" sulfur atom. In the case of K^+ and Cs^+ ions, the replacement of two O atoms by two S atoms in the ligand ring decreases the formation constant by several orders of magnitude (data for Cs^+ ion in Reference 201).

The limiting chemical shift of the K^+•DT18C6 complex, of 6.6±3.7 ppm, is rather imprecise because the chemical shifts could not be measured at high mole ratios. However, it resembles the limiting shifts found for K^+•DB18C6 in various solvents (15). In this last complex, the K^+ ion is "squeezed" in the ligand cavity (see below). The same

reason probably holds for DT18C6 which has a smaller cavity than 18C6 since S atoms are larger than O atoms. However this analogy must be regarded with caution because the electron donor atoms are not the same.

The signals of the K^+ ion complexes with the large dibenzo crowns are rather broad, i.e., 100-220 Hz (Table 27), which increases the experimental error in the chemical shift to such an extent that in most cases a quantitative analysis of the data could not be done. Moreover, without the zero-filling technique (see Experimental part), the time required to perform a complete mole ratio study, i.e., at least 9 spectra, becomes prohibitive when the lines are broad. For these reasons, only the data relative to DB27C9 are presented here (Table 26).

As seen in Figure 26 in pyridine solutions, the experimental points are quite scattered. However, in acetonitrile, the plot of δ vs mole ratio (Figure 26) clearly shows a break at a mole ratio of about 1. This behavior indicates the formation of a rather stable (log $K_f \geq 4$) $K^+ \cdot$DB27C9 complex. It should be emphasized that in the case of ^{39}K NMR, the upper limit of the reliable K_f values measurable with our method is lower than that attainable by ^{133}Cs NMR (10^5) since the experimental error is larger and higher concentrations have to be used. We can estimate this upper limit to be between 5×10^3 and 10^4. For example, a quantitative analysis of the data, shown in

Table 26. Potassium-39 Chemical Shifts and Line Widths for Acetonitrile and Pyridine Solutions Containing $KAsF_6$[a] and DB27C9 at Various Mole Ratios and at 24°C.

Acetonitrile			Pyridine		
$\frac{[DB27C9]}{[K^+]}$	δ[b] (ppm)	$\Delta\nu_{1/2}$ (Hz)	$\frac{[DB27C9]}{[K^+]}$	δ (ppm)	$\Delta\nu_{1/2}$ (Hz)
0 0	- 2.4	12±1	0	0.4±0.2	39±2
0.28	- 5.6	44±3	0.16	- 1.5±0.3	82±3
0.45	- 7.3	52±3	0.44	- 7.0±0.6	105±5
0.59	- 8.5	78±3	0.63	- 9.6±0.6	130±10
0.71	- 9.4	95±5	0.91	-11.3±0.6	170±10
0.91	-11.7	100±5	1.00	-12.2±0.6	188±10
1.00	-11.7	110±5	1.30	-11.0±0.6	240±20
1.09	-12.6	107±5	1.86	-12.4±0.6	220±20
1.21	-12.0	102±5			
1.29	-12.6	97±5			
1.57	-12.2	107±5			
2.22	-12.2	130±5			

[a] $[KAsF_6]$ = 0.075 M.

[b] ±0.3 ppm.

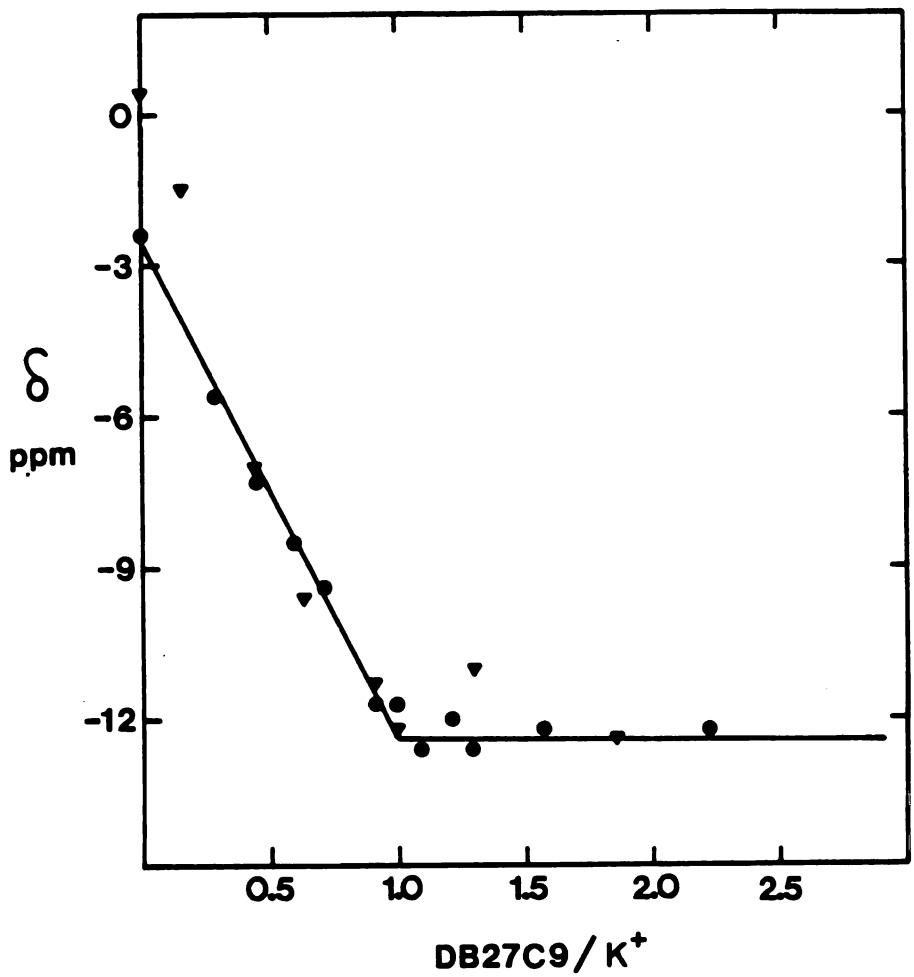

Figure 26. Potassium-39 chemical shift vs. DB27C9/K^+ mole ratio in acetonitrile (●) and pyridine (▼) solutions at 25°C.

Table 27. Potassium-39 Chemical Shifts of Potassium Ion Complexes with Various Crown Ethers in Several Solvents and at 25°C.

	δ(ppm)[a]									
Solvent	(b) $(12C4)_2$	(b) B15C5	(b) $(B15C5)_2$	(b,c) 15C5	(b,c) $(15C5)_2$	(b) DB18C6	(d) 18C6	DB21C7	DB24C8	DB27C9
Nitromethane	-6.0	-16.7	-9.5	-16.9	-11.8				(-15)[e]	
Acetonitrile	-5.7	- 6.1	-9.6	- 4.2	-13.0	7.3		-13[f]	-12	-12.4
Acetone	-7.8			-10.1	-11.6					
Pyridine				- 2.0	-12.7	(13.6)			-11[e]	-12.4
Methanol	-6.6			-7.0	-12.5		-2.5		-13	
DMF				-7.0	-12.0		-3.8			
DMSO				+3.0	-11.7		-1.4			

[a] 0.5-1 ppm depending on the line width. [b] Reference 15. [c] $\Delta\nu_{1/2} \approx$ 40-60 Hz.
[d] See Table 14 for details and line widths. [e] $\Delta\nu_{1/2} \approx$ 200 Hz. [f] $\Delta\nu_{1/2} \approx$ 100-120 Hz.

Figure 26, for the K^+•DB27C9 complex in acetonitrile yielded a formation constant of (8.5±14.6) x 10^3! Although the central value seems reasonable on the basis of that measured for the Cs^+•DB27C9 complex (7.8±0.5) x 10^3 (205), there is ample room for various interpretations! The association constants of the K^+•DB24C8 complexes were measured by ^{13}C NMR (see below).

Unlike the formation constants, the chemical shifts of the K^+• large dibenzo-crowns complexes could be reliably evaluated. Table 27 gives the results together with the chemical shifts of various K^+ ion complexes found in this work or in the literature (15). It is seen in Table 27 that the chemical shift does not vary along the series DB21C7, DB24C8 and DB27C9 and that within experimental error, (0.5-1 ppm for broad lines), it is independent of the solvent for the last two crowns; only one solvent was studied in the case of DB21C7. Thus in the large crowns, the potassium cation seems to be efficiently shielded from the surrounding solvent molecules, as found for example for the K^+•C222 cryptates (138).

The invariance of the shift with the crown as well as its value, -12±1 ppm, call for some comment. A solvent-independent shift of similar magnitude was found by Shih (15) for the "sandwich" K^+•$(15C5)_2$ complex (Table 27). It is the largest ^{39}K NMR diamagnetic shift (with respect to K^+ ion at infinite dilution in water) observed for the

crown complexes (and the cryptates) studied thus far (Table 27). In order to rationalize this behavior, it was necessary to analyze the ^{39}K NMR data in conjunction with other alkali metal NMR data for similar complexes.

The ^{23}Na, ^{39}K, ^{133}Cs and ^{205}Tl NMR chemical shifts of the crown complexes with the corresponding monovalent cations were gathered from the literature (59,148,15,38,204-206,168,169) and collected in Tables 27-30. Figures 27, 28 and 29 illustrate the variation in several solvents of the chemical shifts of the $M^+\cdot(crown)_n$ complexes (n = 1 or 2) with $M^+ = Na^+$, K^+ and Cs^+, respectively. This variation can be fully understood in terms of the repulsive overlap effect. On theoretical grounds, the extent of the paramagnetic shift is expected to depend on the short-range repulsive overlap of the electron donor with the cation (136). This was found to be borne out by experiment in a number of cases such as the "inclusive" $Cs^+\cdot$C222 complex (see Chapter I, Part C). Indeed the application of this model to the data illustrated in Figures 27-29 allows a detailed analysis of the ion size-cavity size relationship, of the conformational properties of the crown ether molecules and of the cation-solvent interactions.

Due to its intermediate size, the K^+ ion forms rather stable complexes with each crown in the series 12C4 . . . DB27C9 (see Table 27). However, the ^{39}K NMR data were the most recently obtained because the measurements are the most difficult. The body of data is now large enough to

Table 28. Sodium-23 Chemical Shifts of Various Na^+·Crown Complexes in Several Solvents at 30°C.

	δ(ppm)							
Solvent	B15C5[a]	15C5[a]	$(15C5)_2$[a]	DA18C6	18C6[a]	DB21C7[b]	DB24C8[b]	DB30C10[b]
Nitromethane	-4.2	-5.3	-11.1	-6.7	-16.7	- 9.4	-7.8	-10.3
Acetonitrile	-4.1	-4.9			-15.3	-10.3	-8.3	- 8.6
Acetone				-8.8	-16.4	- 9.9		
Pyridine	-2.4	-3.2		-7.7		- 9.5	-9.2	- 7.1
DMF	-6.0	-6.8						
DMSO	-3.2	-5.3		-2.9				
THF	-3.8	-4.4			-17			
PC	-5.2				-16.1			
H_2O		-5.3						

[a]Reference 148.

[b]Reference 169.

Table 29. Cesium-133 Chemical Shifts of Various Cs^+·Crown Complexes in Several Solvents at 30°C.

	δ(ppm)[a]							
Solvent	DA18C6[b]	DB18C6[c]	18C6[d]	$(18C6)_2^d$	DB21C7[b]	DB24C8[b]	DB27C9[e]	DB30C10[b]
Nitromethane	+28.1	-37	-23		-24.0	-38.4	-39.6	-18.9
Acetonitrile	+56.5	-10	14.8	-53	8.4	-14.2	-15.6	-10
Acetone	44	-25.1	- 6.4	-47	- 8.1	-29.0	-30.2	-16.2
Pyridine	52	-13.9	10.2	-48	+ 6.0	-20.8	-19.5	-11.4
Methanol	31	-34	-19		-19.3	-36.7	-37	-17.1
DMF		-19	3.4	-48.2	+ 2	-17	-19.2	-13
DMSO		- 3	23.6		15	- 7	- 8	- 8
PC	36.8	-27.1	-10.7	-44.5	-13	-32	-33.3	-18

[a]Predicted values are underlined. [b]Reference 169. [c]Reference 204. [d]Reference [d]Reference 38. [e]Reference 168.

Table 30. Thallium-205 Chemical Shifts of Some Tl^{+}·Crown Complexes in Various Solvents at 30°C.

	(ppm)[a,b]		
Solvent	DA18C6	DB21C7	DB24C8
Nitromethane	-252	-308	-247
Acetonitrile	- 12.4	-274	-250
Acetone	- 32.6	-278	-260
Methanol		-209	(-215)
DMF	- 72.7		(-336)
DMSO		>275	(+150)

[a]Reference 169.

[b]The brackets indicate that the experimental error is large, due in general to the low stability of the complex.

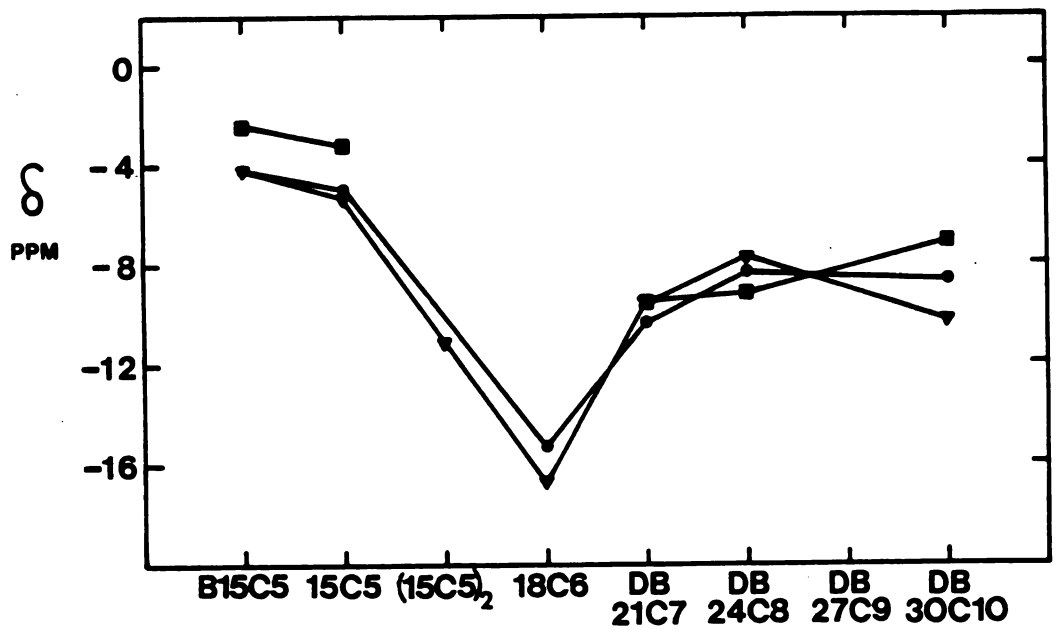

Figure 27. Sodium-23 chemical shifts of various Na^+•crown complexes in several solvents at 30°C. (▼) nitromethane; (●) acetonitrile; (■) pyridine.

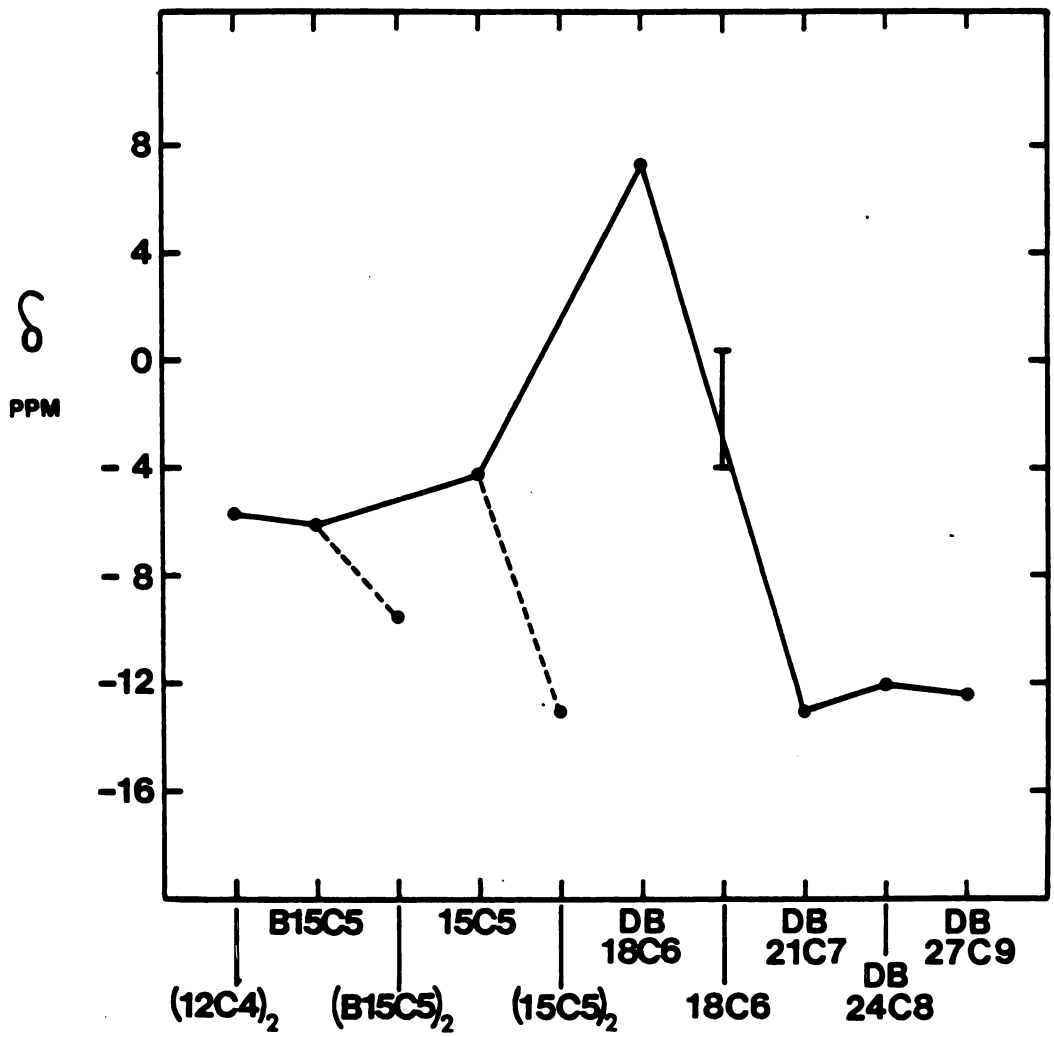

Figure 28. Potassium-39 chemical shifts of various K^+·crown complexes in acetonitrile. The vertical bar for 18C6 represents the range of chemical shifts observed in various solvents (Table 14).

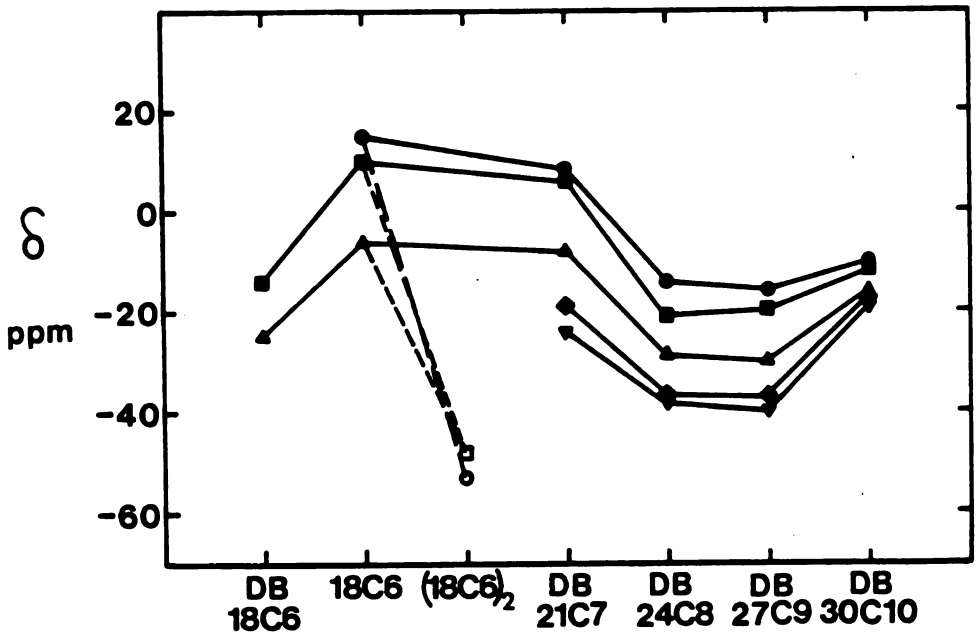

Figure 29. Cesium-133 chemical shifts of various Cs^{+}·crown complexes in several solvents. (●) acetonitrile; (■) pyridine; (▲) acetone; (◆) methanol; (▼) nitromethane.

permit a general interpretation.

The cavity sizes of the large crowns, DB21C7 and above, are larger than the K^+ ion size. As a result, there is not much overlap between the ether oxygens and the K^+ ion; a large upfield shift results (Figure 28). The small solvent dependence of the shifts is consistent with the possibility for the large crowns to "wrap around" the cation (207).

Conversely, the DB18C6 cavity size is smaller than the K^+ ion, and the signal shifts in the paramagnetic direction by about 20 ppm with respect to DB21C7. This is due to the increase in the repulsive overlap between the ether oxygens and the K^+ ion. The chemical shift of K^+·18C6 occupies an intermediate position corresponding to the intermediate size of 18C6 between those of DB18C6 and DB21C7. Since for the K^+·18C6 complex the shift is not known in acetonitrile, the range of shifts in various solvents is shown in Figure 28. As seen in Chapter III, the solvent dependence of the shift is rather limited for this complex.

The large upfield shift observed in going from DB18C6 to 15C5 (Figure 28) indicates that the K^+ ion is displaced from the center of the cavity. If this were not so, a very large paramagnetic shift would have resulted. Thus the K^+ ion lies above the plane of the 15C5 ring and forms an "exclusive" type of complex, as does Cs^+ with DB18C6 (38). This is supported by the very large solvent dependence of the shift (Table 27) and by the formation of a quite stable

2:1 (15C5:K^+) complex (log $K_f \simeq 2$ in MeCN (15)).

It would be interesting to determine the minimum cavity size of a crown ether which could accommodate the K^+ ion in the center of its cavity. This could be done for example by adding a (third) benzene ring to DB18C6 to reduce the cavity size, and by measuring the chemical shift of the resulting K^+•"tribenzo-18C6" complex. If the signal is at lower field than that of K^+•DB18C6, then the K^+ ion should be at the center of the cavity. The opposite result would indicate that the cavity is too small to accommodate the K^+ ion. The difference between the ionic radii and the coordination radii (208) of this and other ions could be estimated by this method.

The ^{39}K chemical shifts of the 2:1 (15C5:K^+) complex is about 8 ppm upfield from that of the 1:1 complex. In a recent review (89) Dye pointed out that the solvent-independent shifts of -48 ppm for Cs^+•$(18C6)_2$ is about that expected for an ether type solvent, indicating that the Cs^+-O interactions are essentially relaxed in this complex (indeed δ for a THF solution of Cs^+ octanoate 0.01 M is -44 ppm (209)). The same explanation probably holds for K^+•$(15C5)_2$. This complex gives a shift of -12 ppm which, as previously mentioned, closely resembles the shifts seen for the large crowns. In both kinds of complexes, the binding sites of the ligand possess a large motional freedom due to the looseness of the fit and behave as

individual ether-type solvent molecules with respect to the cation. It was assumed in Chapter III that the chemical shift of the potassium ion solvated by THF or 1,3-dioxolane is several ppm downfield from -16 ppm. From the results obtained with $K^+\cdot(15C5)_2$, we anticipate a value close to -12 ppm, which would validate our assumption.

The number of binding sites does not seem to be important. In the K^+ ion complexes with DB21C7, DB24C8, DB27C9 and 2 x 15C5, the shift is constant while the number of ether oxygens varies from 7 to 10. This is because the K^+-O interactions are relaxed in the 4 complexes, and the overlap is minimum.

The $K^+\cdot$B15C5 and $K^+\cdot(12C4)_2$ complexes give similar shifts in acetonitrile (Figure 28). What was originally considered (15) as a 1:1 must actually be a 2:1 (12C4:K^+) complex since the shift is virtually solvent independent (Table 27). Both the 1:1 and 2:1 complexes are detectable in the case of B15C5. As found for 15C5, the 2:1 complex gives a signal at higher field than the 1:1 complex in acetonitrile and at lower field in nitromethane.

It is interesting to note that the signal of the 2:1 complex is gradually shifted upfield when 12C4 is replaced by B15C5 and by 15C5 (Figure 28). This might indicate that as the ring size increases, the repulsion between the two rings also increases due probably to the smaller distance of approach of these two rings. This tends to

loosen the fit and to reduce the overlap between the rings and the cation. This explanation seems to be borne out by the higher stability of the $K^+\cdot(B15C5)_2$ complex as compared to $K^+\cdot(15C5)_2$. In acetonitrile log K_f values of 2.7 and 2.0 respectively were reported (15).

The data can also be rationalized by considering that the K^+ ion can or cannot accommodate 10 oxygen atoms around it depending on the spatial arrangement of these atoms. Carbon-13 NMR studies (207) and X-ray diffraction studies (210) have shown that 10 oxygen atoms can be evenly disposed around the K^+ ion when it is complexed by DB30C10 both in solution (207) and in the solid state (210, Figure 30). In this case the 10 oxygen atoms are "wrapped around" the cation like the seam of a tennis ball (same description as for the $K^+\cdot$nonactin complex (211)). When these atoms are located on the two B15C5 rings, they can probably still come into contact with the K^+ ion since the shift of -9.5 ppm for the $K^+\cdot(B15C5)_2$ complex indicates that the K^+-O interactions are not completely relaxed. The benzene rings must not induce steric hindrance since they can easily avoid each other as they do in the solid state (110, Figure 30). In order for the 10 oxygen atoms of the two 15C5 molecules to come into contact with the cation, the two rings should be very close to each other since 15C5 is larger than B15C5. This is not possible due to the repulsive forces between the rings. The potassium cation is then left in a cage

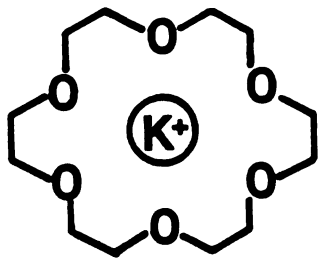

K^+18C6

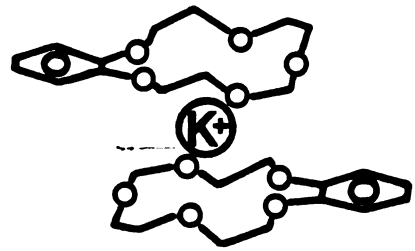

$K^+(B15C5)_2$

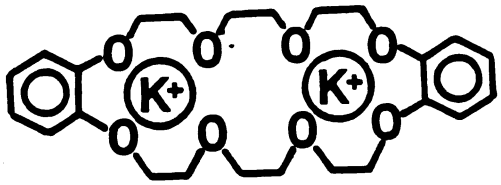

$(K^+)_2DB24C8$

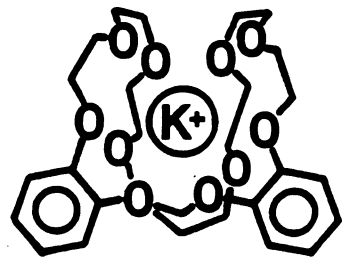

$K^+DB30C10$

Figure 30. Potassium ion-crown ether complexes of various stoichiometries (from Reference 110 except $K^+ \cdot 18C6$ Reference 82).

slightly larger than itself and the overlap is minimum. In the case of $K^+\cdot(12C4)_2$, little repulsion between the two distant rings allows a tighter fit and results in a paramagnetic shift despite the decrease in the number of binding sites.

The ^{39}K NMR data in Figure 28 demonstrate that the steric factors rather than the electron donor abilities of each crown or the number of binding sites determine the chemical shifts of $K^+\cdot$crown complexes. For example the downfield shift observed upon replacement of 18C6 by DB18C6 clearly arises from steric changes. It has been proposed (10) that the addition of benzene rings reduces the cavity size and induces a decrease in the basicity of the ether oxygens. If these oxygens were free to move like solvent molecules, the decrease in basicity should decrease the paramagnetic shift since the solvent paramagnetic shift originates from electron-pair donation from the solvent to the outer p orbitals of the cations (61,141). Contrary to this, however, an increase in the paramagnetic shift is observed due to the larger "squeezing" of K^+ in the smaller DB18C6 cavity.

The notion of "inclusive" and "exclusive" complexes which is well accepted for cryptates (97) may now be extended to the crown complexes. The K^+ ion complexes with DB18C6 (which corresponds to the maximum of the curve) and with all the larger crowns (at the right of this maximum)

are inclusive, as well as the "sandwich" complexes obtained with the small crowns. In an inclusive complex, the cation is located at the center of the crown cavity, or of the cavity formed by two crown molecules. On the other hand the 1:1 complexes with the smaller crowns than DB18C6 are "exclusive", i.e., the cation is displaced from the center of the cavity.

In the case of potassium complexes, both the chemical shift of the complex and the extent of the solvent dependence of this shift may be used to determine the "inclusive" or the "exclusive" character of the complex. The inclusive character is associated with a small or negligible solvent dependence, e.g., less than 5 ppm for K^+•18C6, whereas the exclusive character is reflected by a large solvent dependence of the shift, e.g., 20 ppm for K^+•15C5 (Table 27).

The patterns seen in Figures 27 and 29 for the Na^+ and the Cs^+•crown complexes, respectively, may be rationalized in the same manner. Only the distinctive features of the plots will be discussed. In the case of sodium, there is no sharp maximum of the chemical shift in the series B15C5 . . . DB30C10 (Table 28). However, the very small variation of δ between 15C5 and B15C5 suggests that the maximum is in between these two (closer to B15C5 than to 15C5). This means that the cavities of all the crowns shown except B15C5 are equal to or larger than the Na^+

ion. The chemical shifts exhibit a limited solvent dependence (3 ppm or less). It can be said that the complexes are "inclusive".

Another interesting feature is the very large solvent-independent upfield shift of the Na^+•18C6 complex. The 18C6 cavity is larger than the Na^+ ion but it is too rigid to twist around this cation so that the Na^+-O interactions are even more relaxed than in the large crowns. The larger DB21C7 molecule is able to depart from the planar structure or to contract itself in order to bring the oxygen atoms into contact with the cation. A substantial paramagnetic shift results (Figure 27). The DB24C8 molecule is even more deformable upon complex formation; a "wrap around" complex is formed in this case, as shown by the relative narrowness of the ^{23}Na lines (169).

The DB30C10 molecule seems to be too large to be twisted enough to hold the Na^+ ion tightly, as postulated by Live and Chan (45). The chemical shifts of the Na^+•DB30C10 complexes are somewhat dependent on the solvent (Table 27) and follow the same sequence as the chemical shifts of the solvated Na^+ ions in the various solvents (see for example 164). This behavior strongly indicates that in the complex the Na^+ ion is not completely stripped of solvent molecules. The opposite conclusion was arrived at by Live and Chan (45) who used ^1H NMR. However it is to be expected that the ^{23}Na chemical shift is a much more sensitive probe of

the sodium ion interaction than the ^{1}H chemical shift.

Once again, the shifts seen for the large crown complexes with Na^{+} ions resemble those seen for the Na^{+} ion in ethereal solvents and for the "sandwich" $Na^{+}\cdot(15C5)_2$ complex. This last complex, which is unstable due to the matching of the 15C5 cavity with the Na^{+} ion, could only be detected in the weakly donating nitromethane (148).

The chemical shifts of the $Cs^{+}\cdot$crown complexes do not reach a distinct maximum for any particular crown (Figure 29). However, the pattern observed suggests that the maximum "squeezing" of the Cs^{+} ion would occur for a crown molecule with a size intermediate between those of 18C6 and DB21C7. As seen before, the Cs^{+}-O interactions are relaxed in the $Cs^{+}\cdot(18C6)_2$ complex (89) even more so than in the large crowns. Only the DB30C10 molecule is large enough to "wrap around" the Cs^{+} ion, as indicated by the very limited solvent dependence of the shift. Besides, the downfield shift of the ^{133}Cs resonance upon replacement of DB24C8 or DB27C9 by DB30C10 suggests that the Cs^{+} ion is in direct contact with the ether oxygen atoms of the last ligand whereas the Cs^{+}-O interactions are weaker with the other two ligands.

As previously noted, a change in the number of binding sites does not seem to affect the chemical shift. However, the nature of the electron donor is a predominant factor. It is seen in Table 29, by comparing DA18C6 with 18C6,

that the substitution of two oxygen atoms by two N-H groups in 18C6 shifts the resonance signal of the complex by about 40 ppm in the paramagnetic direction. A large paramagnetic shift was also observed in the case of Na^+ ions (206, see Table 28). The direction of the shift is consistent with the fact that alkali metal NMR resonances are at lower fields in N-donor than in O-donor solvents (135, 195).

The solvent dependences of the chemical shifts of Cs^+•crown complexes are relatively large and follow the sequence DB30C10 < DB18C6 ≈ DB24C8 ≈ DB27C9 ≈ DB21C7 ≤ 18C6. It is noticeable that, in contrast with the Na^+•crown complexes, the Cs^+•crown complexes are of the "exclusive" type with the exception of the Cs^+•DB30C10 and, of course, the "sandwich" Cs^+•$(18C6)_2$ complexes. This "exclusive" character stems directly from the relatively large size of the Cs^+ ion. Even when this ion is located at the center of a crown cavity, such as DB21C7, a large area of the surface of the ion remains exposed to the surrounding solvent molecules or anions. This does not apply to smaller cations.

Two important consequences may be drawn. First the "inclusive" or "exclusive" character of the complex should be defined from the solvent dependence of the chemical shift rather than from the position of the cation in the cavity. Second, the contact and the solvent-separated ion pairs are much more efficiently broken upon complexation

of small cations than large cations by crown ethers.

The parallelism observed in various solvents for the variation of the ^{133}Cs chemical shift as a function of the crown (Figure 29) is interesting in that it allows a reliable prediction of the chemical shifts of a series of $Cs^{+}\cdot$crown complexes in a given solvent, if the chemical shift of only one $Cs^{+}\cdot$crown complex in the same solvent is is known. Some predicted values are underlined in Table 29.

Carbon-13 NMR Studies

The formation constants of some alkali cation crown complexes may be evaluated from the variation of the salt/ ligand ratio. The procedure is nearly the same as that previously described for alkali metal NMR. Wilson (212) reported that with a 100 MHz spectrometer the upper limit of reliable values of formation constants obtainable by ^{13}C NMR is about 100. This observation was confirmed by the results of Shih (15) and of Lin and Popov (59) who used an 80 MHz spectrometer. The purpose of this study was to measure the stability constants of the $K^{+}\cdot$DB24C8 complex in various solvents. Since this complex was found to be quite stable in methanol (log $K_f > 3$, see Table 31), the upper limit of our technique had to be increased by about two orders of magnitude. This was achieved by running the ^{13}C spectra on a 250 MHz spectrometer at a

Table 31. Formation Constants of M^+,DB24C8 Complexes with $M^+ = Na^+$, K^+, Cs^+ and Tl^+ in Various Solvents at 25±5°C.

	Log K_f			
Solvent	Na^{+a}	K^{+b}	Cs^{+a}	Tl^{+a}
Nitromethane	3.74±0.12	≥4	4.11±0.08	>5
Acetonitrile	2.95±0.07	3.70±0.16	3.94±0.07	4.81±0.05
		3.70[c]		4.80[c]
Acetone			3.71±0.09	4.15±0.05
Methanol		3.20[c]	3.65±0.05	3.19±0.07
		3.49[d]	3.78±0.08[d]	3.40[c]
			3.80[c]	
70% MeOH-30% H_2O	1.54[e]	2.42[e]	2.48[e]	
DMF	∿0	1.44±0.08	2.10±0.04	(1.16)
DMSO	∿0		1.61±0.04	<1.0
Pyridine	2.89±0.10	3.46±0.17	4.00±0.03	1.64±0.04

[a]Reference 169 unless otherwise indicated. [b]This work unless otherwise indicated.
[c]Reference 213. [d]Reference 214. [e]Reference 215.

point-to-point resolution of 0.015 ppm.

The variation of the ^{13}C chemical shift with the K^+/DB24C8 molar ratio was studied in nitromethane, acetonitrile, pyridine and DMF. Some spectra obtained in pyridine are shown in Figure 31. The chemical shifts are given in Table 32 and plotted in Figures 32 and 33 as a function of the mole ratio. The DB24C8 molecule has three sets of four aliphatic carbons. The three signals shift upfield upon complexation and the signal at the lowest field shifts the most.

In nitromethane solutions (Figure 32) the addition of potassium hexafluoroarsenate to a DB24C8 solution results in a gradual coalescence of the three signals into a single peak at equimolar concentrations of K^+ ions and the ligand. This behavior, which was previously observed for the K^+·DB30C10 complex (207) in the same solvent, seems to indicate an essentially equal interaction between the 8 oxygen atoms of the polyether ring and the K^+ ion. Such equal interaction is only possible if in solutions the ligand is "wrapped around" the cation in the same manner as found (207) for the DB30C10 complex (Figure 30). The 1:2 (DB24C8:K^+) complex, which exists in the crystalline state (Figure 30), could not be detected in nitromethane solutions. As expected, the log K_f value for the 1:1 complex is larger than 4 in this solvent.

In acetonitrile, pyridine and DMF solutions, the three

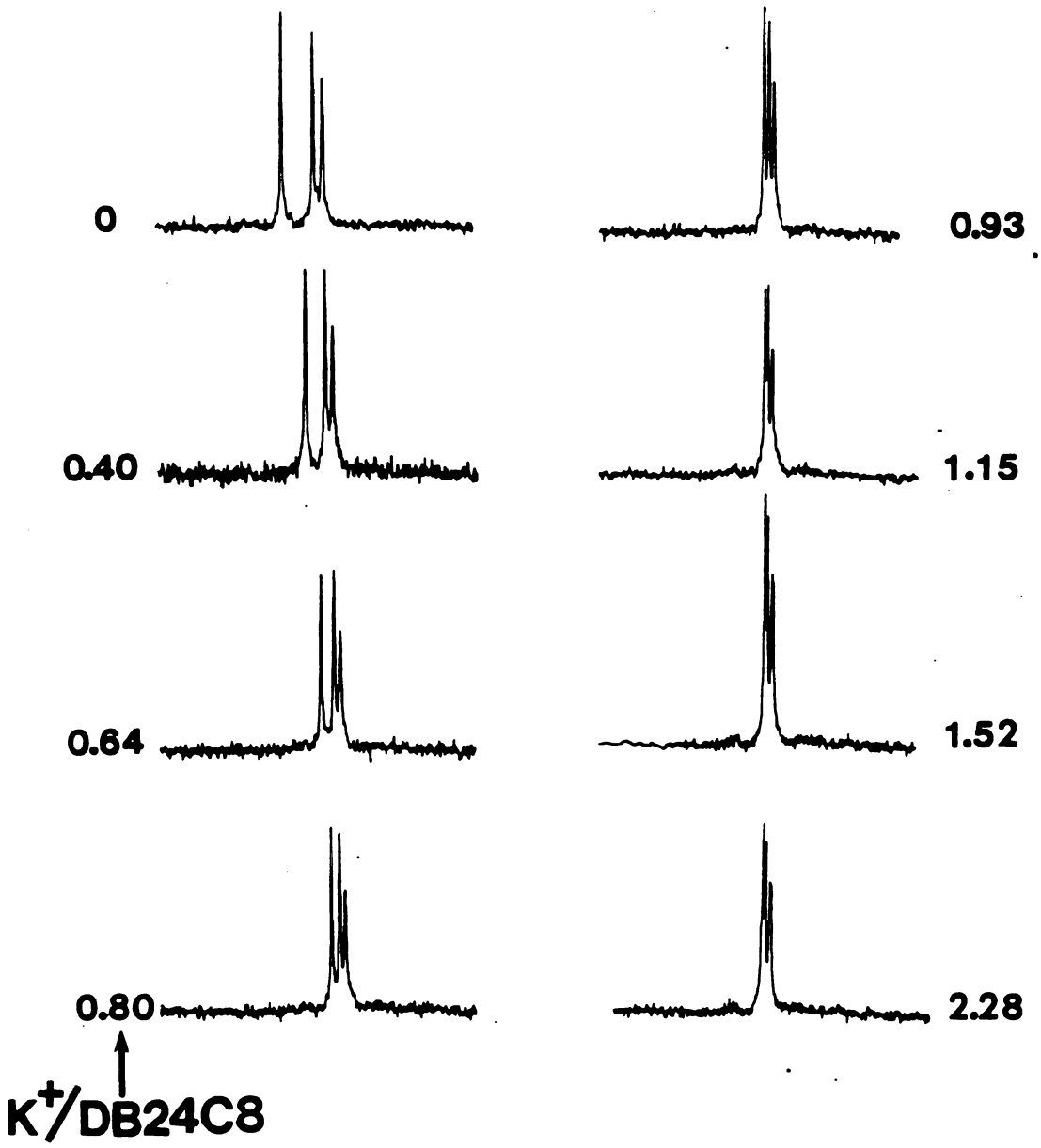

Figure 31. Carbon-13 spectra for pyridine solutions containing $KAsF_6$ and dibenzo-24-crown-8 at various mole ratios and at 25°C.

Table 32. Carbon-13 NMR Chemical Shift-Mole Ratio Data for the $K^+ \cdot DB24C8$ Complex in Various Solvents at 25±1°C.

Pyridine[a]				Acetonitrile[a]			
$\frac{[K^+]}{[DB24C8]}$ [f]	δ_1 [c,d]	δ_2	δ_3	$\frac{[K^+]}{[DB24C8]}$ [f]	δ_1 [c,d]	δ_2	δ_3
0	40.235	40.632	41.955	0	39.966	40.775	41.877
0.395	39.735	40.044	40.897	0.562	39.716	40.113	40.642
0.639	39.456	39.735	40.294	0.711	39.687	39.981	40.392
0.796	39.309	39.559	39.912	0.803	39.642	39.892	40.201
0.934	39.103	39.338	39.544	0.912	39.598	39.804	40.069
1.011	39.103	39.309	39.470	1.04	39.539	39.716	39.892
1.15	39.073	39.294	39.412	1.08	39.539	39.686	39.848
1.52	39.015	39.221	39.338	1.13	39.539	39.657	39.804
1.99	39.015	39.234	39.353	1.31	39.525	39.657	39.804
2.28	39.015	39.221	39.338	1.84	39.539	39.657	39.804
2.52	39.000	39.206	39.323	1.98	39.510	39.642	39.789
4.08	38.956	39.147	39.265				

Table 32 - Continued.

Dimethylformamide[a]				Nitromethane[b]			
$\frac{[K^+]}{[DB24C8]}$[f]	δ_1[c,d]	δ_2	δ_3	$\frac{[K^+]}{[DB24C8]}$[f]	δ_1[e]	δ_2	δ_3
0	40.395	40.777	42.027	0	38.06	38.77	39.84
0.509	40.086	40.556	41.512	0.51	37.86	38.19	38.80
0.776	39.924	40.395	41.277	1.80	37.67	37.67	37.67
0.864	39.865	40.380	41.218				
0.982	39.851	40.350	41.130				
1.16	39.777	40.292	41.012				
1.32	39.718	40.248	40.968				
1.54	39.630	40.174	40.836				
1.80	39.601	40.145	40.747				
2.51	39.498	40.086	40.586				

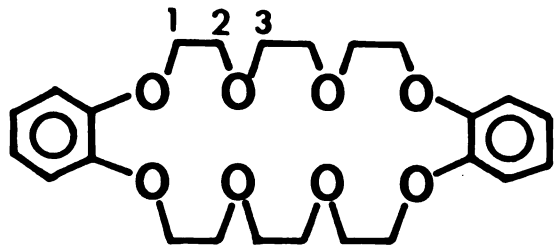

[a]The measurements were made on a Bruker WM-250.

[b]The measurements were made on a Varian CFT-20.

[c]Reference = $\underline{C}D_3$ carbons of pure acetone d6 (see Chapter II).

[d]The experimental error is of the order of the point to point resolution (0.015 ppm). The chemical shifts are corrected for magnetic susceptibilities (Table 7).

[e]Reference = $\underline{C}H_3$ carbons of acetone in water-acetone (50/50 vol%). The chemical shifts (±0.05 ppm) are not corrected.

[f][DB24C8] = 0.05 M except in pyridine (0.07 M).

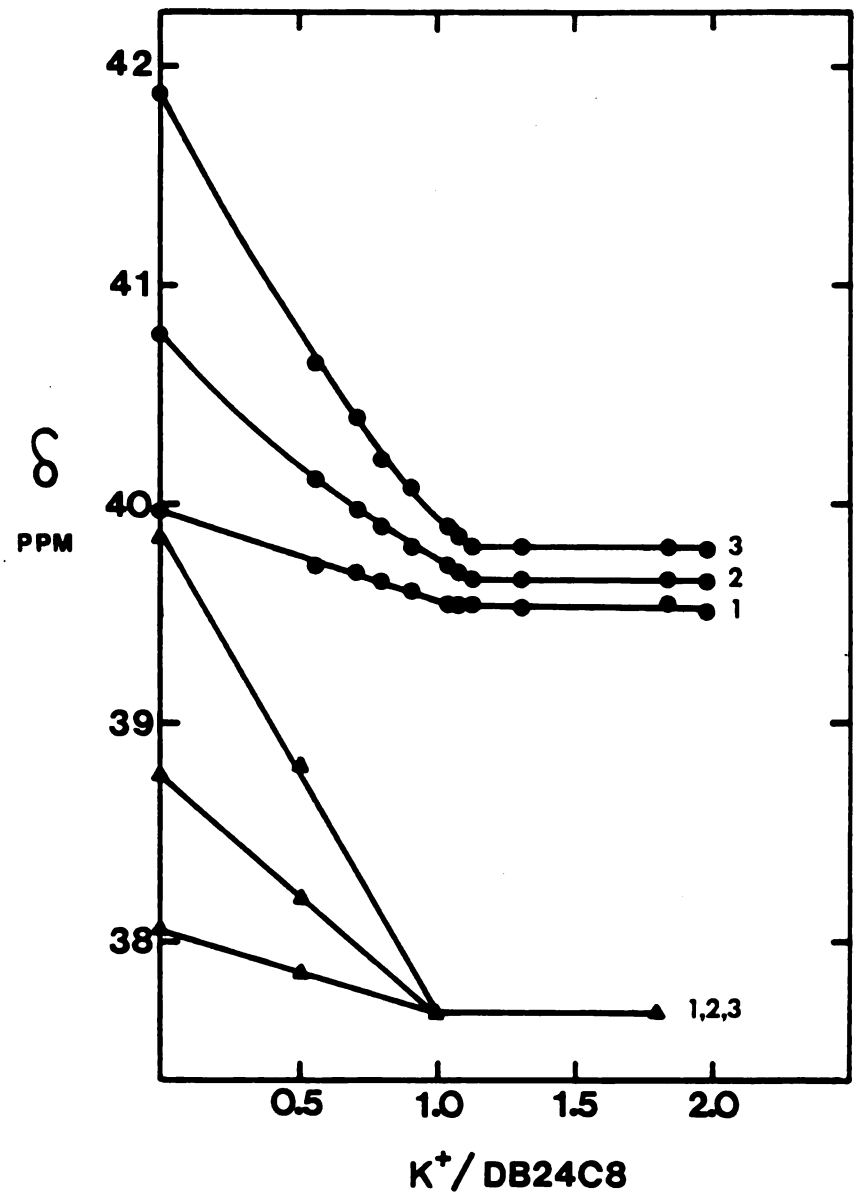

Figure 32. Carbon-13 chemical shifts (vs acetone d_6) as a function of the K^+/DB24C8 mole ratio in (●) acetonitrile and (▲) nitromethane at 25°C.

signals tend to approach each other as the mole ratio increases, but they do not coalesce even at high mole ratio (Figure 33). This behavior is particularly clear in DMF where the spread of the three signals remains quite large (∿1.1 ppm vs ∿0.3 ppm in the other two solvents).

The formation constants, which were measured from the variation of the chemical shift of carbon 3 of the DB24C8 molecule (see Figure 31), are given in Table 31 together with some literature values. In acetonitrile we found the log K_f value to be equal to 3.70±0.16 (K_f = (5±1.8) 10^3), which corresponds to the value obtained by polarography (213). Thus it seems to be possible to measure K_f values much larger than 100 by the ^{13}C NMR technique provided a high field spectrometer is used. However the large standard deviation clearly indicates that the upper limit of the technique is reached.

In pyridine, the signals shift by a large amount upon complexation (Figure 33), which made possible the evaluation of log K_f with each of the three carbons. The three values obtained were identical within experimental error. However, carbons 1 and 2 gave large standard deviations indicating once again the limit of the method. As in other solvents, the log K_f value measured with the carbon 3 was kept (log K_f = 3.46±0.17). It is interesting to note that the DB24C8 ligand selectively complexes K^+ over Tl^+ ions in pyridine while the order is reversed in the other solvents

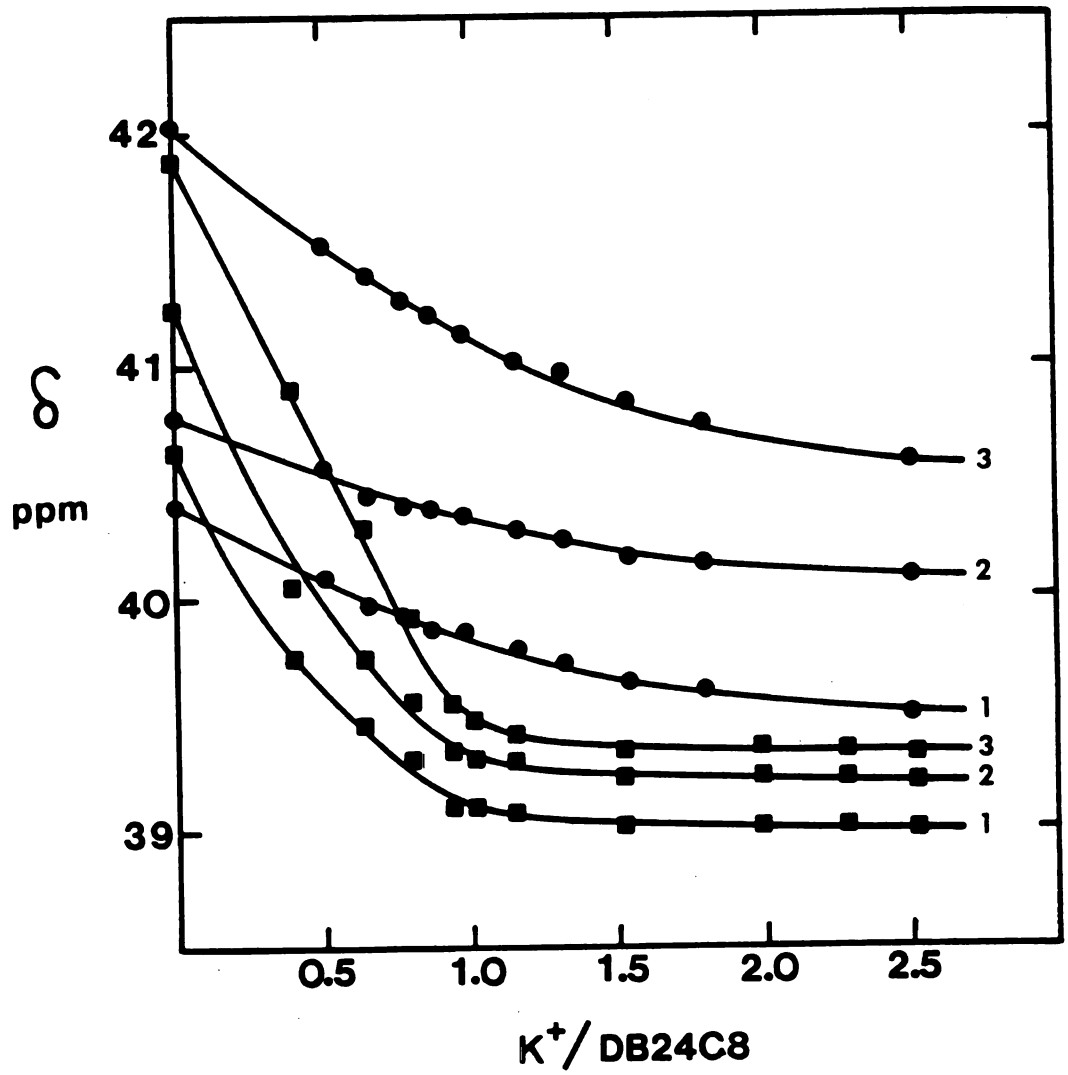

Figure 33. Carbon-13 chemical shifts (vs acetone d_6) as a function of the K^+/DB24C8 mole ratio in (●) DMF and (■) pyridine at 25°C.

studied (Table 31).

This reversal most likely reflects the competition between solvation and complex formation. There is probably some extent of covalency in the Tl^+-pyridine interaction due to the "softness" of both the Tl^+ ion and the nitrogen donor atom of the pyridine molecule (203). The stronger solvation of Tl^+ ions by pyridine results in a weaker complexation. Although pyridine exhibits a strong donor character (150), it does not solvate strongly the hard alkali cations, and the complexes of these cations with crown ethers are usually quite stable (205).

In DMF, which is a good donor, the K^+·DB24C8 complex is much less stable than in the other solvents studied ($\log K_f = 1.44 \pm 0.08$). As found in the other solvents, the stability is lower than that found in the case of Cs^+ ions.

There is a definite relationship between the stability of the K^+·DB24C8 complex and the spreading of the three signals in a given solvent. In the weakly donating nitromethane solvent, the complex is stable and the three peaks coalesce at high mole ratio; a "wrap-around" complex is formed. In acetonitrile and pyridine where the complex is less stable, three signals are distinguishable even at high mole ratio, but the separation of the two extreme signals does not exceed 0.3 ppm; the "wrap-around" complex is almost formed. In DMF, the resonance signals are widely separated ($\delta_1 - \delta_3 \simeq 1.1$ ppm, see Figure 33) even at a mole ratio of 2.5 where about 85% of the DB24C8 are complexed

(with $[DB24C8]_{total}$ = 0.075 M). This behavior suggests that the ligand does not "wrap around" the K^+ ion. In this last case, it is very likely that one or several solvent molecules remain attached to the K^+ ion, as seen for example in the 1:1 complex of DB30C10 with rubidium thiocyanate (216).

It was noted earlier that Cs^+ ions form "wrap-around" complexes with DB30C10 only (in the series of ligands studied), whereas Na^+ ions do so with DB21C7 and DB24C8 (DB27C9 was not investigated). It can be inferred from these results that the DB24C8 molecule must have the minimum size required to surround the K^+ ion. Consequently a strong K^+-solvent interaction might prevent a complete stripping of the solvation shell by the ligand. The stability of the complex and its conformation are intimately related in this case.

B. Potassium Cations Interaction with the Conventional Ligand 2,2'-Bipyridine

Introduction

In general interactions of "conventional", i.e., non macrocyclic, ligands with the alkali ions are quite weak, and often they are beyond the sensitivities of most physicochemical techniques. Therefore, in order to detect the formation of such complexes, it is necessary to use

very sensitive probes of either the ligand or the metal cation. Small changes in the immediate environment of the alkali ions in solutions may be detected by the alkali metal NMR technique.

Hourdakis (218) studied the interactions of alkali metal ions with 2,2'-bipyridine (BP) in several nonaqueous solvents, using ^{7}Li, ^{23}Na, ^{133}Cs and ^{13}C NMR. Recently Vogtle et al. (113) referred to the use of ^{23}Na NMR for a qualitative differentiation of the stability of Na^{+} ion complexes with o-phenanthroline, 2,2',2"-terpyridine and 2,2'-bipyridine and concluded that the last ligand gives the least stable complex. Hourdakis found the stabilities of the BP complexes to be in the order $Li^{+} > Na^{+}$. Complex formation was not detected for the Cs^{+}-BP system. It was of interest to us to complete the study by the "borderline" case which is the K^{+} ion.

Results and Discussion

The variations of the ^{39}K chemical shifts and of the linewidths as a function of the BP/K^{+} mole ratio are given in Table 33 and shown in Figure 34. Since the complexation was expected to be weak, only solvents with intermediate and weak solvating ability were investigated. Both δ and $\Delta\nu_{1/2}$ values show much less change upon addition of BP than was observed with Li^{+} and Na^{+} (140,218), although the range of the chemical shift is larger for ^{39}K than for

Table 33. Potassium-39 Chemical Shifts and Line Widths for Nitromethane Solutions Containing $KAsF_6$ (0.075 M) and 2,2'-Bipyridine at Various BP/K^+ Mole Ratios (MR) and at 25°C.

Nitromethane			THF		
MR	δ(ppm)	$\Delta\nu_{1/2}$ (Hz)	MR	δ(ppm)	$\Delta\nu_{1/2}$ (Hz)
0	-22.8	9	0	-17.8	24
0.75	-21.9	17	1.00	-17.6	26
1.21	-21.5	24	1.98	-17.7	26
1.99	-20.9	30	3.25	-17.4	29
2.50	-20.3	35	4.37	-17.4	30
3.08	-19.9	39	7.75	-17.1	36
3.45	-19.8	41	9.91	-16.6	36
4.25	-19.0	54	11.07	-16.6	38
Acetonitrile			PC		
0	- 2.2	10	0	-15.1	62
1.07	- 2.0	13	0.91	-14.6	80
2.18	- 1.9	14	1.76	-14.7	78
2.96	- 1.8	16	2.93	-14.5	89
3.94	- 1.6	17	3.96	-14.1	95
7.45	- 1.4	21	7.00	-13.8	115
10.63	- 1.2	28	9.86	-13.4	145

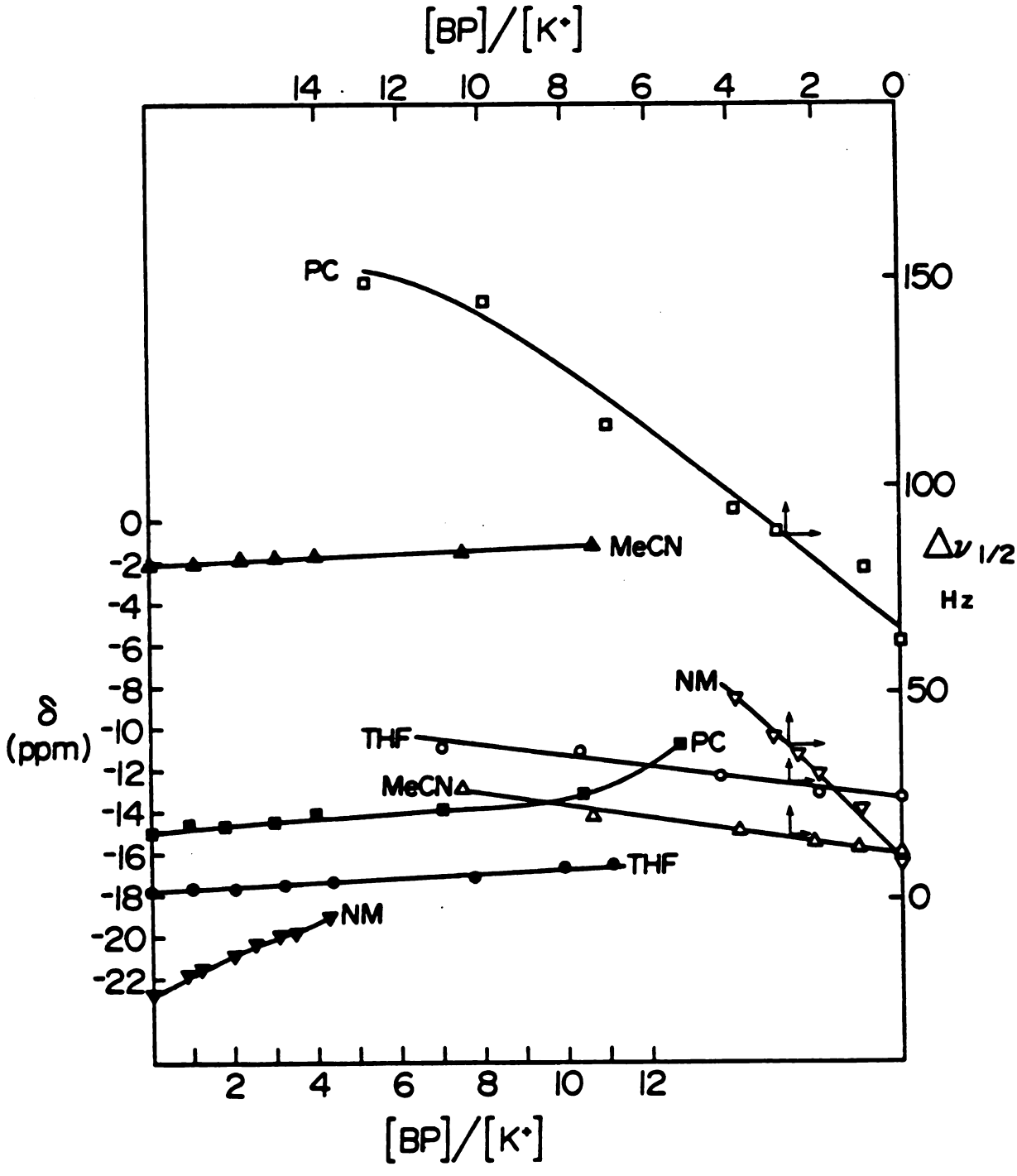

Figure 34. Variation of the ^{39}K chemical shift and line width as a function of the 2,2'-bipyridine (BP)/ K^+ ratio in various solvents.

^{7}Li or ^{23}Na. It is obvious that the K^{+}-BP interaction is very weak even in nitromethane solutions. Except in this last solvent, the increase in the line width reflects that in the viscosity. It should be noted that while Grillone and Nocilla (109) succeeded in isolating solid $(K{\cdot}BP)^{+}Ph_4B^{-}$ complex, in order to do so they had to have a 6-7 fold excess of the ligand.

Hourdakis (218) found that the limiting chemical shift in nitromethane is 4.0 ppm (vs $LiClO_4$ 4 M in H_2O). This value seems to be the largest downfield ^{7}Li chemical shift observed thus far for solutions of lithium salts, and it is considerably further downfield than that observed for dilute lithium salt solutions in pyridine (+2.5 ppm (219)). On the other hand, the highest upfield shift seems to be that of fluorenllithium diethyl ether complex in ether solvent of -6.2 ppm (220). Although two different references were used for these measurements, 4.0 M $LiClO_4$ and 20% solution of LiCl (both aqueous), the difference between the two is smaller than the experimental error.

These results seem to support the explanation proposed by Maciel et al. (221) for the very high and low shieldings of ^{7}Li in acetonitrile and pyridine solutions, respectively. The neighbor anisotropy effect is even stronger for the $Li(BP)_2^{+}$ complex than for Li^{+} ion in pyridine solutions. In the $Li(BP)_2^{+}$ complex, Li^{+} ion is coordinated to the nitrogen in the plane of the ring, while in the $Li^{+}Fl^{-}{\cdot}Et_2O$

complex it is located directly above the plane of the aromatic carbanion (220). The resulting ^{7}Li shifts are 10 ppm apart, about twice as much as the total range of ^{7}Li shifts in dilute solutions of lithium salts in common solvents (219,221).

It is clearly seen from the above results and from the Hourdakis' results that 2,2'-bipyridine does complex Li^{+}, Na^{+} and K^{+} ions in nonaqueous solvents, and that the strength of the interaction varies in the order $Li^{+} > Na^{+} > K^{+}$; it also varies inversely with the solvating ability of the solvents.

CHAPTER VI

NUCLEAR MAGNETIC RESONANCE IN MOLTEN SALTS

A. Introduction

In the presence of a solvent, the anion competes with the solvent molecules for the cation and such factors as the dielectric constant and the donor character of the solvent, the sizes and the charge densities of the species in solution determine the result of this competition. In a molten salt only cation and anions are present; however, the nature and the extent of the cation-anion interaction may vary in a large extent, depending on the species present and on the temperature.

Nuclear magnetic resonance has proven to be a sensitive technique for the study of cation-anion interactions. Besides, it has been shown (121-125) that NMR can provide valuable information about the structure of molten salts and the identification of the species present (Chapter I, Part C). The reported studies were made by ^{205}Tl, ^{7}Li and ^{23}Na NMR. The relatively low melting points of some potassium salts or their mixtures with other alkali metal salts (Table 34) led us to extend our ^{39}K NMR studies to molten salts.

B. Experimental Part

Most measurements were carried out on a highly modified single-coil, multinuclear Varian DA-60 spectrometer

Table 34. Physical Properties of Some Alkali Metal Salts and Eutectic Mixtures.[a]

System	Composition mol %	m.p. °C	Density$^{temp.}$ g.cm^{-3}	ε	η$^{temp.}$ cp
NaSCN		323		2.7[b]	
KSCN		173	$1.60^{173-200}$	2.4[b]	7.87^{200}
NaSCN-KSCN	30-70	133			
NaSCN-KNO_3	36.5-63.5	140			
$LiNO_3$		252	1.771^{270}	2.5	5.05^{300}
$NaNO_3$		310	1.896^{320}	1.9	3.00^{310}
KNO_3		338	1.861^{350}	1.45	2.73^{350}
$LiNO_3$-KNO_3	43-57	132		2.3[b]	
$LiNO_3$-$NaNO_3$	54-46	193			
$LiNO_3$-$NaNO_3$-KNO_3	27-18-55	125			
NaOH-KOH		<227			
NaCl-$AlCl_3$	33-67	154			

[a]Data from G. J. Janz, Molten Salt Handbook, Academic Press (1967).
[b]Calculated with $\varepsilon = \rho^2$ (ρ = refractive index).

equipped with an external ^{1}H lock system. Special probe inserts were made by W. Burkhardt for various frequency ranges. A high melting glue was used for the attachment of the radio frequency coil to the glass part of the insert. The designs of the inserts and of the home built probe allowed measurements to be made at temperatures up to ∿250°C.

Preliminary measurements were made on a Bruker WH-180 spectrometer described in Chapter II. With this instrument, measurements are not possible at temperatures over 150°C or 200°C depending on the core diameter.

Samples (∿5 ml) were prepared by directly weighing appropriate amounts of purified salts (purification methods were described in Chapter II) in the NMR sample tubes (Wilmad, 15 mm O.D.). In all cases studied, pressure caps were sufficient to resist to the pressure resulting from the heating of the samples.

For the measurements, the samples were heated in a sand bath at the temperature of the measurement and rapidly transferred to the probe which was preheated at the same temperature. A few minutes were allowed in order to reach equilibrium. Depending on the composition of the sample and on the line width, the number of scans varied between 1 and 100.

The highly moisture sensitive chloroaluminate mixtures were directly inserted in NMR sample tubes under nitrogen atmosphere.

C. Results and Discussion

The ^{39}K chemical shifts and line widths of the systems investigated are given in Table 35. At 200°C, the signals are quite narrow despite the relative viscosity of molten salts (Table 34). The line widths are comparable to those observed in concentrated aqueous solutions of potassium salts at 23°C (Table 36). At a given temperature, the line widths were nearly the same for all systems investigated.

The chemical shifts vary in a large range. The shift of -17 ppm observed for the $LiNO_3$-KNO_3 eutectic mixture at 200°C approaches that observed for the K^+ ion solvated in nitromethane at 25°C (-21.1 ppm (15)). Bloor and Kidd (142) studied the anion and the concentration dependence of the ^{39}K chemical shift in aqueous potassium salt solutions. These authors found that the paramagnetic shielding of the cation induced by the anion is related to the ability of the anion to overlap with the cation. In the molten salt as in aqueous solution, the NO_3^- ion gives an upfield shift of the ^{39}K resonance with respect to the solvated K^+ ion, indicating that the K^+-NO_3^- overlap is smaller than the K^+-H_2O overlap.

In KSCN and in NaSCN-KSCN mixtures, a shift of 13 ppm is observed. The chemical shifts obtained in aqueous potassium thiocyanate solutions are given in Table 36 and plotted in Figure 35. In this figure it is seen that

Table 35. Potassium-39 Chemical Shifts and Line Widths for Some Molten Salts and Molten Salt Mixtures.

System	Composition mol %	t °C	δ ±0.5 ppm	$\Delta\nu_{1/2}$ Hz
KSCN		200	13.1	23
NaSCN-KSCN	10-90	200	12.8	26
	20-80	200	12.6	27
	30-70	200	11.4	28
		190	10.9	35
		170	10.9	52
$LiNO_3$-KNO_3	43-57	200	-17.0	24
($LiNO_3$-KNO_3)-KSCN	90-10	200	-14.1	31
		130	-14.8	104
$LiNO_3$-$NaNO_3$-KNO_3	27-18-55	200	-17.4	23
		190	-16.8	27
		180	-16.9	30
		170	-17.2	34
		160	-17.3	42
		150	-17.2	52
		140	-17.8	63
NaOH-KOH	50-50	240	43	33

Table 36. Potassium-39 Chemical Shifts for Aqueous Solutions of KSCN at Various Concentrations.[a]

Concentration M	δ^b ppm	$\Delta\nu^c_{1/2}$ Hz
0.097	0.06	8
0.200	0.06	8
0.296	0.06	10
0.403	0.15	10
0.502	0.15	10
0.593	0.21	11
0.807	0.30	11
0.985	0.35	11
2.010	0.79	11
3.986	1.95	13
9.028	5.58	20
9.028 (58°C)	4.71	14
9.028 (75°C)	4.42	12
9.028 (87°C)	3.11	11

[a]At 23°C unless otherwise indicated.

[b]±0.05 ppm.

[c]±1 Hz.

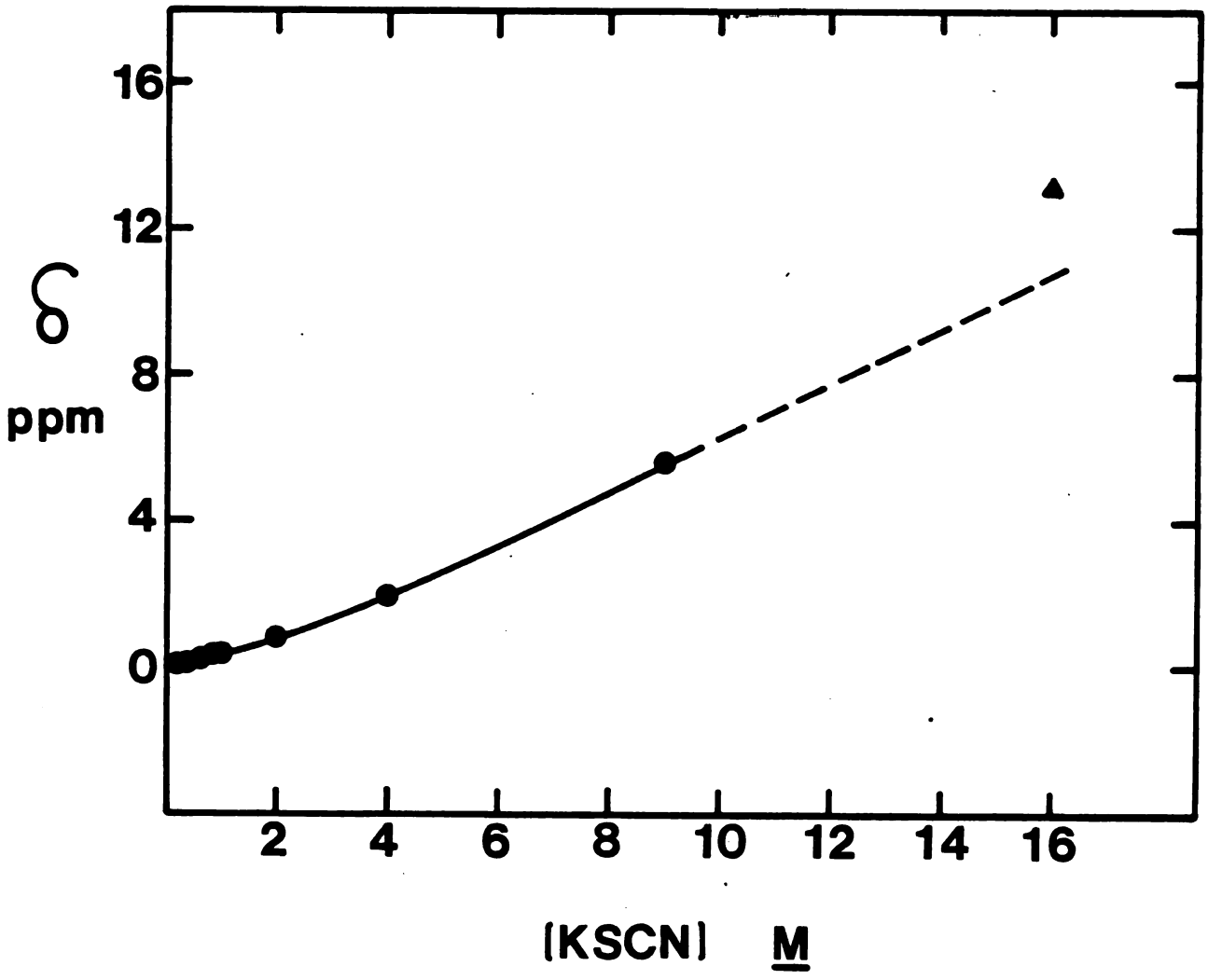

Figure 35. Variation of the potassium-39 chemical shift as a function of the KSCN concentration in water at 23°C. The dashed line is an extrapolation. The triangle is for the molten KSCN at 200°C.

an extrapolation of the chemical shifts observed in aqueous KSCN solutions to the concentration of the pure salt (∿16 M) gives a value of about 11 ppm in fair agreement with the value of 13 ppm measured in the molten salt. As more and more NCS^- ions are disposed around the potassium ion, the environment of this ion resembles more and more that in molten KSCN; the extent of the electron donation of NCS^- to K^+ seems to be comparable in both media since the chemical shifts are nearly the same.

It should be noted that the strong temperature dependence of the chemical shift in aqueous solution (Table 36) is not observed in molten salts (at least in the few cases studied). The upfield shift with increasing temperature is a quite general phenomenon in solutions (Chapter III). It is probably related to the loosening of the cation solvation shell.

Sahm and Schwenk (133) obtained values of 23.0, 49.6, 57.6 and 62.5 ppm for the ^{39}K chemical shift of crystalline powders of KF, KCl, KBr and KI respectively. The order of the shifts is the same as that observed for aqueous solutions of these salts (15,142). Therefore it appears that there is a correlation between the chemical shifts in aqueous solutions and those in molten salts or in crystals

A decrease in temperature does not significantly affect the chemical shift, nor does a change in the cation composition of the mixture as long as the anion remains the same.

This behavior, which was observed for the nitrates as well as the thiocyanates mixtures (Table 35), is consistent with the fact that the nearest neighbors of the cations remain the same. Nevertheless, it should be noted that a change in the composition of a mixture results in a slight change in the average K^+-anion distance, due to the differences in electrostatic attractions of different cations for the common anion (125). The change in distance should, in turn, affect the chemical shift. In fact the chemical shift variation is too small to be detected in the mixtures investigated here. Harold-Smith (125) could not detect any ^7Li chemical shift upon changing the cation composition in $LiNO_3$-KNO_3 mixtures. Likewise, we could not detect any ^{39}K chemical shift upon replacing in part $LiNO_3$ by $NaNO_3$ in the same mixtures (Table 35). Relaxation times are more sensitive than chemical shifts to changes in the composition of the mixtures (125).

The upfield shift observed in going from the pure KSCN to the NaSCN-KSCN (30-70 mol %) mixture is only three times larger than the experimental error, which precludes any interpretation. However, it is noticeable that the direction of the shift is that expected from an increase in the K^+-NCS^- distance due to the stronger electrostatic attraction of the sodium ion for the nitrate ion.

When the anion composition is changed, the chemical shift should change according to the respective populations

of the various anions in the mixture. Indeed when 10% of KSCN replace 10% of $LiNO_3$-KNO_3 mixture, the ^{39}K resonance signal shifts downfield by 3 ppm, which is 10% of the difference in chemical shift between KSCN and the nitrates mixture (Table 35).

The large paramagnetic shift of 43 ppm observed in the molten NaOH-KOH (50-50 mol%) mixture at 240°C is nearly the same as that observed for the crystalline powder of KCl, 49.6 ppm (133). In molten hydroxides the shift is large considering that, in an aqueous solution of NaOH and KOH (5 M each), the chemical shift is only 6.8 ppm.

A few ^{23}Na and ^{27}Al NMR measurements were made in chloroaluminate melts. At 193°C, in the $AlCl_3$-NaCl-KCl (66-20-14 mol %) eutectic mixture (mp = 89°C) which corresponds to the $(Na,K)Al_2Cl_7$ stoichiometry, the ^{27}Al chemical shift is 105 ppm, which is in the range of shifts found for the species $AlCl_4^-$ and Al_2Cl_6 in various solvents (85). In the same mixture the line width broadens from 350 to 700 Hz in going from 193 to 144°C, which makes the chemical shifts measurements difficult at the lower temperatures.

The ^{27}Al signals are much narrower, i.e., $\Delta\nu_{1/2} \approx$ 100 Hz at 160°C, in the $AlCl_3$-NaCl (50-50 mol %) mixture (mp 154°C (115)), due to the tetrahedral environment around the Al nucleus in the $AlCl_4^-$ species. Within experimental error, the chemical shift is identical to that measured for the previous ternary system, so that chemical shifts

cannot be used to identify the various species present in chloroaluminate melts.

Conclusion

The ^{39}K chemical shift range, which is about 40 ppm in dilute solutions, extends to about 100 ppm in molten salts and in crystals due probably to the closer distance of approach of cations and anions in these systems. In molten salts, potassium-39 lines are relatively narrow. The chemical shifts observed in molten salts correlate those found in aqueous solutions of the corresponding salts and do not vary significantly with the temperature or the cation composition of the mixtures.

APPENDIX 1

APPLICATION OF THE COMPUTER PROGRAM KINFIT TO THE CALCULATION OF COMPLEX FORMATION CONSTANTS FROM NMR DATA

The KINFIT computer program was used to fit the potassium-39 and carbon-13 NMR chemical shift vs mole ratio data to Equation (3) of Chapter V which was used as the SUBROUTINE EQN.

$$\delta_{obs} = [(K_f C_M^t - K_f C_L^t - 1) + (K_f^2 C_L^{t2} + K_f^2 C_M^{t2} -$$

$$2K_f^2 C_L^t C_M^t + 2K_f C_L^t + 2K_f C_M^t + 1)^{1/2}] \left(\frac{\delta_M - \delta_{ML}}{2K_f C_M^t}\right) + \delta_{ML} \quad (3)$$

Equation (3) has two unknown quantities, δ_{ML} and K_f, designated as U(1) and U(2) respectively in the FORTRAN code. The two input variables are the analytical concentration of the ligand (C_L^t, M) and the observed chemical shift (δ_{obs}, ppm) which are denoted as XX(1) and XX(2) respectively in the FORTRAN code. Starting with a reasonable estimate for the value of K_f and δ_{ML}, the program

fits the calculated chemical shifts (the right hand side of equation (3) to the observed ones by iteration method.

The first control card contains the number of data points (columns 1-5 (Format I5)), the maximum number of iterations allowed (columns 11-15 (F I5)), the number of constants (columns 36-40 (F I5)) and the convergence tolerance (0.0001 works well) in columns 41-50 (F 10.6). The second control card contains any title the user desires. The third control card contains the values of CONST(1) (C_M^t, $\underline{M}$) in columns 1-10 (F 10.6) and CONST(2) (δ_M, ppm) in columns 11-20 (F 10.6); other constants can be listed in columns 21-30, 31-40, etc. The fourth and final control card contains the initial estimates of the unknowns U(1) = δ_{ML} and U(2) = K_f, in columns 1-10 and 11-20 (F 10.6) respectively. The fifth through N cards are the data cards which contain XX(1) = C_L^t in columns 1-10 (F 10.6), the variance on XX(1) in columns 11-20, XX(2) = the chemical shift at XX(1) in columns 21-30 (F 10.6) and the variance on XX(2) in columns 31-40 (F 10.6) followed by the same parameters for the next data point. Each card may contain two data points. The SUBROUTINE EQN is given below.

APPENDIX 2

SUBROUTINE EQN

```
      COMMON NOUNT,ITAPE,JTAPE,IWT,LAP,XINCR,NOPT,NOVAR,NOUNS,X,U,ITMAX,  EQN6
     1WTX,TEST,I,AV,RESID,IAR,EPS,ITYP,XX,RXTYP,DXII,FOP,FO,FU,P,ZL,TO,E EQN6
     2IGVAL,XST,T,DT,L,M,JJJ,Y,DY,VECT,NCST,CONST,NOAT,JOAT,MOPT,LOPT,    EQN6
     3YYT,CONSTS
      COMMON/FREDT/IMETH
      COMMON/POINT/MOPT,JOPT,XXX
      DIMENSION X(6,100),U(20),WTX(4,300),XX(4),FOP(300),FO(300),FU(300) EQ
     1,P(29,21),VECT(20,21),ZL(300),TO(20),EIGVAL(20),XST(300),Y(10),
     2DY(10),CONSTS(50,16),NCST(50),ISMIN(50),RXTYP(50),DXII(50),IRX(50)
     3,MOPT(50),LOPT(50),YYY(50),CONST(16),XXX(15)
      GO TO (2,3,4,5,6,7,8,9,10,11,12)  ITYP
    1 CONTINUE
      ITAPE=40
      JTAPE=41
      NOUNS=2
      NOVAR=2
      RETURN
    2 CONTINUE
      RETURN
    3 CONTINUE
      RETURN
    4 CONTINUE
      IF(IMETH.NE.-1) GO TO 35
      RETURN
   35 CONTINUE
      A=(U(2)**2)*(XX(1)**2)
      B=(U(2)**2)*(CONST(1)**2)
      C=-2.0*(U(2)**2)*(XX(1))*CONST(1)
      D=2.0*(U(2))*(XX(1))
      E=2.0*(U(2))*(CONST(1))
      AA=(U(2))*(CONST(1))
      BB=-(U(2))*XX(1)
      CC=(CONST(2)-U(1))/(2.*(CONST(1))*(U(2)))
      S=((AA+BB-1.)+SQRT(ABS(A+B+C+D+E-1.)))*CC)-U(1)
      RESID=S-XX(2)
      RETURN
    5 CONTINUE
      RETURN
    6 CONTINUE
      RETURN
    7 CONTINUE
      RETURN
    8 CONTINUE
      IF(IMETH.NE.-1) GO TO 20
      RETURN
   20 CONTINUE
      RETURN
    9 CONTINUE
      RETURN
   10 CONTINUE
      RETURN
   11 CONTINUE
      RETURN
   12 CONTINUE
      RETURN
      END
```

APPENDIX 3

DERIVATION OF THE EXPRESSION OF THE RECIPROCAL LIFETIME OF THE SOLVATED SPECIES (EQUATION 11 CHAPTER III)

Equation (7) of Chapter III reads

$$\frac{1}{T'_A} = \frac{1}{2}[(\frac{1}{T_A} + \frac{1}{T_B} + \frac{1}{\tau_B} + \frac{1}{\tau_A}) - [(\frac{1}{T_B} - \frac{1}{T_A} + \frac{1}{\tau_B} - \frac{1}{\tau_A})^2 + \frac{4}{\tau_A \tau_B}]^{1/2}] \quad (1)$$

The equilibrium condition is $\frac{P_A}{\tau_A} = \frac{P_B}{\tau_B}$ with $P_A + P_B = 1$ from which we get:

$$\frac{1}{\tau} = \frac{1}{\tau_A P_B} - \frac{1}{\tau_A} \quad (2)$$

Rearrangement of (1) and replacement of T'_A by T_2 leads to

$$[\frac{1}{T_2} - \frac{1}{2}(\frac{1}{T_B} + \frac{1}{T_A} + \frac{1}{\tau_B} + \frac{1}{\tau_A})]^2 = \frac{1}{4}[(\frac{1}{T_B} - \frac{1}{T_A} + \frac{1}{\tau_B} - \frac{1}{\tau_A})^2 + \frac{4}{\tau_A \tau_B}] \quad (3)$$

$$\frac{1}{T_2^2} - \frac{1}{T_2T_B} - \frac{1}{T_2T_A} - \frac{1}{T_2P_B\tau_A} + \frac{1}{4}\left(\frac{1}{T_B^2}+\frac{1}{T_A^2}+\frac{1}{\tau_A^2P_B^2}+\frac{2}{T_AT_B}+\frac{2}{T_BP_B\tau_A}+\frac{2}{T_AP_B\tau_A}\right) =$$

$$\frac{1}{4}\left[\frac{1}{T_B^2}+\frac{1}{T_A^2}+\frac{1}{\tau_B^2}+\frac{1}{\tau_A^2}-\frac{2}{T_AT_B}-\frac{2}{\tau_A\tau_B}-\frac{2}{T_B\tau_A}-\frac{2}{\tau_A\tau_B}+\frac{2}{\tau_AT_A}+\frac{2}{\tau_BT_B}+\frac{4}{\tau_BT_B}\right] \tag{4}$$

$$\frac{1}{\tau_A}\left[-\frac{1}{T_2P_B}+\frac{1}{4\tau_AP_B^2}+\frac{1}{2P_B\tau_B}+\frac{1}{2T_AP_B}-\frac{1}{4\tau_A}-\frac{1}{4\tau_AP_B^2}-\frac{1}{4\tau_A}+\frac{1}{2\tau_AP_B}-\frac{1}{2\tau_AP_B}+\frac{1}{2\tau_A}\right.$$

$$\left.+\frac{1}{2T_B}-\frac{1}{2T_A}-\frac{1}{2P_BT_B}+\frac{1}{2T_B}+\frac{1}{2P_BT_A}-\frac{1}{2T_A}\right] = -\frac{1}{T_2^2}+\frac{1}{T_2T_B}+\frac{1}{T_2T_A}-\frac{1}{2T_AT_B}-\frac{1}{2T_AT_B} \tag{5}$$

$$\frac{1}{\tau_A}\left[\frac{1}{T_B}\frac{1}{T_A}+\frac{1}{T_AP_B}\frac{1}{T_2P_B}\right] = \left(\frac{1}{T_B}-\frac{1}{T_2}\right)\left(\frac{1}{T_2}-\frac{1}{T_A}\right) \tag{6}$$

$$\frac{1}{\tau_A}\left[\frac{1}{T_B}+\frac{1}{T_A}\frac{P_A}{P_B}-\frac{1}{T_2P_B}\right] = \left(\frac{1}{T_B}-\frac{1}{T_2}\right)\left(\frac{1}{T_2}-\frac{1}{T_A}\right) \tag{7}$$

$$\frac{1}{\tau_A} = \frac{P_B\left(\frac{1}{T_B}-\frac{1}{T_2}\right)\left(\frac{1}{T_2}-\frac{1}{T_A}\right)}{\frac{P_B}{T_B}+\frac{P_A}{T_A}-\frac{1}{T_2}}$$

APPENDIX 4

CALCULATION OF THE STANDARD DEVIATION ON $1/\tau_A$ VALUES (SEE TABLES 17-19 and 21)

The reciprocal lifetime of the solvated species is given by Equation (11) of Chapter III

$$1/\tau_A = P_B \frac{(1/T_{2B} - 1/T_2)(1/T_2 - 1/T_{2A})}{1/T_{2av.} - 1/T_2}$$

If $P_B = 0.5$ and if we set

$$A = 1/T_{2B} \qquad B = 1/T_{2A} \qquad C = 1/T_2$$

we have $$1/\tau_A = \frac{(A-C)(C-B)}{A+B-2C}$$

Then, considering A, B and C as independent variables in the intermediate region, we can write the absolute standard deviation S_{1/τ_A} as a function of the standard deviation S_A, S_B and S_C on A, B and C respectively.

$$S^2_{1/\tau_A} = \left(\frac{\delta(1/\tau_A)}{\partial A}\right)^2 S^2_A + \left(\frac{\delta(1/\tau_A)}{\partial B}\right)^2 S^2_B + \left(\frac{\delta(1/\tau_A)}{\partial C}\right)^2 S^2_C$$

$$S^2_{1/\tau_A} = \left(\frac{B-C}{A+B-2C}\right)^4 S^2_A + \left(\frac{A-C}{A+B-2C}\right)^4 S^2_B + \left[\frac{(A-C)^2+(C-B)^2}{(A+B-2C)^2}\right]^2 S^2_C$$

A, B and C values are given in Chapter III. S_A, S_B and S_C values are selected by taking into account both the experimental error and the error due to the extrapolations involved in the obtention of A and B.

REFERENCES

REFERENCES

1. C. Moore and B. C. Pressmann, Biochem. Biophys. Res. Comm. **15**, 562 (1964).

2. R. J. P. Williams, Quart. Rev., **24**, 331 (1970).

3. D. C. Tosteson, Sci. Am., **244**, 164 (April 1981).

4. (a) C. J. Pedersen, J. Am. Chem. Soc., **89**, 2495 (1967).
   (b) Ibid., **89**, 7017 (1967).

5. B. Dietrich, J. M. Lehn and J. P. Sauvage, Tetrahedron Lett., 2885 (1969).

6. J.-M. Lehn, Struct. Bonding (Berlin), **16**, 1 (1973).

7. J.-M. Lehn, Acc. Chem. Res., **11**, 49 (1978).

8. G. Schroder and W. Witt, Angew. Chem. Int. Ed. Engl., **18**, 311 (1979).

9. A. I. Popov and J.-M. Lehn, in "Coordination Chemistry of Macrocyclic Compounds", G. A. Melson ed., Plenum Press (1979), p. 537.

10. J. D. Lamb, R. M. Izatt, J. J. Christensen and D. J. Eatough, Ibid., p. 145.

11. "Progress in Macrocyclic Chemistry", R. M. Izatt and J. J. Christensen eds., Wiley Interscience (1979).

12. I. M. Kolthoff, Anal. Chem., **51**, 1R (1979).

13. N. S. Poonia and A. V. Bajaj, Chem. Rev., **79**, 389 (1979).

14. A. I. Popov, Pure Appl. Chem., **51**, 101 (1979).

15. J. S. Shih, Ph.D. Thesis, Michigan State University (1978).

16. P. B. Chock, F. Eggers, M. Eigen and R. Winkler, Biophys. Chem., **6**, 239 (1977).

17. E. Grell, T. Funck and F. Eggers in "Membranes", G. Eisenmann ed., Vol. III, Dekker, New York, p. 1-171.

18. R. A. Schwind, T. J. Gilligan and E. L. Cussler in "Synthetic Multidentate Macrocyclic Compounds", R. M. Izatt, J. J. Christensen eds., Academic Press (1978), p. 302.

19. G. W. Liesegang and E. M. Eyring, ibid. p. 245.

20. H. Degani, Biophys. Chem., 6, 345 (1977).

21. B. G. Cox, J. Garcia Rosas and H. Schneider, J. Am. Chem. Soc., 103, 1054 (1981).

22. H. Diebler, M. Eigen, G. Ilgenfritz, G. Maass and R. Winkler, Pure Appl. Chem., 20, 93 (1969).

23. G. G. Hammes, "Principles of Chemical Kinetics", Academic Press (1978).

24. P. Laszlo, Progress in NMR Spectrosc., 13, 257 (1980).

25. E. L. Yee, O. A. Gansow, and M. Weaver, J. Am. Chem. Soc., 102, 2278 (1980).

26. B. G. Cox, H. Schneider, J. Am. Chem. Soc., 99, 2809 (1977).

27. B. G. Cox, H. Schneider, and J. Stroka, J. Am. Chem. Soc., 100, 4746 (1978).

28. B. G. Cox, D. Knop, and H. Schneider, J. Am. Chem. Soc., 100, 6002 (1978).

29. B. G. Cox, H. Schneider, J. Am. Chem. Soc., 102, 3628 (1980).

30. B. G. Cox, J. Garcia-Rosas, and H. Schneider, J. Am. Chem. Soc., 103, 1054 (1981).

31. R. Gresser, D. W. Boyd, A. M. Albrecht-Gary and J. P. Schwing, J. Am. Chem. Soc., 102, 651 (1980).

32. J.-M. Lehn, J.-P. Sauvage, B. Dietrich, J. Am. Chem. Soc., 92, 2916 (1970).

33. J. M. Ceraso, J. L. Dye, J. Am. Chem. Soc., 95, 4432 (1973).

34. J. M. Ceraso, P. B. Smith, J. S. Landers, and J. L. Dye, J. Phys. Chem. 81, 760 (1977).

35. Y. M. Cahen, J. L. Dye, and A. I. Popov, J. Phys. Chem., 79, 1292 (1975).

36. E. Mei, J. L. Dye, and A. I. Popov, J. Am. Chem. Soc., 99, 5308 (1977).

37. E. Mei, A. I. Popov, and J. L. Dye, J. Am. Chem. Soc. 99, 6532 (1977).

38. E. Mei, A. I. Popov, and J. L. Dye, J. Phys. Chem. 81, 1677 (1977).

39. G. W. Liesegang, M. M. Farrow, N. Purdie, and E. M. Eyring, J. Am. Chem. Soc., 98, 6905 (1976).

40. G. W. Liesegang, M. M. Farrow, F. A. Vazquez, N. Purdie, and E. M. Eyring, J. Am. Chem. Soc., 99, 3240 (1977).

41. L. J. Rodriguez, G. W. Liesegang, R. D. White, M. M. Farrow, N. Purdie, and E. M. Eyring, J. Phys. Chem., 81, 2118 (1977).

42. G. W. Liesegang, M. M. Farrow, L. J. Rodriguez, R. K. Burnham, and E. M. Eyring, Int. J. Chem. Kinetics, X, 471 (1978).

43. B. Tümmler, G. Maass, E. Weber, W. Wehner, and F. Vögtle, J. Am. Chem. Soc., 99, 4683 (1977).

44. P. B. Chock, Proc. Nat. Acad. Sci., 69, 1939 (1972).

45. D. Live and S. I. Chan, J. Am. Chem. Soc. 98, 3769 (1976).

46. E. Shchori, J. Jagur-Grodzinski, Z. Luz, and M. Shporer, J. Am. Chem. Soc., 93, 7133 (1971).

47. E. Shchori, J. Jagur-Grodzinski, and M. Shporer, J. Am. Chem. Soc., 95, 3842 (1973).

48. M. Shporer, Z. Luz, J. Am. Chem. Soc., 97, 665 (1975).

49. J. Krane, J. Dale and K. Daasvatn, Acta Chem. Scand. B34, 59 (1980).

50. G. Borgen, J. Dale, K. Daasvatn and J. Krane, Acta Chem. Scand. B34, 249 (1980).

51. D. N. Reinhoudt and F. deJong in "Progress in Macrocyclic Chemistry", R. M. Izatt and J. J. Christensen eds., John Wiley and Sons (1979), p. 157.

52. J. Krane and T. Skjetne, Tetrahedron Lett., 1775 (1980).

53. J. S. Bradshaw, G. E. Maas, J. D. Lamb, R. M. Izatt and J. J. Christensen, J. Am. Chem. Soc., 102, 467 (1980).

54. G. Binsch and H. Kessler, Angew. Chem. Int . Ed. Engl., 19, 411 (1980).

55. K. H. Wong, G. Konizer, and J. Smid, J. Am. Chem. Soc. 92, 666 (1970).

56. E. Kauffmann, J.-M. Lehn and J.-P. Sauvage, Helv. Chim. Acta, 59, 1099 (1976).

57. B. Lindman and S. Forsen in "NMR and the Periodic Table", R. K. Harris and B. E. Mann eds., Academic Press, New York (1979).

58. A. M. Grotens, J. Smid, and E. deBoer, Chem. Commun., 759 (1971).

59. J. D. Lin and A. I. Popov, J. Am. Chem. Soc., in press.

60. J. P. Kintzinger, J.-M. Lehn, J. Am. Chem. Soc., 96, 3313 (1974).

61. C. Deverell, Progress in NMR Spectrosc., 4, 278 (1969).

62. D. E. Woessner, J. Chem. Phys., 35, 41 (1961).

63. D. E. Woessner and J. R. Zimmermann, J. Phys. Chem., 67, 1590 (1963).

64. K. J. Laidler, "Chemical Kinetics", McGraw-Hill (1965), p. 206.

65. Ibid, p. 251.

66. J. Krane, E. Amble, J. Dale and K. Daasvatn, Acta Chem. Scand. B34, 255 (1980).

67. J. Krane and O. Aune, Acta Chem. Scand. B34, 397 (1980).

68. M.-C. Fedarko, J. Magn. Res., 12, 30 (1973).

69. F. deJong, D. N. Reinhoudt, C. J. Smit and R. Huis, Tetrahedron Lett. 4783 (1976).

70. F. deJong, D. N. Reinhoudt and C. J. Smit, Tetrahedron Lett., 1371 (1976).

71. D. A. Laidler and J. F. Stoddart, J. C. S. Chem. Comm., 979 (1976).

72. J. Smid, Angew. Chem. Int. Ed. Engl., 11, 112 (1972).

73. M. Szwarc in "Ions and Ion Pairs in Organic Reactions", M. Szwarc ed., Wiley Interscience (1972), Vol. 1, p. 1.

74. J. Smid in "Ions and Ion Pairs in Organic Reactions", M. Szwarc ed., Wiley Interscience (1972), Vol. 1, p. 85.

75. S. Khazaeli, Ph.D. Thesis, Michigan State University (1981).

76. C. Carjaval, K. J. Tölle, J. Smid and M. Szwarc, J. Am. Chem. Soc., 87, 5548 (1965).

77. D. N. Bhattacharyya, C. L. Lee, J. Smid, and M. Szwarc, J. Phys. Chem., 69, 612 (1965).

78. W. F. Edgell and D. Harris, J. Sol. Chem. 9, 649 (1980).

79. D. Moras and R. Weiss, Acta Cryst. B29, 400 (1973).

80. M. A. Bush and M. R. Truter, J. Chem. Soc. Perkin II, 345 (1972).

81. D. Bright and M. R. Truter, J. Chem. Soc. B, 1544 (1970).

82. P. Seiler, M. Dobler and J. D. Dunitz, Acta Cryst. B30, 2744 (1974).

83. M. Dobler and R. P. Phizackerley, Acta Cryst. B30, 2746, 2748 (1974).

84. M. Dobler, J. D. Dunitz and P. Seiler, Acta. Cryst. B30, 2741 (1974).

85. J. F. Hinton and R. W. Briggs in "NMR and Periodic Table", R. K. Harris and B. E. Mann eds., Academic Press, New York (1979), p. 279.

86. P. R. Mallison and M. R. Truter, J. Chem. Soc. Perkin II, 1818 (1972).

87. W. Sheldrick, J. Kroner, F. Zwaschka, and A. Schmidpeter, Angew. Chem. Int. Ed. Engl. 18, 934 (1979).

88. T-P. I. and E. Grunwald, J. Am. Chem. Soc., 96, 2879 (1974).

89. J. L. Dye in Reference 11, page 63.

90. H. E. Simmons, C. H. Park, J. Am. Chem. Soc., 90, 2428 (1968).

91. C. H. Park, H. E. Simmons, J. Am. Chem. Soc., 90, 2429 (1968).

92. F. Mathieu, B. Metz, D. Moras and R. Weiss, J. Am. Chem. Soc., 100, 4412 (1978).

93. B. Dietrich, J.-M. Lehn and J. P. Sauvage, Tetrahedron, 29, 1647 (1973).

94. D. Moras and R. Weiss, Acta Cryst., B29, 396 (1973).

95. D. Moras, B. Metz and R. Weiss, Acta Cryst. B29, 383, 388 (1973).

96. B. Metz, D. Moras and R. Weiss, J. C. S. Chem. Comm., 444 (1971).

97. E. Kauffmann, J. L. Dye, J.-M. Lehn and A. I. Popov, J. Am. Chem. Soc., 102, 2274 (1980).

98. A. Knöchel, J. Oehler, G. Rudolph and V. Sinnvell, Tetrahedron, 33, 119 (1977).

99. J. Gutknecht, H. Schneider and J. Stroka, Inorg. Chem., 17, 3326 (1978).

100. S. Villermaux and J.-J. Delpuech, J. C. S. Chem. Comm., 478 (1975).

101. M.-F. Lejaille, M.-H. Livertoux, C. Guidon, J. Bessiere, Bull. Soc. Chim. Fr. I373 (1978).

102. M. H. Abraham, A. F. Danil deNamor and W. H. Lee, J. C. S. Chem. Comm., 893 (1977).

103. M. H. Abraham, E. Contreras Viguria, A. F. Danil de-Namor, and T. Hill, Inorg. Chem., 19, 54 (1980).

104. M. H. Abraham, E. Contreras Viguria, and A. F. Danil de Namor, J. C. S. Chem. Comm., 374 (1979).

105. M. H. Abraham, A. F. Danil de Namor and R. A. Schulz, J. C. S. Faraday I, **76**, 869 (1980).

106. I. M. Kolthoff and M. K. Chantooni, Jr., Proc. Natl. Acad. Sci. USA, **77**, 5040 (1980).

107. P. Pfeiffer and W. Christeleit, Z. Anorg. Allg. Chem., **239**, 133 (1938).

108. N. S. Poonia, Inorg. Chim. Acta, **23**, 5 (1977).

109. M. D. Grillone and M. A. Nocilla, Inorg. Nucl. Chem. Lett. **14**, 49 (1978).

110. M. R. Truter, Struct. Bonding (Berlin), **16**, 71 (1973).

111. N. S. Poonia and M. R. Truter, J. C. S. Dalton, 1791 (1972).

112. D. E. Fenton and R. Newman, J. C. S. Dalton, 655 (1974).

113. F. Vögtle, W. M. Müller and W. Rabhoffer, Isr. J. Chem., **18**, 246 (1979).

114. D. H. Kerridge, Pure Appl. Chem., **41**, 355 (1975).

115. B. Tremillon and G. Letisse, J. Electroanal. Chem., **17**, 371 (1968).

116. G. Letisse and B. Tremillon, J. Electroanal. Chem., **17**, 387 (1968).

117. A. M. Shams El Din, H. D. Taki El Din and A. A. El Hosary, Electrochim. Acta, **13**, 407 (1968).

118. A. A. El Hosary and A. M. Shams El Din, J. Electroanal. Chem., **35**, 35 (1972).

119. L. Sabbatini, B. Morelli and P. Zambonin, J. C. S. Faraday I, **75**, 2628 (1979).

120. G. Picard, F. Seon and B. Tremillon, J. Electroanal. Chem., **102**, 65 (1979).

121. T. J. Rowland and J. P. Bromberg, J. Chem. Phys., **29**, 626 (1958).

122. S. Hafner and N. Nachtrieb, J. Chem. Phys., **40**, 2891 (1964).

123. S. Hafner and N. Nachtrieb, J. Chem. Phys., 42, 631 (1965).

124. D. Harold-Smith, J. Chem. Phys., 59, 4771 (1973).

125. D. Harold-Smith, J. Chem. Phys., 60, 1405 (1974).

126. D. O'Reilly and E. Patterson, J. Chem. Phys., 55, 2155 (1971).

127. G. G. Bombi and G. A. Sachetto, J. Electroanal. Chem., 34, 319 (1972).

128. K. Furukawa, Disc. Faraday. Soc., 32, 53 (1961).

129. U. Anders and J. A. Plambeck, Inorg. Nucl. Chem. Lett., 40, 387 (1978).

130. P. B. Brekke, J. H. von Barner, and N. J. Bjerrum, Inorg. Chem. 18, 1372 (1979).

131. C. A. Angell and J. W. Shuppert, J. Phys. Chem., 84, 538 (1980).

132. J. Robinson, R. C. Bugle, H. L. Chum, D. Koran and R. A. Osteryoung, J. Am. Chem. Soc., 101, 3776 (1979).

133. W. Sahm and A. Schwenk, Z. Naturforsch 29A, 1754 (1974).

134. A. Delville, C. Detellier, A. Gerstman and P. Laszlo, J. Magn. Res., 42, 14 (1981).

135. J. S. Shih and A. I. Popov, Inorg. Nucl. Chem. Lett., 13, 105 (1977).

136. J. Kondo and J. Yamashita, J. Phys. Chem. Solids, 10, 245 (1959).

137. A. Abragam, "The Principles of Nuclear Magnetism", Oxford University Press, London (1961).

138. J. S. Shih and A. I. Popov, Inorg. Chem., 19, 1689 (1980).

139. F. W. Cope and R. Damadian, Physiol. Chem. Phys., 11, 143 (1979).

140. E. Schmidt, A. Hourdakis and A. I. Popov, Inorg. Chim. Acta., in press.

141. C. Deverell and R. E. Richards, Mol. Phys., **10**, 551 (1966).

142. E. G. Bloor and R. G. Kidd, Can. J. Chem., **50**, 3926 (1972).

143. F. W. Cope and R. Damadian, Nature, **228**, 76 (1970).

144. R. Damadian and F. W. Cope, Physiol. Chem. Phys., **5**, 511 (1973).

145. F. W. Cope and R. Damadian, ibid, **6**, 17 (1974).

146. R. Damadian and F. W. Cope, ibid, **6**, 309 (1974).

147. F. W. Cope and R. Damadian, ibid, **9**, 461 (1977).

148. J. D. Lin, Ph. D. Thesis, Michigan State University (1980).

149. V. Gutmann and E. Wychera, Inorg. Nucl. Chem. Lett., **2**, 257 (1966).

150. V. Gutmann, "The Donor-Acceptor Approach to Molecular Interactions", Plenum Press, New York (1969).

151. M. ST. J. Arnold and K. J. Packer, Mol. Phys., **10**, 141 (1966).

152. K. J. Packer and E. L. Muetterties, Proc. Chem. Soc., London, 147 (1964).

153. A. L. Van Geet, J. Am. Chem. Soc., **94**, 5583 (1972).

154. C. J. Pedersen, J. Am. Chem. Soc., **94**, 386, 391 (1972).

155. R. M. Izatt, N. E. Izatt, B. E. Rossiter and J. J. Christensen, Science, **199**, 994 (1978).

156. C. J. Pedersen in "Synthetic Multidentate Macrocyclic Complexes", R. M. Izatt, J. J. Christensen eds., Academic Press (1978), p. 1.

157. C. Cambillau, G. Bram, J. Corset, C. Riche and C. Pascard-Billy, Tetrahedron, **36**, 1043 (1980).

158. J. F. Garst, R. A. Klein, D. Walmsley and E. R. Zabolotny, J. Am. Chem. Soc., **87**, 4080 (1965).

159. I. M. Kolthoff and M. K. Chantooni, Jr., Anal. Chem., **51**, 1301 (1979).

160. N. S. Poonia, J. Inorg. Nucl. Chem., **37**, 1855 (1975).

161. M. K. Kuya and O. A. Serra, J. Coord. Chem., **10**, 13 (1980).

162. W. DeWitte and A. I. Popov, J. Sol. Chem., **5**, 231 (1976).

163. "Nonaqueous Electrolytes Handbook", G. J. Janz and R. P. T. Tomkin eds., Academic Press (1972), Vol. I.

164. R. H. Erlich, E. Roach and A. I. Popov, J. Am. Chem. Soc., **92**, 4989 (1970).

165. T. R. Griffiths and D. C. Pugh, Coord. Chem. Rev., **29**, 129 (1979).

166. G. W. Gokel and D. J. Cram, J. Org. Chem., **39**, 6 (1974).

167. G. W. Gokel, D. J. Cram, C. L. Liotta, H. P. Harris and F. L. Cook, J. Org. Chem., **39**, 2445 (1974).

168. G. Rounaghi, Ph.D. Thesis, Michigan State University (1980).

169. M. Shamsipur, Ph.D. Thesis, Michigan State University (1979).

170. See Vogel's method in "Organic Solvents", J. A. Riddick and W. B. Bunger, Wiley Interscience (1970), p. 748.

171. G. E. Hiegel and K. C. Selk, Appl. Spectrosc., **33**, 528 (1979).

172. M. St. J. Arnold and K. J. Packer, Mol. Phys., **14**, 249 (1968).

173. D. Live and S. I. Chan, Anal. Chem., **42**, 791 (1970).

174. "Handbook of Chemistry and Physics", The Chemical and Rubber Company, 47th edition (1966-1967).

175. S. Brownstein and J. Bornais, J. Magn. Res., **38**, 131 (1980).

176. E. D. Becker, J. A. Ferretti and P. N. Gambier, Anal. Chem., **51**, 1413 (1979).

177. J. C. Lindon and A. G. Ferridge, Prog. in NMR Spectrosc. **14**, 27 (1980).

178. A. I. Popov and A. J. Smetana, J. P. Kintzinger and T. T. Nguyen, Helv. Chim. Acta, **63**, 668 (1980).

179. V. A. Nicely and J. L. Dye, J. Chem. Educ., **48**, 443 (1971).

180. T. E. Burke and S. I. Chan, J. Magn. Res., **3**, 55 (1970).

181. M. Nicolas, M. Malineau and R. Reich, Phys. Chem. Lig., **10**, 11 (1980).

182. P. Beronius and L. Pataki, Acta Chem. Scand. **A33**, 675 (1979).

183. P. Beronius, Acta. Chem. Scand. **A33**, 79 (1979).

184. I. M. Kolthoff and M. K. Chantooni, Jr., Anal. Chem., **52**, 1039 (1980).

185. L. S. Frankel, T. R. Stengle and C. H. Langford, Chem. Commun., 393 (1965).

186. A. I. Popov in "Solute-Solvent Interactions", J. F. Coetzee and C. D. Ritchie eds., Marcel Dekker (1976), p. 305.

187. H. Schneider, ibid, p. 187.

188. T. Kagiya, Y. Sumida and T. Inoue, Bull. Chem. Soc. Japan, **41**, 767 (1968).

189. L. L. Chan and J. Smid, J. Am. Chem. Soc., **90**, 4654 (1968).

190. A. I. Shatenstein, E. S. Petrov, M. I. Belouseva, K. G. Yanova, and E. A. Yakov va, Dokl. Akad. Nauk. SSSR, **151**, 353 (1963).

191. G. J. Templeman and A. L. Van Geet, J. Am. Chem. Soc., **94**, 5578 (1970).

192. K. H. Wong, M. Bourgoin, and J. Smid, J. C. S. Chem. Comm., 715 (1974).

193. J. Smid and A. M. Grotens, J. Phys. Chem., **77**, 2377 (1973).

194. S. Boileau, P. Hemery, and J. C. Justice, J. Sol. Chem., **4**, 873 (1975).

195. R. H. Erlich and A. I. Popov, J. Am. Chem. Soc., **93**, 5620 (1971).

196. (a) K. J. Laidler, "Chemical Kinetics", McGraw-Hill (1965), p. 219.

197. J. D. Lamb, Ph.D. Thesis, Brigham Young University (1978).

198. W. F. K. Wynne-Jones and H. Eyring, J. Chem. Phys., **3**, 493 (1935).

199. A. J. Parker, Chem. Rev. **69**, 1 (1969).

200. J. J. Christensen, D. J. Eatough, and R. M. Izatt, Chem. Rev. **74**, 351 (1974).

201. G. Rounaghi and A. I. Popov, J. Inorg. Nucl. Chem. **43**, 911 (1981).

202. L. Pauling, "The Nature of the Chemical Bond", 3rd Ed., Cornell University Press, Ithaca, N.Y., 1960.

203. R. G. Pearson, J. Am. Chem. Soc., **85**, 3535 (1963).

204. E. Mei, Ph.D. Thesis, Michigan State University (1977).

205. M. Shamsipur, G. Rounaghi, and A. I. Popov, J. Sol. Chem., **9**, 701 (1980).

206. M. Shamsipur and A. I. Popov, Inorg. Chim. Acta **43**, 243 (1980).

207. M. Shamsipur and A. I. Popov, J. Am. Chem. Soc., **101**, 4051 (1979).

208. R. T. Myers, Inorg. Nucl. Chem. Lett. **16**, 329 (1980).

209. E. Kauffmann, Thése de Doctorat d'Etat, Université Louis Pasteur, Strasbourg (1979).

210. M. A. Bush and M. R. Truter, J. C. S. Perkin II, 345 (1972).

211. B. T. Kilbourn, J. D. Dunitz, L. A. R. Pioda, and W. Simon, J. Mol. Biol. **30**, 559 (1967).

212. N. A. Wilson, J. Phys. Chem., **83**, 2649 (1979).

213. A. Hofmanova, J. Koryta, M. Brezina and M. L. Mittal, Inorg. Chim. Acta, 28, 73 (1978).

214. H. K. Frensdorff, J. Am. Chem. Soc., 93, 600 (1971).

215. R. M. Izatt, R. E. Terry, D. P. Nelson, Y. Chan, D. J. Eatough, J. S. Bradshaw, L. D. Hansen, and J. J. Christensen, J. Am. Chem. Soc., 98, 7626 (1976).

216. J. Hasek, K. Huml and D. Hlavata, quoted in Reference 217.

217. J. D. Owen and M. R. Truter, J. C. S. Dalton, 1831 (1979).

218. A. R. Hourdakis, Ph.D. Thesis, Michigan State University (1978).

219. Y. M. Cahen, P. R. Handy, E. T. Roach and A. I. Popov, J. Phys. Chem., 79, 80 (1975).

220. J. A. Dixon, P. A. Gwinner and D. C. Lini, J. Am. Chem. Soc., 87, 1379 (1965).

221. G. E. Maciel, J. K. Hancock, L. F. Lafferty, P. A. Mueller and W. K. Mucher, Inorg. Chem., 5, 554 (1966).

222. B. G. Cox, G. R. Hedwig, A. J. Parker and D. W. Watts, Aust. J. Chem. 27, 477 (1974).

223. F. Hinz, D. W. Margerum, J. Am. Chem. Soc., 96, 4993 (1974).

224. F. Hinz and D. W. Margerum, Inorg. Chem., 13, 2941 (1974).

225. D. K. Cabbiness and D. W. Margerum, J. Am. Chem. Soc. 91, 6540 (1969).

226. F. A. L. Anet, C. H. Bradley and G. W. Buchanan, J. Am. Chem. Soc. 93, 258 (1971).

227. R. C. Lord and M. N. Siamwiza, Spectrochimica Acta, 31A, 1381 (1975).

228. J. A. Caruso and A. I. Popov, J. Phys. Chem., 72, 918 (1968).

229. J.-M. Lehn and J.-P. Sauvage, J. C. S. Chem. Comm., 440 (1971).

230. D. Gudlin and H. Schneider, Inorg. Chim. Acta 33, 205 (1979).